IMPACTS OF CLIMATE CHANGE ON STREAMFLOW AND HYDROLOGICAL EXTREMES IN THE SOUTH PHUTHIATSANA CATCHMENT, LESOTHO

BY

MAKOANYE MAPHUTSENG

201001779

DISSERTATION SUBMITTED TO THE NATIONAL UNIVERSITY OF LESOTHO WATER INSTITUTE IN PARTIAL FULFILLMENT OF THE REQUIREMENTS FOR THE DEGREE OF MASTERS OF SCIENCE IN INTEGRATED CATCHMENT AND WATER RESOURCES MANAGEMENT

NATIONAL UNIVERSITY OF LESOTHO

OCTOBER 2025

Declaration

The work contained in this dissertation was carried out and completed by MAKOANYE MAPHUTSENG, 201001779, at the National University of Lesotho Water Institute, National University of Lesotho. I hereby declare that this study constitutes my original work and has never been submitted for the award of a degree or diploma to any university. To the best of my knowledge, this dissertation contains no material written by another person except where due reference is made in the dissertation itself.

Signature _____ **Date** _____**13th October 2025**_____

As the candidate's supervisor, I certify the above statement to be correct to my knowledge and have recommended this dissertation for submission.

Dr. Liphapang Khaba _____ **Date** 13th October 2025 _____

Acknowledgements

I would like to thank the following organisations for the role they played in my MSc in ICWRM at the National University of Lesotho.

- The Government of Lesotho in general and the ReNOKA Movement in particular, which initiated and coordinated the implementation of the Integrated Catchment Management Programme in Lesotho.
- The EU and the German government for availing the funds for my full scholarship at the NUL.
- Deutsche Gesellschaft für Internationale Zusammenarbeit (GIZ) for providing the necessary technical assistance in the implementation of the ICM programme under which the MSc in ICWRM Programme was initiated.
- WaterNet for managing the scholarship fund for MSc in ICWRM.
- The National University of Lesotho in general and the Water Institute in particular for running the MSc in ICWRM Programme.
- The Department of Water Affairs for providing access to the hydrological flow data used in this study
- The Lesotho Meteorological Services for making available the historical precipitation and temperature records
- The Water and Sewage Company for providing reservoir operations data

I would also like to extend my deepest gratitude to several key individuals whose support was invaluable during my MSc journey:

- My sincere thanks go to my supervisor, Dr. Liphapang Khaba, for his expert guidance, insightful feedback, and unwavering support throughout my dissertation. His dedication was truly instrumental.
- To my family and friends, thank you for your constant encouragement, understanding, and patience. Specifically, I want to express my heartfelt appreciation to my wife, Mamona Maphutseng; my daughter, Mamosa Maphutseng; and my incredible mum, Mamakoanye Maphutseng. Your unwavering belief in me was a huge motivation, especially during

challenging times. I am grateful to my sister and brothers for their continuous support and encouragement.

- Finally, I am grateful to my colleagues and fellow students for their camaraderie and the enriching discussions that made my academic experience even more valuable

Abstract

Global climate change is predicted to significantly modify hydrological processes, which will have a big impact on ecosystem sustainability, flood risk, and water availability. Knowing how future climate changes may impact river systems is especially important in southern Africa, where population increase and fluctuating rainfall are already placing a strain on water resources. One such critical system is the South Phuthiatsana catchment, which serves as a vital supply of water for Maseru and the other metropolitan areas.

This study explores how projected climatic shifts may influence streamflow behavior and the occurrence of hydrological extremes within the South Phuthiatsana watershed, an essential source of water for Maseru and surrounding urban communities. Bias-adjusted data from the MPI-ESM1-2-LR global climate model, along with two sample emissions trajectories for the mid-21st century (2041–2080), were used to project climate inputs. Suboptimal performance indicators showed that the process-based model (SWAT+), which was used to simulate streamflow, was not very reliable in capturing historical daily flow patterns. SWAT+ was therefore thought to be insufficient for predicting future hydrological reactions in this context.

A machine learning approach using the XGBoost algorithm was adopted to address this challenge. This data-driven model was trained on bias-corrected climate variables and observed streamflow, providing a more reliable tool for future streamflow prediction. The results from XGBoost revealed substantial and complex hydrological shifts. A consistent warming trend combined with highly variable seasonal precipitation patterns was evident across both emission scenarios. Extreme high flows, represented by the 98th percentile (Q98), are projected to decline by more than 52% compared to historical values, suggesting a reduced risk of flooding. In contrast, low flows are expected to increase dramatically; the 1st percentile (Q1) flow is projected to rise from near-zero values historically to approximately 9.0 m^3/s, indicating a significant shift toward more perennial flow conditions.

Mid-range flows (Q25, Q50, and Q75) are also expected to increase substantially, depending on the flow percentile and scenario. While the absolute magnitude of low flows improves, the number

of days with historically low flow conditions may still increase during certain months, highlighting a shift in the intra-annual flow variability.

These findings point to a future with altered hydrological regimes in the South Phuthiatsana catchment characterised by diminished flood peaks, elevated baseflows, and more frequent low-flow conditions during critical periods. Despite initial limitations with the process-based model, the machine learning approach provided robust insights that form a valuable foundation for developing adaptive, forward-looking water resource management strategies. These results underscore the need for resilient planning to ensure long-term water security under evolving climate conditions.

Keywords: SWAT+, XGBoost, Climate Change, Streamflow, Hydrological Extremes

List of tables

List of figures

Contents

Abbreviations

ANN	Artificial Neural Networks
CMIP6	Coupled Model Intercomparison Project Phase 6
DEM	Digital Elevation Model
DSMW	Digital Soil Map of the World
DWA	Department of Water Affairs
ENSO	El-Niño Southern Oscillation
GEV	Generalised Extreme Value
GCM	Global Climate Model
IOD	Indian Ocean Dipole
IPCC	Intergovernmental Panel on Climate Change
LDC	Least Developed Countries
LMS	Lesotho Meteorological Services
LSTM	Long-Short Term Memory
ML	Machine Learning
RCM	Regional Climate Models
RCP	Representative Concentration Pathway
SADC	Southern African Development Community
SRTM	Shuttle Radar Topography Mission
SSP	Shared Socioeconomic Pathway
SWAT+	Soil and Water Assessment Tool Plus
XGBoost	eXtreme Gradient Boosting

1 Introduction

1.1 Background

Climate change refers to long-term shifts in average climate conditions and variability, driven by both internal dynamics such as ocean-atmosphere interactions, solar radiation and external forcings such as volcanic activity and anthropogenic greenhouse gas emissions (Abdulahi et al., 2022; IPCC, 2021). These changes have led to observable impacts including rising temperatures, altered precipitation patterns, and increased frequency of extreme weather events (Ayalew et al., 2022).

Globally, climate change poses serious risks to water security, with nearly half the world's population experiencing seasonal shortages due to climatic and human factors (IPCC, 2023). Vulnerable populations particularly in Africa, Asia, Central and South America, the Arctic, Small Island Developing States (SIDS), and Least Developed Countries (LDCs) face disproportionate exposure to climate hazards. Between 2010 and 2020, mortality from floods, droughts, and storms was up to 15 times higher in these regions compared to more resilient areas (Ali et al., 2023; IPCC, 2023).

Africa is especially sensitive to climate variability, with Sub-Saharan regions relying heavily on rain-fed agriculture, which accounts for 96% of production (Assfaw et al., 2023). Southern Africa, including Lesotho, is characterised by semi-arid conditions and highly variable rainfall, ranging from 100 mm to 2000 mm annually (Nicholson et al., 2018). These climatic pressures exacerbate water scarcity and threaten livelihoods dependent on agriculture and natural resources (Nhemachena et al., 2020).

Numerous studies have shown that climate variability significantly affects hydrological systems and fluvial dynamics (Wang et al., 2023). Key impacts include increased frequency and severity of floods and droughts, changes in water quality, and altered flow regimes due to shifts in soil moisture, humidity, and runoff (Teweldebrihan & Dinka, 2024). Combined with human pressures such as land use change, population growth, and economic development, climate variability intensifies water supply strain (Saedi et al., 2022).

Robust surface water modeling is essential for understanding and managing watershed dynamics. Hydrological models like SWAT are widely used to simulate streamflow, sediment transport, and the impacts of land use and climate change (Abbaspour et al., 2015; Nath et al., 2024). In this study, SWAT will be calibrated at the Masianokeng gauging station, which provides long-term streamflow data and represents the catchment's hydrological behavior (Maliehe & Mulungu, 2017).

In Lesotho, understanding catchment-level hydrological responses to climate change is critical for sustainable water resource planning. The South Phuthiatsana Catchment, which supports domestic use, agriculture, and hydropower, is particularly vulnerable to shifts in streamflow and hydrological extremes. This study focuses on assessing climate-induced changes in streamflow patterns and evaluating their implications for water management in the region, with the goal of supporting adaptive planning and sustainable resource use in the South Phuthiatsana Catchment.

1.2 Problem Statement

In Lesotho, the annual average temperature is projected to rise by 1.78–2.2 degrees Celsius (°C) by 2060, contributing to shifts in seasonal precipitation and water availability (Irish Aid, 2015). Additionally, Lesotho's climate change scenarios indicate substantial changes in the northern region by 2050, with a significant increase in rainfall between March and May until 2100. These changes pose serious risks to water resources, agriculture, and ecosystem resilience. While increased rainfall may enhance water availability, it can also trigger extreme events like floods and soil erosion, threatening infrastructure and livelihoods. Conversely, rising temperatures could intensify evapotranspiration, leading to dry spells that counteract the benefits of increased precipitation. Lesotho's dependence on water for domestic use, agriculture, hydropower, and export highlights the need to assess how climate change may impact future catchment-level streamflow, supporting better resource planning and climate resilience.

1.3 Aim

To assess the impacts of climate change on streamflow patterns and hydrological extremes (floods and droughts) in the South Phuthiatsana Catchment, Lesotho, with the aim of improving hydrological modeling accuracy and supporting adaptive planning under future climate scenarios.

1.4 Specific Objectives

a) To assess historical trends and variability in key climate variables within the South Phuthiatsana Catchment.
b) To evaluate projected changes in precipitation and temperature under SSP2-4.5 and SSP5-8.5 scenarios for the South Phuthiatsana Catchment.
c) To simulate future streamflow patterns in the catchment using hydrological modeling based on projected climate scenarios.
d) To analyse the effects of projected climate change on hydrological extremes in the catchment through hydrological modeling.

This study aims to generate insights that can inform catchment-level water resource planning and support improvements in surface water management policies in the South Phuthiatsana Catchment, particularly in response to climate-induced hydrological changes.

1.5 Research Questions

a) What are the possible effects of climate change on streamflow dynamics and hydrologic irregularities under two distinct climatic scenarios (SSP2-4.5 and SSP5-8.5)?
b) How will climate change alter streamflow dynamics in the South Phuthiatsana catchment?
c) Under different climate scenarios, what are the projected alterations in streamflow extremes (low and high flows) in the South Phuthiatsana catchment?

1.6 Justification

The South Phuthiatsana catchment plays a key role in national water resource management, supporting efforts to increase water accessibility and ensure a dependable supply for Maseru's

urban and peri-urban zones, as well as nearby communities such as Morija, Roma, Mazenod, and Teyateyaneng (Maliehe & Mulungu, 2017). Lesotho's climate is moderately temperate and largely influenced by rainfall patterns, making the country especially vulnerable to the adverse impacts of climate change (LMS, 2021). As such, assessing climate-related variability in streamflow and the occurrence of hydrological extremes at the catchment level is essential. Anticipating these changes early enables more informed planning and the development of robust adaptation and mitigation frameworks.

1.7 Research Gap

Recent studies in the South Phuthiatsana catchment (Maliehe & Mulungu, 2017; Fobo, 2009) have advanced hydrological modeling and land use change understanding. However, they often overlook the complex interactions among hydrological extremes, climatic variations, and land use changes. Notably, few studies assess climate change impacts on streamflow in Lesotho, particularly using CMIP6 data with new scenarios like SSP2-4.5 and SSP5-8.5. Predicting long-term river flow dynamics and extreme hydrological events remains challenging. This study aims to improve predictions of future hydrological extremes by incorporating advanced climate projections and comprehensive land use classifications into hydrological models. Climate change impacts often trigger recurring disasters, including extreme or low precipitation and rising temperatures, which disrupt streamflow patterns.

2 Literature Review

2.1 Introduction

This chapter reviews key literature on the impacts of climate change on streamflow and hydrological extremes using SSP2-4.5 and SSP5-8.5 scenarios in the South Phuthiatsana catchment. It begins by outlining the relationship between climate change and hydrology, followed by a review of climate modeling approaches, including downscaling techniques and future climate scenarios such as the RCPs and SSPs. It also examines hydrological modeling approaches used in climate impact studies, including the application of process-based models and data-driven models. Finally, the chapter discusses model performance and limitations, highlighting challenges in simulating hydrological responses under changing climatic conditions. Crucially, the review provides the foundation for adopting a hybrid modeling strategy, utilising the process-based Soil and Water Assessment Tool (SWAT+) for understanding physical processes and the machine learning model Extreme Gradient Boosting (XGBoost) for robust prediction of hydrological extremes, thereby addressing the limitations inherent in using a single modeling approach.

2.2 Climate Change and Hydrology Overview

Global climate change plays a critical role in altering the hydrological cycle, with notable impacts on river flow, evaporation rates, and rainfall distribution (Assfaw et al., 2023; Sun et al., 2022). The primary drivers behind rising atmospheric greenhouse gas levels are anthropogenic activities, particularly the combustion of fossil fuels (Islam & Van Amstel, 2021). Since the 1950s, human-induced climate change has likely contributed to a rise in the occurrence and severity of compound weather extremes such as intense rainfall, droughts, and associated flooding events (IPCC, 2021). Numerous studies have investigated these hydrological shifts across Sub-Saharan Africa, a region especially exposed to climatic fluctuations and extreme weather (Bekele et al., 2019; Serdeczny et al., 2017). The IPCC (2014) also notes that climate change disproportionately affects developing countries, especially those with economies heavily dependent on agriculture.

Often described as the “water tower” of water-scarce Southern Africa, Lesotho plays a critical role in supplying water to neighboring regions. At the same time, the country was ranked 127th out of 181 in the Global Climate Risk Index 2021, reflecting its high vulnerability to climate-related hazards (Eckstein et al., 2021). This vulnerability stems largely from increasing variability in temperature extremes, rainfall patterns, and snowmelt timing, which directly affect streamflow regimes and the frequency of hydrological extremes such as droughts and floods. Lesotho's water resources are extremely vulnerable to climatic variations because of its rain-fed hydrology, vulnerable mountain catchments, and damaged soils (Hlalele, 2020). This becomes even more severe due to the nation's inadequate institutional ability and adaptive infrastructure to cope with these extremes, which reduces the resilience of its river systems, wetlands, and watersheds, particularly during times of either excess or insufficient runoff. This is made worse by the nation's inadequate institutional ability and adaptive infrastructure to deal with these extremes, which makes its river systems, wetlands, and catchments less resilient, particularly during times of either excess or inadequate runoff. Understanding and measuring how climate change affects streamflow behavior is crucial for safeguarding Lesotho’s water resources and supporting regional water security in Southern Africa.

2.3 Climate Models

Numerous studies have emphasised the significance of global climate models (GCMs) in predicting temperature trends and assessing the impact of climate change on hydrological extremes (Daniel & Abate, 2022; Meresa et al., 2022; Tarekegn et al., 2021). The effectiveness of these models, however, depends largely on their ability to replicate past and present climate patterns at both regional and global levels, making them essential tools in climate research (Fan et al., 2020). Fan et al. (2020) also highlight that GCM outputs offer insights into potential 21st-century climate scenarios and their broader implications. Despite their value, simulating diverse climate variables remains complex. These models must be evaluated for their precision in reproducing historical conditions and in projecting short- and long-term climate developments (Oo et al., 2019).

The sixth phase of the Coupled Model Intercomparison Project (CMIP6) was developed with a more decentralised framework to address the complexity of climate system modeling. It also

introduced a wider range of experimental scenarios compared to earlier phases (Fan et al., 2020). Oo et al. (2019) report that CMIP6 models exhibit significant improvements over CMIP5, including enhanced spatial resolution, refined physical processes such as cloud dynamics, and the integration of additional Earth system factors like nutrient impacts on the land carbon cycle and interactions with ice sheets. These upgrades allow for better simulation of extreme weather events and provide greater detail at regional scales. Overall, using a multi-model ensemble combining several GCMs from various institutions offers more robust assessments of water resources than relying on a single model, particularly when the uncertainty in climate projections exceeds that of hydrological models (Li & Fang, 2021).

2.3.1 Downscaling of Climate Models

Two methods have been used in previous research to downscale GCM projections: the statistical downscaling technique and the dynamic downscaling method (El-Samra et al., 2024). The outputs generated by GCMs necessitate the implementation of downscaling methodologies to yield well-organised data on regional scales relevant to impact evaluations, policy formulation, and climate advisory services, among other applications (Kreienkamp et al., 2018). As stated by Kreienkamp et al. (2018), empirical statistical downscaling utilises transfer functions that are derived from observational data at the coarse resolution of GCMs and regional datasets, whereas dynamical downscaling employs Regional Climate Models (RCMs) that are informed by GCM outputs at the peripheries of a constrained geographical area (for example, Africa) and subsequently computes atmospheric phenomena within this region on a significantly finer spatial grid. Compared to dynamic downscaling, statistical downscaling approaches often take less time and effort and are less expensive to compute. However, statistical downscaling depends on the crucial principle of stationarity, which holds that the local climate and the coarsely simulated climate from GCM will always be related (El-Samra et al., 2024). Generally, statistical downscaling methods try to connect the large-scale atmospheric predictor variables to local or regional weather data series (Enayati et al., 2021).

On the other hand, Enayati et al. (2021) stated that dynamic downscaling methods use finer gridded models known as the RCMs to define climate change predictions at a regional scale from the

projections of the coarse GCMs. It is done in multiple steps, with each step improving the detail and decreasing the area of the simulated region. Although dynamic downscaling allows trading off area spatial extent for resolution, it is computationally expensive for larger areas; for example, downscaling a model from 100-kilometer resolution to a 10-kilometer resolution. Being computationally intensive limits, the number of processes run in parallel, hence leading to gaps in data and incomplete model uncertainty assessment and internal variability in regional climate projections (Lopez-Gomez et al., 2025). Therefore, statistical downscaling is best for computational efficiency and broader regional applications where high-resolution projections are needed without the heavy resource demands of dynamic modeling.

Statistical downscaling is frequently chosen in hydrological impact studies due to its computational efficiency and ease of generating large ensembles, which makes it appropriate for broad-scale assessments. In contrast, dynamical downscaling, particularly when employing high-resolution regional climate models, provides more topographically accurate and physically consistent representations of extreme precipitation and streamflow processes, especially in mountainous catchments (Legrand et al., 2024; Byun et al., 2022). The trade-off between computing cost, ensemble breadth, and the need for detailed process fidelity thus determines the best option.

2.3.2 Future Climate Scenarios: From Representative Concentration Pathways (RCPs) to Shared Socio-economic Pathways (SSPs)

The assessment of future climate change impacts relies on climate scenarios that project potential greenhouse gas concentrations and subsequent radiative forcing. Earlier climate research, particularly under the CMIP5 framework, utilised the Representative Concentration Pathways (RCPs) (Van Vuuren et al., 2011). These pathways were defined primarily by the radiative forcing stabilisation level (in W/m^2) they achieve by 2100. For instance, scenarios like RCP 4.5 (medium emissions) and RCP 8.5 (high emissions) focused solely on the physical climate system response.

The latest climate projections, however, are based on the more comprehensive Shared Socioeconomic Pathways (SSPs), which form the core of the CMIP6 framework (IPCC, 2021).

The SSPs represent five distinct global storylines of socioeconomic development covering future demographic, economic, and policy trends that influence society's capacity to both mitigate and adapt to climate challenges (Van Vuuren et al., 2017).

The SSPs are typically linked with a specific radiative forcing level from the RCP concept, for example, SSP2 combined with 4.5 W/m^2). This integration provides a more robust and contextualised projection than RCPs alone. The five SSP storylines range from a focus on sustainability (SSP1) to a fragmented, regional rivalry path (SSP3), to the fossil-fuel-intensive development path (SSP5) (Cheng et al., 2024), with SSP2 representing the "middle-of-the-road" scenario (O'Neill et al., 2014). Consequently, the CMIP6 Scenarios, including those aligned with the IPCC's Sixth Assessment Report (2021), now utilise scenarios like SSP1-1.9, SSP2-4.5, and SSP5-8.5 (Siabi et al., 2023). CMIP6 models also offer improvements over CMIP5, including enhanced spatial resolution and greater attention to the socioeconomic drivers of climate change (Siabi, 2021).

The current research focuses on projections under the SSP2-4.5 and SSP5-8.5 scenarios, which are considered updated versions of the earlier RCP 4.5 and 8.5 pathways (Arfasa et al., 2024; Khan et al., 2023). This selection provides a representative range of potential futures:

a) **SSP2-4.5 (Middle-of-the-Road):** This moderate scenario reflects a future with emissions peaking mid-century and then declining, making it appropriate for evaluating impacts under modest mitigation efforts (O'Neill et al., 2017).
b) **SSP5-8.5 (Fossil-Fuelled Development):** This high-emission, fossil-fuel-intensive pathway represents a business-as-usual future with limited mitigation, highlighting the upper bounds of expected warming and hydrological extremes by the end of the century (O'Neill et al., 2017).

In Southern Africa, the SSPs are complex and represent the region's particular socioeconomic and environmental issues. A study by the United Nations Convention to Combat Desertification (UNCCD) predicts that under different SSP scenarios, Sub-Saharan Africa will see substantial shifts in land use and greater pressure on remaining resources, which could put additional strain

on local economies (UNCCD, 2022). Furthermore, studies show that since low-income communities depend on climate-sensitive industries like agriculture, they are particularly affected by climate change. According to a World Agroforestry Centre assessment, climate variability might result in decreased agricultural productivity and limited resources, which is crucial for the economy of Lesotho.

2.4 Impacts of Climate Change on Streamflow Regimes

Climate change is increasingly altering streamflow regimes worldwide, as shifts in temperature and precipitation disrupt the timing, magnitude, and variability of river flows (IPCC, 2021; Brunner et al., 2020). Shifts in climate variables, particularly temperature, often affect precipitation and surface runoff due to the interdependent nature of climate components (IPCC, 2021). As the atmosphere warms, its capacity to hold moisture increases by roughly 6–7% per degree Celsius, creating the potential for more intense precipitation and shifts in regional rainfall patterns (Chen et al., 2023). However, this relationship is not linear; increased evapotranspiration does not always result in heavier rainfall, as outcomes depend strongly on meteorological conditions, storm tracks, and geographic setting (Dierauer et al., 2021). These changes directly influence the amount and timing of water entering river system, thereby modifying streamflow regimes.

Observed records confirm that streamflow regimes are already shifting, and such changes are projected to intensify under continued climate change (Brunner et al., 2020). For example, in snowmelt-dependent basins, warmer temperatures are causing earlier snowmelt, which shifts peak flows to earlier in spring while reducing summer discharge (Dierauer et al., 2021). This re-timing of flows reduces water availability during periods of peak demand. Importantly, impacts are not uniform but vary with catchment characteristics such as reliance on snowmelt versus rainfall, basin topography, and geographic location.

In Southern Africa, climate change impacts on streamflow are already evident, with projections showing rising temperatures alongside declining or more variable rainfall (Coumou et al., 2016). The frequency of extreme events, including floods and droughts, has increased, contributing to greater variability in river discharge and heightened risks for water resource management (WRC,

2022). These patterns highlight the importance of localised assessments of streamflow response and the development of tailored adaptation strategies (Pierre et al., 2016).

2.5 Impacts on Hydrological Extremes (High and Low flows)

Globally, the probability of drought and the yearly occurrence of heavy precipitation are predicted to increase before 2070, and they will only worsen if global temperature rises by an additional 2.0 degrees Celsius (Li et al., 2024). Numerous studies have predicted that future climate change will influence hydrological extremes, primarily across main river basins worldwide, leading to increased large-scale floods (Taye & Dyer, 2024; Lane & Kay, 2021). In regions already vulnerable to significant rainfall, the increase in atmospheric moisture brought on by global warming will likely increase precipitation extremes (IPCC, 2021; Alfieri et al., 2017). As a result, as precipitation patterns are changing and floods and flash floods become more unpredictable, there is an increasing danger of damage to infrastructure, public safety, and ecosystems.

On the other hand, it is also predicted that future climatic scenarios will result in more frequent and severe droughts (Markus et al., 2019). Li et al., (2024) stated that changes in precipitation patterns and rising temperatures may cause extended droughts in areas already struggling with a water shortage. In dry and semi-arid environments, increased evapotranspiration exacerbates drought conditions by combining with decreased soil moisture. This results in less reliable water resources. Droughts influence ecosystem health, agriculture, and water delivery systems, which raises questions about food security and sustainable water usage (Pereira, 2017).

Global warming causes an increase in the average amount of precipitation and evaporation worldwide (IPCC, 2023). Undoubtedly, this will exacerbate the change in streamflow and hydrological extremes. Beyond climate-induced change, anthropogenic activities also significantly modify hydrological processes and extreme events such as changes in land use and cover, water use, urbanisation, and dam construction have also affected hydrological processes (Zhang et al., 2021). Human activities can drastically impact flow and may lead to altered water quality and quantity thereby affecting aquatic ecosystems. For example, human activities may influence how much water enters a stream, divert flow through constructed channels, or alter stream shape and

position. In addition to changing downstream flow patterns and the river's sediment load, reservoirs are essential for managing water resources (Sirisena et al., 2021). According (Montanari et al., 2013), the Internation Association of Hydrological Sciences (IAHS) emphasised in 2013 that human interactions with water are still poorly understood. The observed flows must therefore be separated into their natural and man-made components (Terrier et al., 2021).

Numerous methodologies have been established to quantify the effects of hydrologic factors on flow alterations, categorised into four types: statistical approaches, paired catchment, field study, and hydrological simulation methods (Van Loon et al., 2019). The statistical analysis approach, while useful, does not account for hydrological-physical processes or watershed spatial heterogeneity. The paired catchment technique, although robust, is often limited by the difficulty of selecting comparable test catchments and its time-consuming nature. In some cases, naturalised flow can be inferred through on-site measurements, though doing so requires comprehensive records of human influence, which are often incomplete or lacking. Finally, hydrological simulation models (such as SWAT and HBV) offer physically meaningful and detailed reconstructions of naturalised flows through process-based modeling (Sheng et al., 2023).

Recent studies in Africa and other data-scarce regions highlight the importance of naturalisation in climate-impact hydrology. For instance, Akoko et al. (2021) demonstrated the value of model-based natural flow reconstructions for East African basins using SWAT, particularly where hydrological data is limited or affected by human activity. Analysis of 471 catchments was conducted worldwide and it was discovered that adding human-impact parameterisations like dams, abstractions, and land use greatly improves the accuracy of streamflow simulations and extremes (Veldkamp et al., 2018). This highlights the significance of flow naturalisation in both managed and near-natural systems.

2.6 Hydrological Modeling in Climate Change Impact Assessment

Hydrological modeling techniques are valuable tools for examining climate change's effects on a particular watershed's hydrology (Pandey et al., 2016). Hydrological models are critical for simulating water cycle components and evaluating the impacts of climatic and anthropogenic

changes (Ibrahim & Dan'azumi, 2020). According to Ibrahim & Dan'azumi (2020), the concept of hydrological modeling focuses on the interactions between soil, land use, water, and climate. Hydrological models can be categorised as process-based (or physical/conceptual) or data-driven (statistical or machine learning) and further as distributed or lumped and stochastic or deterministic.

Recent developments in water resource planning have seen a growing use of hydrological models that incorporate detailed features such as reservoirs, irrigation systems, water quality parameters, and feedback mechanisms at both regional and global levels (Dobson et al., 2024; Abeshu et al., 2023). Among these, tools like the Soil and Water Assessment Tool (SWAT) are widely utilised. SWAT is a semi-distributed, process-oriented model that simulates hydrological behavior based on physical watershed characteristics (Shiferaw et al., 2018). These models rely heavily on the quality of input data; accurate and comprehensive datasets are essential for producing reliable simulations, while poor data quality often results in significant inaccuracies.

SWAT and its modified version, SWAT+ (Chawanda et al., 2020), are particularly helpful resources for analysing how streamflow and hydrological extremes respond to climate change by simulating water balance components and transport processes within a watershed (Li & Fang, 2021). For example, (Gradiyanto et al., 2025) used an ensemble of CMIP6 and ten GCMs in the SWAT model under the SSP2-4.5 and SSP5-8.5 scenarios to assess the impacts of climate change on Kupang River flow and hydrological extremes over two different periods. Several studies recommend the adoption of the modified version, SWAT+, based on its successful application and performance in different catchments (Gujree et al., 2022; Kakarndee & Kositsakulchai, 2020; Bieger et al., 2016). While physically based models are often preferred for climate change impact studies due to their ability to represent underlying hydrological processes and their response to altered climatic conditions (Parajuli & Risal, 2021), they require extensive input data and calibration.

2.6.1 Machine Learning Models in Hydrology

The use of data-driven models, especially machine learning (ML) techniques, for hydrological forecasting and climate change impact assessment has significantly increased as a result of the

growing complexity of hydrological systems, as well as the expansion of computational power and a variety of datasets (Khan et al., 2023; Eccles et al., 2019). Unlike process-based models that rely on explicit physical equations, ML models learn complex, non-linear relationships directly from historical climate and streamflow data (Martel et al., 2024). When compared to traditional models, they frequently perform better at capturing the complex nature of climate change impacts on streamflow because of this feature, which gives them great flexibility in addressing non-linearities and responding to a range of hydrological and climatic conditions (Martel et al., 2024; Phetanan et al., 2024).

Among the advanced machine learning techniques, Extreme Gradient Boosting (XGBoost), one of the most sophisticated machine learning methods, has become an efficient and very successful algorithm for a range of regression and classification applications, including hydrological modeling (Niazkar et al., 2024). An ensemble learning technique called XGBoost makes use of a gradient boosting framework. It generates a succession of decision trees one after the other, training each one to fix the mistakes of the one before it. Its exceptional accuracy and resilience are a result of the regularisation approaches and iterative error correction (Chen & Guestrin, 2016).

Key advantages of XGBoost in hydrological applications include its proven high predictive accuracy for both mean flows and hydrological extremes (Li et al., 2024), its excellent capability to capture complex, non-linear relationships inherent in hydrological processes, and its robustness to noise and missing data often found in environmental datasets. Furthermore, XGBoost can provide insights into the relative importance of different input features such as rainfall, temperature, and antecedent streamflow in driving streamflow responses, aiding in hydrological understanding (Szczepanek, 2022; Yang & Chui, 2020). Its computational efficiency also makes it scalable for large datasets.

XGBoost has been successfully applied in numerous hydrological contexts, including streamflow forecasting, runoff prediction, and integrated water resource modeling (Wang & Peng, 2024; Niazkar et al., 2024). For instance, studies have leveraged XGBoost for daily and monthly streamflow forecasting (Fan et al., 2020), predicting flood and drought occurrences (Li et al., 2024), and assessing impacts of climate change on water resources (Martinho et al., 2023).

Comparative studies have often shown that advanced ensemble ML models like XGBoost can achieve comparable or even superior predictive performance to traditional physically based or conceptual models, especially for complex hydrological phenomena or in catchments with limited detailed process data (Solanki et al., 2025; Kumar et al., 2023).

2.7 Model Performance and Limitations

In hydrological modeling using tools like SWAT+, objective functions play a crucial role in assessing how well the model replicates streamflow behavior. These functions compare simulated discharge with observed data and are essential during both calibration and validation stages (Pulighe et al., 2021). To evaluate model performance, several statistical indicators are commonly used, such as the Nash-Sutcliffe Efficiency (NSE), Percent Bias (PBIAS), Root Mean Square Error (RMSE), Mean Square Error (MSE), Coefficient of Determination (R^2), and the Kling-Gupta Efficiency (KGE) (Rufino et al., 2023). The equations for these objective functions are as follows:

NSE

$$NSE = 1 - \frac{\sum_{i=1}^{n}(Q_{obs} - Q_{sim})^2}{\sum_{i=1}^{n}(Q_{obs} - Q_{mean})^2} \qquad \textit{Equation 1}$$

PBIAS

$$PBIAS = \left[\frac{\sum_{i=1}^{n}(Q_{obs} - Q_{sim}) * 100}{\sum_{i=1}^{n} Q_{obs}}\right] \qquad \textit{Equation 2}$$

RMSE

$$RMSE = \sqrt{\frac{\sum_{i=1}^{n}(Q_{obs} - Q_{sim})^2}{n}} \qquad \textit{Equation 3}$$

KGE

$$KGE = 1 - \sqrt{(r-1)^2 + \left(\frac{\alpha_{sim}}{\alpha_{obs}} - 1\right)^2 + \left(\frac{\mu_{sim}}{\mu_{obs}} - 1\right)^2} \qquad \textit{Equation 4}$$

Where; Q_{obs} – Observed discharge, Q_{sim} – Simulated discharge, and Q_{mean} – Observed mean discharge, r - linear correlation coefficient between Q_{obs} and Q_{sim}, α - $\alpha_{sim}/\alpha_{obs}$ (ratio of standard deviations), β - μ_{sim}/μ_{obs} (ratio of means).

NSE is a performance metric varying from $-\infty$ to 1, where values near 1 suggest high model reliability (Althoff & Rodrigues, 2021). The Percent Bias (PBIAS) evaluates whether a model systematically overestimates or underestimates observed values, with ideal results being near zero. The overall error is measured by the Root Mean Square Error (RMSE), where lower numbers indicate more accuracy. To provide a comprehensive measure of model performance, the Kling–Gupta Efficiency (KGE) combines correlation, bias, and variability (Bai & Liu, 2018). ***Table 1*** displays the generally used hydrological model performance metrics.

Table 1 - Classification of Model Performance Based on Statistical Evaluation Criteria (Lopez-Ballesteros et al., 2023)

Objective function	**Performance Rating**				
	Very Good	**Good**	**Satisfactory**	**Acceptable**	**Unsatisfactory**
NSE	$0.75 < NSE \leq 1.00$	$0.65 < NSE \leq 0.75$	$0.50 < NSE \leq 0.65$	$0.4 < NSE \leq 0.50$	$NSE \leq 0.4$
PBias	$PBIAS < \pm 10$	$\pm 10 \leq PBIAS < \pm 15$	$\pm 15 \leq PBIAS < \pm 25$		$PBIAS \geq \pm 25$
KGE	$KGE > 0.75$	$0.65 < KGE \leq 0.75$	$0.50 < KGE \leq 0.65$	$0.40 < KGE \leq 0.50$	$KGE \leq 0.40$
RMSE	Values below half the standard deviation are considered satisfactory				

Although the SWAT+ model is frequently used for hydrological simulations, it has a number of drawbacks that may impair its effectiveness, particularly when considering how climate change may affect streamflow and hydrological extremes. Underestimating daily peak discharges, being sensitive to the availability and quality of input data, reservoirs in the catchment, and having difficulties adequately capturing some hydrological processes, like snow dynamics and hydropeaking occurrences, are common problems (Rahman et al., 2022). The model's performance is also influenced by watershed characteristics, such as area, land cover, soil data, and streamflow

distribution, as well as the period and quality of climate data used for calibration and validation (Marin et al., 2020).

SWAT+ is often applied in data-scarce regions, but its performance is limited by the lack of high-quality observational data, which can lead to poor simulation accuracy and increased uncertainty in model outputs (Samimi et al., 2020). This data scarcity can lead to reduced simulation accuracy and increased uncertainty, with manual calibration efforts typically achieving only moderate performance (for example, NSE values of 0.47-0.64). Furthermore, SWAT+ may struggle to capture complex hydrological responses, particularly under changing climate conditions or for predicting extreme events (Rahman et al., 2022; Nyeko, 2015). Technical and structural limitations such as applying the SCS-CN method universally can reduce model accuracy, as it was originally designed for specific event-based scenarios and often captures high flows better than low flows in continuous simulations (Mulu et al., 2025). Its direct applicability to highly dynamic river systems is limited unless integrated with other approaches (Phetanan et al., 2024).

Recognising these inherent limitations in some process-based hydrological models, especially concerning their ability to capture hydrological extremes and complex non-linear climate-streamflow relationships, research has increasingly explored the robust predictive capabilities of data-driven models (Rajib et al., 2020). Advanced machine learning models like XGBoost are gaining popularity for streamflow simulations precisely because of their strength in handling complex, non-linear dynamics and their capacity to achieve high predictive accuracy where process-based models might face challenges, particularly for extreme events (Moges et al., 2024). Although process-based hydrological models offer deep insights into physical processes, data-driven and hybrid approaches have emerged as powerful alternatives, frequently demonstrating superior predictive performance, especially in complex or data-limited environments (Slater et al., 2023).

2.7.1 Rationale for a Hybrid Modeling Approach

Process-based models, specifically SWAT+, are invaluable for providing physically meaningful insights into the hydrological cycle such as separating surface runoff from groundwater

contributions and how these components respond to climate change. However, as noted, SWAT+ faces inherent challenges in data-scarce regions and often struggles to accurately capture the full magnitude of hydrological extremes (Rahman et al., 2022). Conversely, data-driven models like XGBoost excel at capturing the complex, non-linear relationships between climatic drivers and observed streamflow, frequently offering superior predictive accuracy for high and low flows, even without explicit physical knowledge (Moges et al., 2024). Therefore, this study adopts a hybrid modeling approach by utilising the process-based SWAT+ for detailed physical assessment and the data-driven XGBoost for robust prediction and benchmarking of high and low flow extremes under the SSP2-4.5 and SSP5-8.5 scenarios. This dual approach provides a powerful cross-validation of results, mitigating the limitations of relying on a single model type and ensuring a comprehensive assessment of streamflow impacts in the South Phuthiatsana catchment.

2.8 Conceptual Framework and Chapter Summary

The literature reviewed encompassing climate drivers, hydrological impacts, and model limitations forms the necessary foundation for the study's design. The need to overcome the limitations of single-model assessments, particularly in predicting hydrological extremes, necessitates the adoption of a hybrid modeling approach. This approach ensures both processes understanding through SWAT+ and predictive robustness through XGBoost.

This framework, conceptually outlined in **Figure *1***, demonstrates how this hybrid strategy addresses the research objectives. The foundation of this assessment relies entirely on the quality of the observed data; consequently, the process begins by utilising Historical Climate Data and Streamflow to ensure both the process-based and data-driven models are accurately initialised and rigorously evaluated. This initial step of Model Performance and Comparative Assessment is essential to confirming that both modeling approaches are robust and reliable for the South Phuthiatsana catchment. Upon validation against the literature's performance standards, these established models can then be reliably applied to the Downscaled Future Climate Data (SSP Scenarios) based on the best performing model to confidently project the impacts on South Phuthiatsana streamflow and extremes. This dual-model synthesis represents the most comprehensive way to assess future water security in the region.

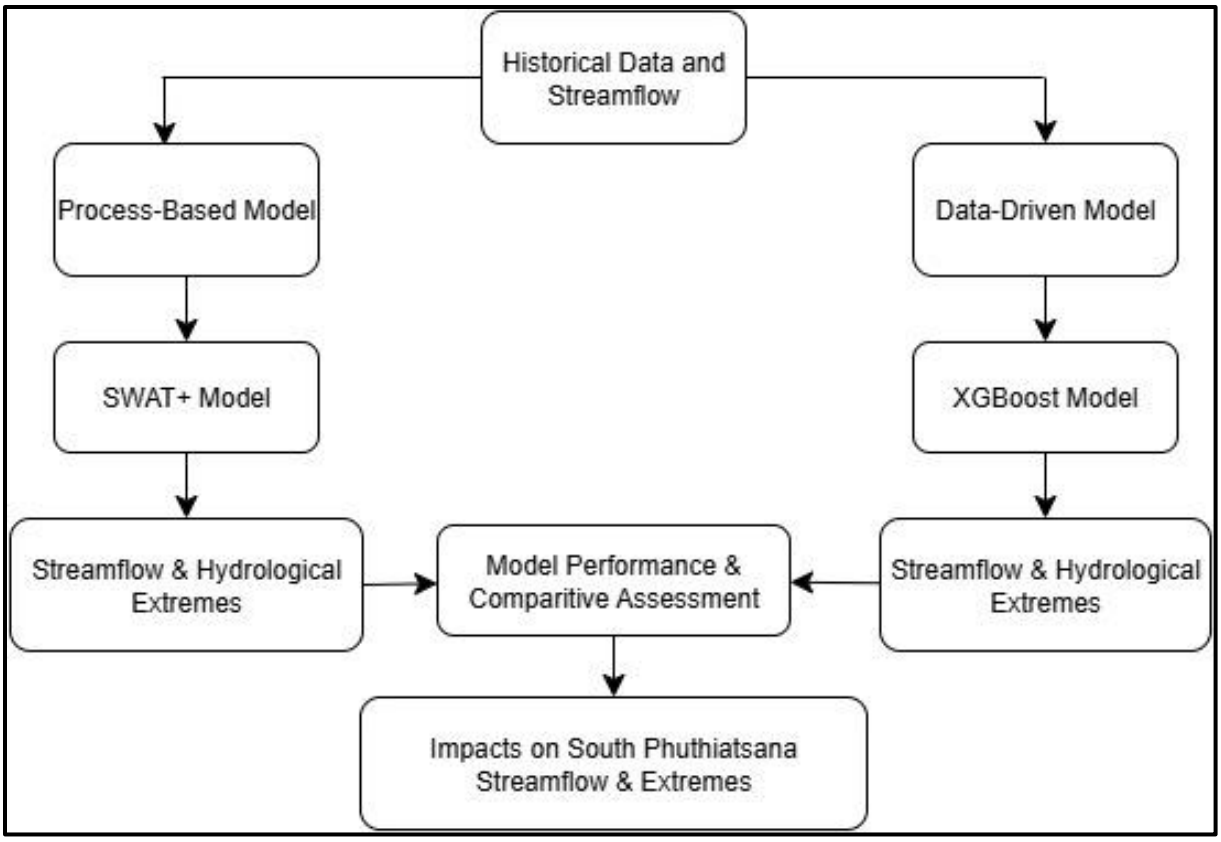

Figure 1 - Conceptual Framework of the Hybrid Modelling Approach

3 Methodology

3.1 Introduction

This chapter presents the methodology used to investigate the impacts of climate change on streamflow and hydrological extremes in the South Phuthiatsana catchment. It outlines the data sources, modeling approaches, and analytical procedures employed to achieve the study objectives. The chapter also details the framework for integrating climate projections with hydrological modeling to assess future changes in streamflow dynamics.

3.2 Study Area Description

Lesotho, a landlocked country entirely encircled by South Africa, is especially vulnerable to the effects of climate change due to its rugged terrain and the ongoing economic challenges faced by its rural communities. Positioned in the southeastern part of Southern Africa, the country lies approximately between 28°S–31°S latitude and 27°E–30°E longitude. It spans a total area of about 30,355 km², extending roughly 230 km from north to south and up to 210 km in width. Elevation varies significantly from 1,388 m in the lowlands to 3,482 m in the highlands. Lesotho's landscape is classified into four major regions, each with distinct climatic and ecological traits: the Lowlands (17%), Foothills (15%), Mountains (59%), and the Senqu River Valley (9%) (LMS, 2017).

The climate of Lesotho is continental temperate, characterised by four distinct seasons: spring, summer, autumn, and winter (LMS, 2021). According to LMS (2021), the country receives most of its rainfall between October and April, with an annual average of 700 mm. The Lesotho Land Cover Statistics tool (2023) indicates that the South Phuthiatsana catchment (CC23) experiences an average yearly precipitation of 690.7 mm and an average yearly evapotranspiration of 402.3 mm. Grassland, cropland, and trees are the 2 dominant land cover classes in the catchment, with 46.9%, 34.4%, and 9.9% of land cover distribution, respectively (FAO, 2023). Other land uses share the remainder of the land distribution, and these include built-up areas, water bodies, wetlands, shrubland, bare surfaces, irrigated cropland, and gullies. Irrigated cropland area is zero in the catchment.

The South Phuthiatsana catchment, as delineated for this study; draining to the Masianokeng gauging station, extends between latitudes 29°12'50" and 29°37'50" and longitudes 27°25'5" and 28°2'5", with elevations between 1560 and 3010 meters above sea level. South Phuthiatsana's area is approximately 651.7 km². A tributary of the Caledon River (Mohokare). Below is the South Phuthiatsana catchment as displayed by **Figure 2** with stream networks delineated using the digital elevation model (DEM), utilising the hydrology toolbox in QGIS, catchment outlet (gauging station), and climate stations in the catchment. The South Phuthiatsana River is perennial and it begins in the highlands of the Berea district (Middle Caledon/Mohokare) in Pulane and flows through some parts of the Maseru district, a significant portion of its course traverses' plains and foothills. It joins the Mohokare/Caledon River at 1486 meters above sea level (m.a.s.l.) with the mean annual runoff (MAR) of 128.47 m^3/year (Fobo, 2009). The Mohokare/Caledon River, a tributary of the Orange-Senqu River Basin (Botswana, Lesotho, Namibia, and South Africa), forms the border between Lesotho and South Africa.

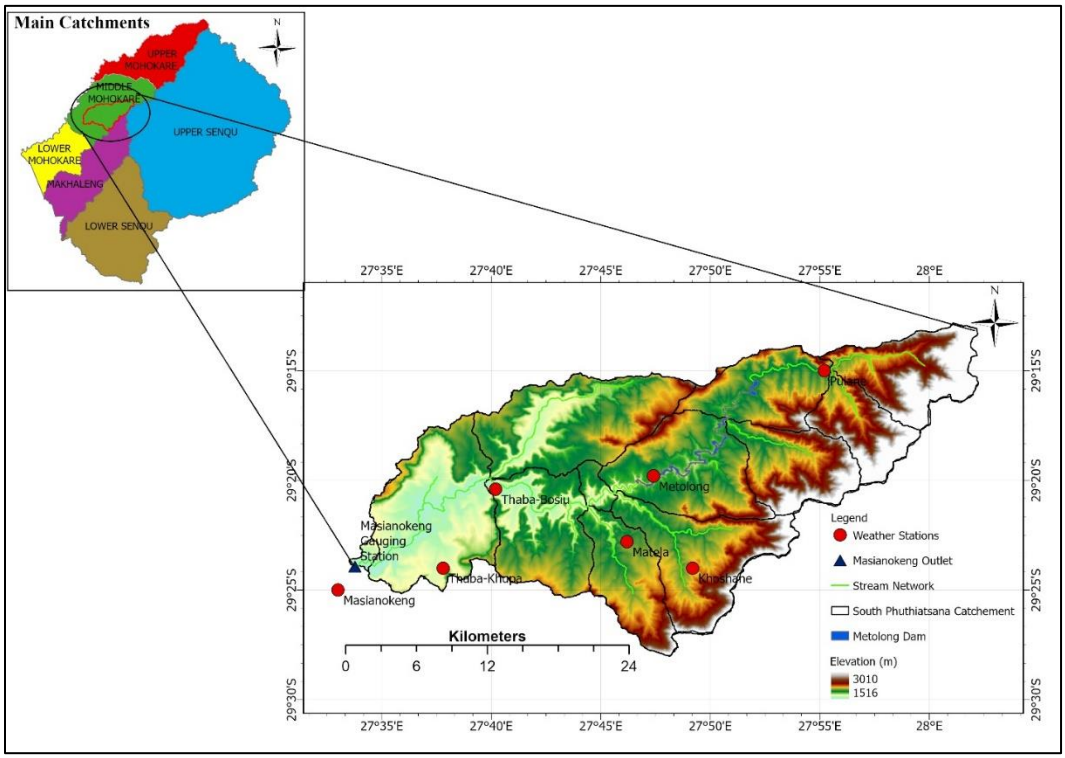

Figure 2 - Study Area Map showing stream network and the elevation

3.3 Methodological Framework

This research integrates hydrological modeling with climate change projections to evaluate their effects on streamflow and hydrological extremes in the South Phuthiatsana catchment. The process comprises several essential components. Initially, future climate scenarios for the period 2041 to 2080 are generated utilising various GCMs, emission scenarios SSPs, and bias correction methodologies. These climate scenarios provide essential input data for the hydrological model utilised in the study for future streamflow simulation.

Calibration and validation of the SWAT+ hydrological model were conducted using observed streamflow data. However, limitations were identified in its ability to simulate streamflow behavior and extreme hydrological events accurately within the South Phuthiatsana catchment. This was primarily due to the model's difficulty in capturing highly variable daily flow patterns and its sensitivity to input data resolution and quality, which affected its ability to reproduce extreme high and low flows. Because of this, and the general complexity of using physically based models for future climate projections, SWAT+ was applied only for analysing past streamflow patterns and naturalisation. t was not used for future simulations due to its limited performance in capturing daily flow variability and extremes under projected climate conditions. To address these challenges and better predict future conditions, the XGBoost machine learning model was adopted as the main tool for streamflow simulation and assessing climate change impacts. The XGBoost was used to analyse projected variations in streamflow and hydrological extremes under different climate scenarios. **Figure *3*** outlines the methodological process, highlighting the sequence of steps followed to achieve the study's objectives. The framework also guided the investigation of how climate variables influence runoff and extreme flow behavior in the catchment.

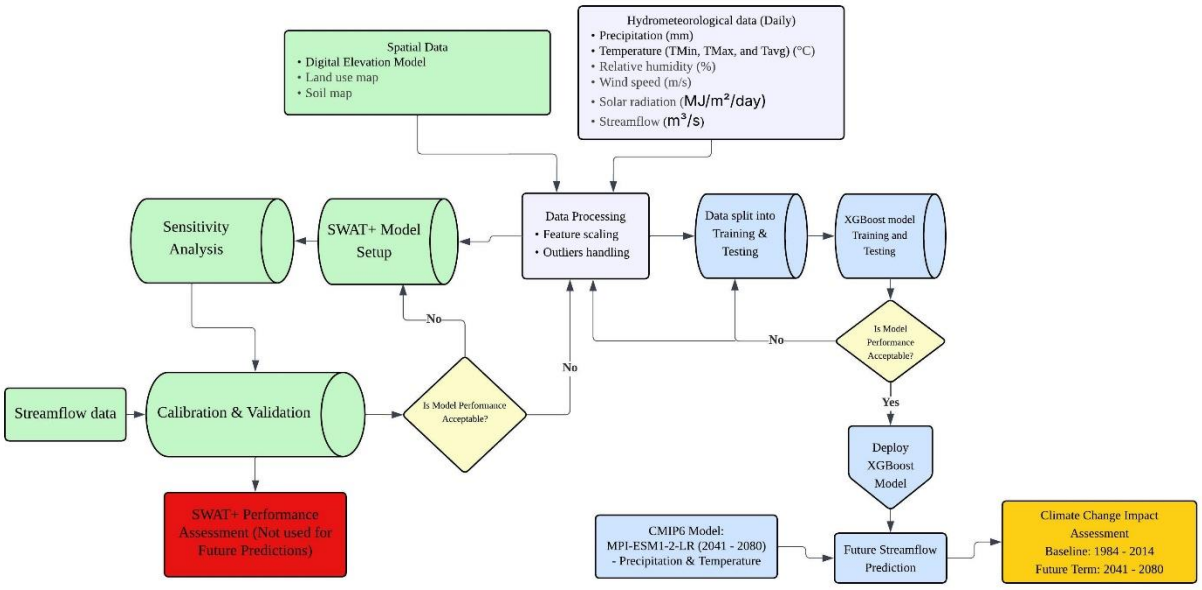

Figure 3 – Schematic representation of the integrated analytical framework employed in the study, detailing the sequential deployment and specialised functions of the SWAT+ and XGBoost models

3.4 Data Requirements

3.4.1 GIS Data

The hydrological modeling process incorporated three main datasets into the QGIS environment: topography (through the Digital Elevation Model), land use, and soil characteristics, along with meteorological variables such as precipitation, maximum and minimum temperatures, solar radiation, wind speed, and relative humidity. These inputs are essential for simulating watershed dynamics accurately. The DEM, a key element for capturing terrain features like slope and elevation, was obtained from the Shuttle Radar Topography Mission (SRTM) dataset through the USGS Earth Explorer. To enhance the accuracy of surface flow representation, the 30-meter resolution DEM was subjected to sink-filling procedures prior to analysis (Uuemmaa et al., 2020). The SRTM collects elevation data using space-based interferometric radar, operating in both C-band and X-band frequencies (Muhammed et al., 2023). From the processed DEM, essential terrain features such as slope gradients and stream network patterns were derived for the catchment.

The soil map (250 m), which comprises key soil properties for the South Phuthiatsana catchment, was obtained from the WateriTech portal (WateriTech, 2023). The Lesotho Soil Information System (LESIS) contains updated data on Lesotho soils; however, the soil attributes necessary for SWAT+ are missing from this database, necessitating the utilisation of the Food and Agriculture Organisation Digital Soil Map of the World (DSMW). The DSMW repository had only 2 soil types for the South Phuthiatsana watershed. The classifications are Eutric Planosols (We-FAO 74) and Lithosols (I-FAO) (Cruz-Gaistardo et al., 2016). Planosols are soils distinguished by a light-hued, coarse-textured surface layer that abruptly overlays a dense, slowly permeable subsurface containing considerably more clay than the surface layer. This sudden alteration in texture results in hindered downward water percolation, inducing temporary decreasing circumstances characterised by a stagnic colour pattern, particularly around the abrupt textural transition. Lithosols are soils constrained in depth by solid, cohesive rock located within 10 cm of the surface (Dondeyne et al., 2014) as shown in **Figure 4**. The land use/land cover map, as one of the required datasets was obtained from the (FAO, 2023) in raster format as required by SWAT+. **Table 2** below displays all the data types used in this investigation.

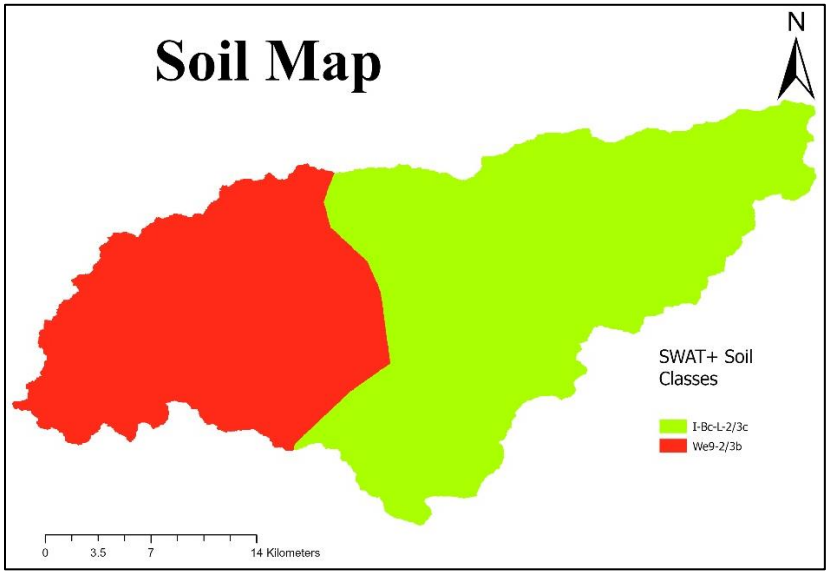

Figure 4 - South Phuthiatsana catchment soil map (WateriTech, 2023)

Table 2 - Comprehensive details of various data types utilised in this investigation

Data	Resolution	Description	Source
DEM	30 m	Elevation	(USGS, 2000)
Land use land cover	10 m	Land use classes	(FAO, 2023)
Soil map	250 m	Soil properties (chemical and physical)	(WateriTech, 2023)
Meteorological data	Daily	Precipitation, Temperature, Relative humidity, Solar radiation, wind speed	LMS and (CDS, 2021) EarthData-Giovanni
Hydrological data	Daily	River discharge	DWA

3.4.2 Observed Hydrometeorological Data

Meteorological data specifically, daily records of precipitation and minimum/maximum temperatures spanning January 1, 1984, to December 31, 2014 were obtained from the Lesotho Meteorological Services (LMS), with station metadata provided in **Table 3**. In the absence of in-situ records for solar radiation, wind speed, and relative humidity, supplementary climate variables were sourced from NASA's EarthData-Giovanni platform (NASA/GSFC/HSL, 2018), which offers satellite-derived datasets with relatively high spatial and temporal resolution. Additional meteorological inputs were acquired from the Climate Data Store (CDS) to complete the required parameters for hydrological modeling. Observed daily streamflow data, essential for model calibration and validation, were procured from the Department of Water Affairs (DWA) under the Ministry of Natural Resources. These records, obtained at the Masianokeng gauging station, spanned from 1972 to 2014 and were nearly complete, with only a single missing entry on December 31, 2014. The continuity and quality of this streamflow dataset rendered it highly suitable for robust hydrological model performance assessment.

Table 3 - Description of the Climate Stations in the South Phuthiatsana Catchment

ID	Latitude (°S)	Longitude (°E)	Elevation (m)
Thaba-Bosiu	-29.34	27.67	1575
Pulane	-29.25	27.92	1820
Metolong	-29.33	27.79	1700
Thaba-Khupa	-29.4	27.63	1626
Matela	-29.38	27.77	1785
Khoshane	-29.4	27.82	1834
Masianokeng	-29.42	27.55	1512

3.5 Streamflow Naturalisation

Human activities like reservoir construction and operation, land-use changes, and water withdrawals frequently modify streamflow in a watershed. These alterations could potentially influence hydrological extremes (both high and low flows), potentially complicating the evaluation of climate change impacts. Therefore, it is critical to differentiate between anthropogenic and climatic-driven changes in order to properly evaluate how streamflow dynamics are affected by climate change. Streamflow naturalisation is a process used to estimate what the flow conditions would have been in the absence of human interventions, thereby providing a baseline for evaluating climate change effects (Terrier et al., 2021).

While various methods for streamflow naturalisation exist, including reconstitution, water balance, routing, extension, paired catchment, and regionalisation (or neighbourhood) (Terrier et al., 2021), this study leverages the simulation capabilities of SWAT+ model to derive naturalised flows. Instead of post-processing observed data using statistical methods like reconstitution, SWAT+ achieves naturalisation by configuring the model itself to represent the watershed under pre-disturbance or minimally impacted conditions.

This is accomplished during the model build-up and parameterisation phase by systematically excluding or modifying representations of major anthropogenic influences:

Representation of hydraulic structures (reservoirs or dams): Naturalised conditions are simulated by excluding reservoir objects from the SWAT+ project setup. In the current study, reservoirs are not defined in the project setup; hence, the decision tables that control reservoir operations are thus not used. Water abstraction for domestic water use and irrigation is also omitted from the model inputs for the naturalised simulation; these activities depend on the availability of data. Land use and management practices include the current land cover, agricultural practices, and potential natural vegetation in the catchment. The management schedules (.mgt files) are used to incorporate such activities in the model setup. Furthermore, management schedules for agricultural land uses include parameters like fertiliser application and crop rotations.

This simulation-based approach, commonly employed in studies using SWAT/SWAT+ for naturalisation and climate impact assessment (Yin et al., 2017; Zhang et al., 2016; De Girolamo et al., 2015), provides the necessary baseline flow series against which the results from other model scenarios (current conditions, future climate scenarios) can be compared to isolate the impact of climate change or specific human activities. The selection of input data for defining the “natural” state is guided by data availability, as generally suggested by frameworks like the one proposed by Terrier, et., (2021) in **Figure 5** below.

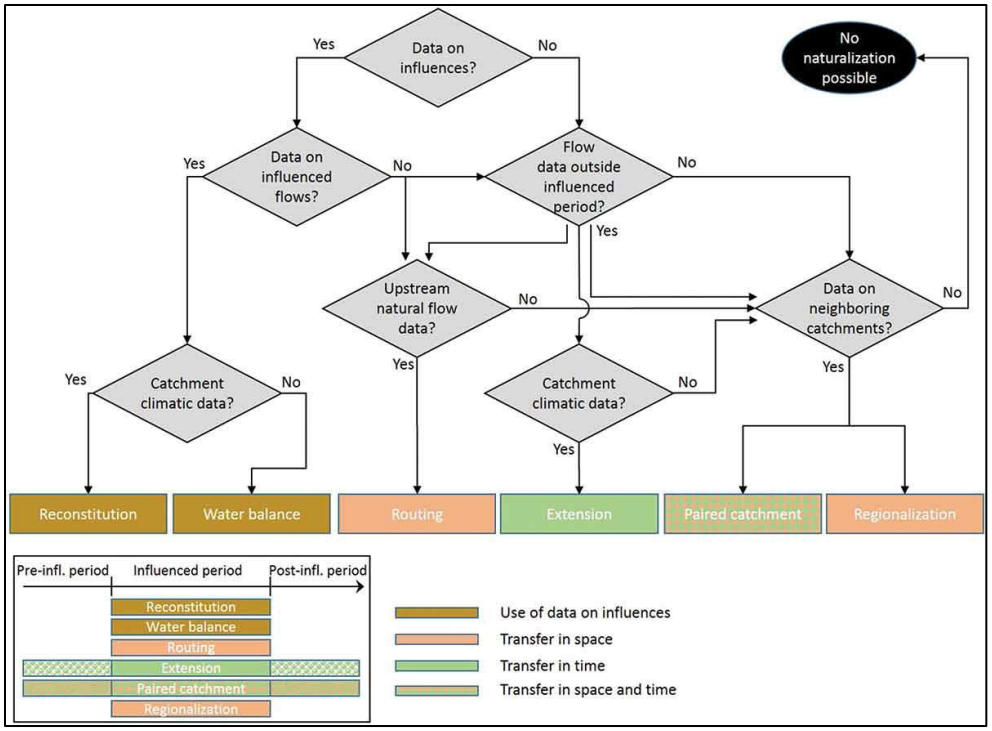

Figure 5 - Diagram of the choice of naturalisation according to the available data (Terrier et al., 2021)**.**

3.6 Remotely Sensed Hydrometeorological Data

CMIP6 (Coupled Model Intercomparison Project Phase 6) represents a large-scale collaboration among more than 110 climate modeling institutions worldwide. Supported by infrastructures like the Earth System Grid Federation, its goal is to enhance the understanding and simulation of climate systems (Cohen, 2021). For this research, air temperature and precipitation variables were retrieved from CMIP6 datasets available through the Climate Data Store (CDS, 2021). These global climate models were chosen due to their improved sensitivity and extended historical simulation span (1850–2015), which also overlaps with the period covered by the earlier CMIP5 models (1850–2005) (Tokarska et al., 2020).

This study adopts two future greenhouse gas emission scenarios; SSP2-4.5 and SSP5-8.5 to assess climate-induced hydrological changes in the South Phuthiatsana Catchment. SSP2-4.5 represents a “middle-of-the-road” pathway, assuming moderate mitigation efforts and socio-economic

development, while SSP5-8.5 reflects a fossil-fuelled development trajectory with high emissions and limited climate policy intervention (IPCC, 2021). These scenarios were selected to capture a broad range of plausible futures, from intermediate stabilisation to worst-case outcomes, thereby enabling a more comprehensive assessment of streamflow sensitivity under varying climate forcing conditions. Their use aligns with CMIP6 protocols and recent regional climate impact studies, which emphasise the importance of scenario diversity in hydrological modeling (Alexander et al., 2023; Goswami et al., 2025). Lower-emission scenarios such as SSP1-2.6 were excluded due to their limited representation of current global emission trends and reduced relevance for stress-testing water resource systems under high-impact conditions.

This study analyses two distinct 20-year future periods for climate projections: 2041–2060 (referred to as the near future or "2040s") and 2061–2080 (the mid-future or "2080s"), using the historical period from 1984 to 2014 as a baseline. The combined 40-year span from 2041 to 2080 was selected to balance scientific rigor with methodological efficiency. Although the IPCC Sixth Assessment Report (AR6) defines future climate intervals as near-term (2021–2040), mid-term (2041–2060), and long-term (2081–2100) (IPCC, 2023), this study specifically focuses on a continuous window that bridges near- and mid-century projections. This approach reduces dependence on longer-term estimates, which often carry greater uncertainty, while providing a more cohesive view of climate trends across upcoming decades.

3.6.1 GCM Models (CMIP5 & CMIP6 Datasets)

In climate change impact research, careful selection of meteorological input for impact models is crucial and involves criteria such as past performance, climate change signal spread, and model independence. There are several methods used in the selection process of GCMs, such as bias correction, Taylor diagrams, multi-criteria decision-making techniques, and clustering either by applying the principal component analysis (PCA) or K-Means (Song et al., 2019; Mendlik & Gobiet, 2016) as they aim to identify the most suitable models for local climates. Nevertheless, model performance can differ depending on the time of year and the location, so careful selection is required for particular applications.

However, this study selected eight most appropriate models based on literature, available computer resources, and the GCMeval tool, which is an interactive tool for selection and evaluation of global climate models (Parding et al., 2020). Furthermore, principal component analysis was used to convert the original variables into a set of diagonal components that capture the majority of the variance with the aim to manage the high dimensionality and multicollinearity present in climate model datasets (Ma et al., 2024). This step facilitates the identification of dominant patterns and reduces noise in the data.

Subsequently, Recursive Feature Elimination (RFE) was employed to iteratively rank feature importance by training models while progressively removing the least significant features, optimising the trade-off between model complexity and accuracy. The RFE results are summarised in **Figure 6**.

To further assess the contributions of the selected climate models to streamflow predictions, Shapley Additive exPlanations (SHAP) analysis was performed. SHAP quantifies the marginal contribution of each climate model to the simulation output, providing a robust measure of influence. **Figure *7*** shows the SHAP values for the chosen GCMs, illustrating both the magnitude and direction of their impact on model predictions. Higher SHAP values indicate stronger influence, while the colour gradient reflects relative feature values. Together, PCA, RFE, and SHAP analyses form a comprehensive methodology framework for feature selection and interpretation in streamflow modeling under climate change scenarios.

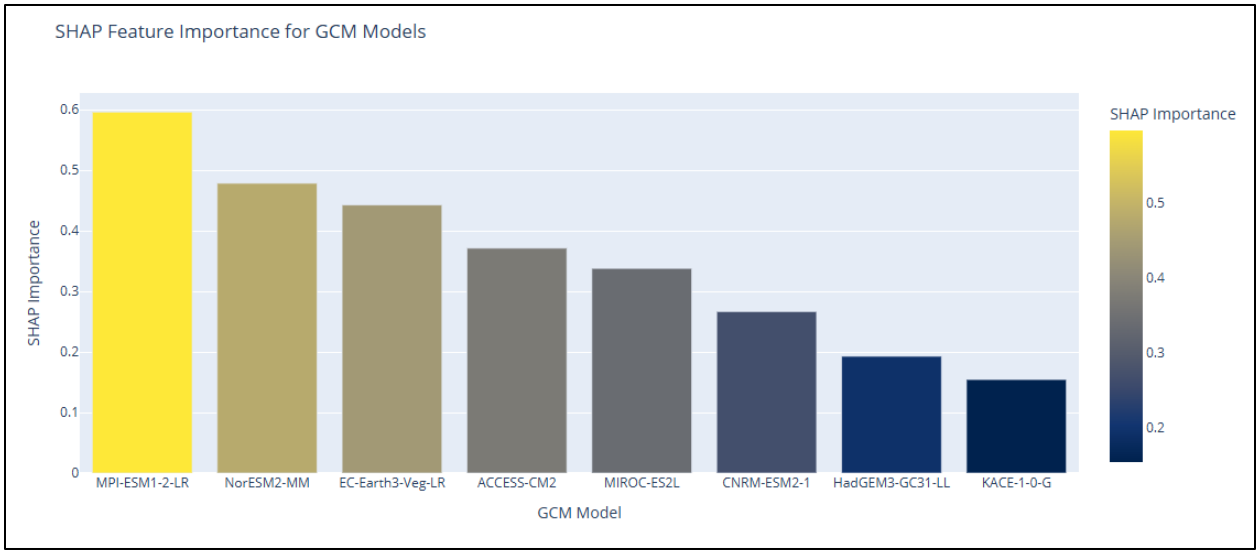

Figure 6 - RFE ranked GCMs based on their predictive contribution

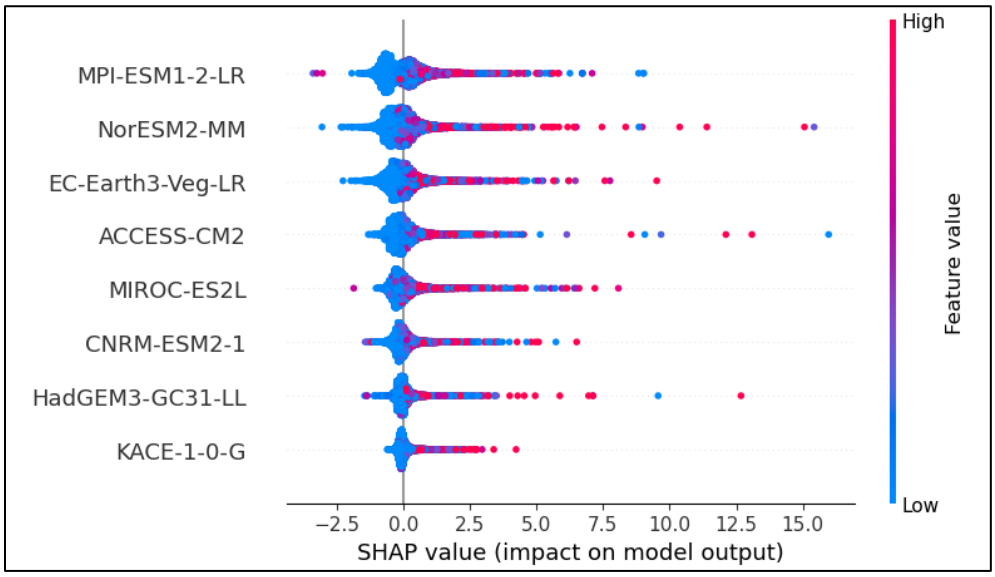

Figure 7 - SHAP Analysis for Model Interpretability in GCM-Influenced Climate Patterns

Historical and projected climate datasets were sourced from the MPI-ESM1-2-LR global climate model, aligned with the CMIP6 framework and two Shared Socioeconomic Pathway scenarios: SSP2-4.5 and SSP5-8.5 (Max Planck Institute for Meteorology, 2021). The MPI Earth System Model version 1.2 (low resolution) offers detailed daily inputs on precipitation and maximum and

minimum temperature for the South Phuthiatsana catchment, employing the r1i1p1f1 ensemble member configuration. With an approximate spatial resolution of 1.9° × 1.9°, its structural design and simulation capabilities are presented in **Table 4** (Gutjahr et al., 2019). This particular GCM was selected due to its data availability for both historical and future scenarios, as well as its spatial resolution.

Table 4 - CMIP6 GCMs considered for the South Phuthiatsana catchment, with the selected model (MPI-ESM1-2-LR) marked (*)

Institute	**Country**	**Resolution (Lat/Lon)**	**Description**	**Agency**
MPI-ESM1-2-LR*	'Germany	1.87° × 1.87°	Max Planck Institute for Meteorology-Earth System Model version 1.2 Low Resolution	Max Planck Institute for Meteorology
MIROC-ES2L	Japan	2.81° × 2.81°	Model for Interdisciplinary Research on Climate - Earth System Model version 2 for Long-term simulations	Japan Agency for Marine Earth - Science and Technology, Atmosphere and Ocean Research Institute (The University of Tokyo), and National Institute for Environmental Studies
KACE-1-0-G	South Korea	1.25° × 1.25°	Korea Advanced Institute of Science and Technology (KAIST) Climate Model version 1.0	Korea Institute of Atmospheric Prediction Systems (KIAPS), National Institute of Meteorological Sciences (NIMS), Korea Meteorological Administration (KMA)
EC-Earth3-Veg-LR	Europe	0.70° × 0.70°	EC-Earth Earth System Model Version 3 with Dynamic Vegetation Component	EC-Earth Consortium
CNMR-ESM2-1	France	1.4° × 1.4°	Centre National de Recherches Météorologiques Coupled Global Climate Model, version 5	Centre National de Recherches Meteorologiques/Centre European de Recherche et Formation Avancees en Calcul Scientifique
HadGEM3-GC31-LL	UK	1.875° × 1.25°	Hadley Centre Global Environment Model version 3 - Global Coupled 3.1 Low-resolution	Met Office Hadley Centre (MOHC)
NorESM2-MM	Norway	1.9° × 2.5°	Norwegian Earth System Model version 2 - Medium Resolution	Norwegian Climate Centre (NCC)'

3.6.2 Bias Correction

Even though the models have been improved over time, bias remains in them, which is concerning for climate research (Maraun, 2016). To enhance the accuracy of the modelled hydrological components, bias correction techniques were applied to the GCM using the CMhyd model to bias correct the GCM at catchment scale. 'The Climate Model data for hydrological modeling tool (CMhyd) model has been globally applied for bias correction and statistical downscaling of general climate models using observed climate variables, which has several statistical downscaling techniques for temperature and precipitation (Mukheef et al., 2024)'. Quantile mapping is particularly recommended for hydroclimatic modeling (Tootoonchi et al., 2023). Therefore, the distribution mapping (quantile mapping) method was employed for temperatures (minimum and maximum), and the linear scaling (multiplicative) method for precipitation, under the SSP2-4.5 and SSP5-8.5 scenarios. Downscaling was applied to GCM outputs for both the baseline period (1984–2014) and the future period (2041–2080). This process involved merging daily temperature and precipitation projections from the GCM with corresponding daily historical data (1984–2014) from the same model to perform bias correction. Furthermore, bias correction is usually performed as the spatial resolution of the GCMs is too coarse to be used directly (Saade et al., 2021).

QM methods use statistical changes for final adjustments of climate modeling results. These statistical changes involve adjusting the distribution patterns of the modeled variables to match the observed ones using a mathematical formula, which can be mathematically written as shown in **Equation 5** (Enayati et al., 2021):

$$X^0 = f(x^m) \qquad \textbf{\textit{Equation 5}}$$

Where x^0 = observed variable, x^m = modeled variable, and f^0 = transformation function.

3.7 Hydrological Modeling Approaches

This study employs a strategic hybrid modeling approach utilising both the process-oriented SWAT+ model and the data-centric Extreme Gradient Boosting (XGBoost) machine learning model. This integration is designed to leverage the distinct strengths of each model while mitigating their respective limitations, ensuring a robust and comprehensive assessment of climate change impacts.

3.7.1 SWAT+ Model Setup and Application

The Soil and Water Assessment Tool (SWAT), originally developed by the Agricultural Research Service of the USDA (Arnold et al., 2012), is a semi-distributed, process-oriented hydrological model tailored for continuous, long-term simulations at the watershed scale. It functions on a daily timestep and can be deployed through geospatial platforms such as ArcGIS and QGIS, where it incorporates essential spatial inputs including land cover classification, soil properties, topographic elevation (DEM), and climatic parameters (Sane et al., 2020). In this study, the advanced SWAT+ version was applied within the QGIS framework through the QSWAT+ interface to replicate catchment-scale hydrological behavior in the South Phuthiatsana basin (Arnold et al., 2012). SWAT+ extends the original model's architecture by enabling enhanced spatial modularity and more flexible representation of land-use practices, hydrological pathways, and channel flow networks (Bieger et al., 2016). It is widely applied for assessing land use and climate change impacts on hydrology, water quality, and non-point source pollution at scales ranging from small watersheds to large river basins (Jain & Singh, 2017).

Water balance is the fundamental concept of SWAT+ hydrologic modeling. SWAT+ estimates surface runoff using the SCS-CN technique, which considers antecedent moisture conditions, soil, and regional land use. The model uses the Hargreaves, Priestley-Taylor, and Penman-Monteith methods to determine how much water is lost by evaporation and transpiration (Nair et al., 2025). The SWAT+ also models how water moves in the watershed by taking into account precipitation, runoff, evapotranspiration, infiltration, and groundwater flow at a daily time step using the water balance approach shown in **Equation 6** (Pandi et al., 2023).

$$SW_t = SW_o + \sum_{i=1}^{t}\left(R_{day} - Q_{sur} - E_a - W_{seep} - Q_{qw}\right) \qquad \textbf{\textit{Equation 6}}$$

Where;

a) **SWt** represents soil water content at the end of the day (mm)
b) **SWo** is the soil water content at the beginning of the day (mm)
c) **Rday** denotes daily precipitation (mm)
d) **Qsur** refers to surface runoff generated on that day (mm)
e) **Ea** is the amount of evapotranspiration occurring daily (mm)
f) **Wseep** indicates the volume of water percolating from the soil profile into the vadose zone (mm)
g) **Qw** corresponds to the return flow or baseflow contribution for the day (mm)

The digital elevation model (DEM) was used to delineate the catchment and define hydrological features such as sub-basins, stream networks, terrain slope, and channel slope using QSWAT+ tool (Bieger et al., 2016). The maximum elevation according to the DEM is the 3010 meters above sea level and the minimum elevation 1515 meters above sea level. DEM was used to classify slope into three categories: 0 – 15%, 15 – 30%, and 30 – 999%, using QGIS, which is flat, medium and steep slope respectively as shown in **Figure 8** below. Land cover had 8 land cover types as shown in ***Table 5*** and ***Figure 12*** below. Bare surfaces and gullies were merged to form one land cover type due to their similar features. The land cover types were categorised and encoded into SWAT+ land cover codes as mandated.

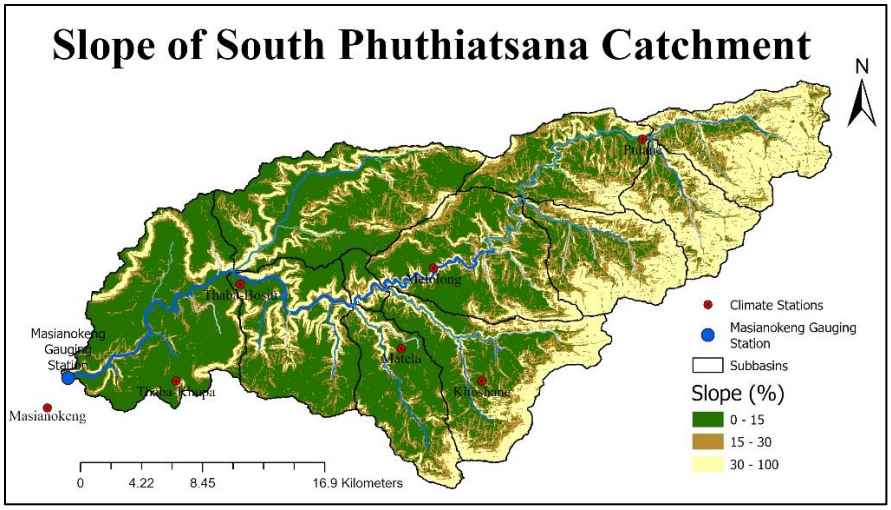

Figure 8 - Slope of South Phuthiatsana catchment showing the gauging station and climate stations

Table 5 - Land cover types and SWAT+ codes in the South Phuthiatsana catchment

Land Cover Type	SWAT Code	Area (ha)	Area (km^2)	Area (%)
Built-Up (Urban)	URBN	469.74	4.70	0.72
Cropland (Agriculture)	AGRL	23506.64	235.07	36.07
Trees (Forest)	FRST	6093.96	60.94	9.35
Water Body	WATR	386.04	3.86	0.59
Wetland	WETL	418.91	4.19	0.64
Shrubland	SRHB	2351.07	23.51	3.61
Grassland (Rangeland)	RNGE	30137.34	301.37	46.24
Bare Surfaces	BARR	1807.41	18.07	2.77

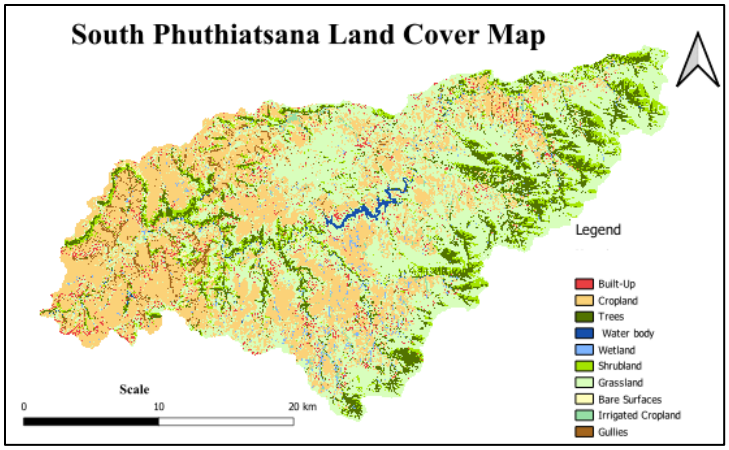

Figure 9 - Land use/Land cover map of South Phuthiatsana catchment (FAO, 2023)

SWAT+ subdivides the catchment into sub-catchments called subbasins, which are subsequently further subdivided into Hydrological Response Units (HRUs) according to distinct land use, soil, and slope characteristics. The HRUs were delineated using default threshold values recommended in the SWAT+ framework: 10% for land use, 20% for soil classes, and 20% for slope classes, to simplify the landscape representation and manage model complexity (Tetra Tech, 2015). Generally, there were 23 subbasins and 1244 HRUs.

The last phase of model configuration entails adjusting the QGIS-generated datasets in the SWAT+ Editor. A weather generator module creates synthetic weather input datasets based on the statistical parameters specified in the SWAT+ weather generator database. Long-term climate data (1984–2014) was input into the SWAT+ Editor to facilitate model execution before the calibration and validation stages. The data encompass precipitation, minimum and maximum temperatures, wind velocity, relative humidity, and solar radiation. SWAT+ Editor functions as an intuitive desktop interface that streamlines the arrangement and modification of all necessary input files. It functions as a standalone application devoid of GIS, facilitating seamless collaboration across QSWAT+ users. A 10-year warm-up phase was established prior to the simulation, alongside factors such as water routing as a variable storage mechanism and the curve number, which depends on soil moisture. The model was executed utilising SWAT+ version 61.0.1 (SWAT+ Editor 3.0.8) executable. The SWAT+ Editor offers two calibration methods: soft calibration, which emphasises mass balance, and hard calibration, which aims to align simulated and real hydrographs as nearly

as feasible. In the present investigation, the results from the successful model run were preserved and then analysed in the SWAT+ Toolbox due to its superior calibration and validation capabilities relative to the SWAT+ Editor.

3.7.1.1 Evaluation of SWAT+ Performance through Calibration and Sensitivity Analysis

The SWAT+ Toolbox, a free tool intended for uncertainty and calibration analysis, along with model verification, was employed to perform sensitivity analysis, calibration, and validation of the SWAT+ model. The comparison of empirical and simulated data facilitates the optimisation of model performance, consequently finalising the calibration process. Calibration is the procedure of determining the ideal set of model parameters that produces outputs closely aligned with the empirical data. Daily streamflow data from 1984 to 2014 at the Masianokeng gauging station (Outlet) was used to evaluate model performance, perform parameter sensitivity analysis, and conduct calibration and validation.

A statistical split optimisation technique was used to guarantee an objective separation of the dataset into calibration and validation periods. This was achieved by applying Welch's T-test to evaluate several potential split dates as applied in (Zheng et al., 2012) and the F-test as well as the Kolmogorov-Smirnov test to evaluate variations in distributions, variances, and means, respectively (Kini et al., 2024). The date on which the calibration and validation subsets showed the highest statistical similarity was determined to be the optimal split point, which was July 1997. Therefore, the calibration period spanned from 01/01/1984 to 31/12/2006, and the validation period was from 01/01/2007 to 31/12/2014.

3.7.1.2 Parameter Sensitivity Analysis

The initial five years of the dataset were allocated as a warming-up period. A global sensitivity analysis was subsequently performed utilising the Sobol approach, as executed in the SWAT+ Toolbox (v3.0.4). This method was configured with a fixed random seed value of 200 to ensure reproducibility, and 1500 parameter samples were generated to comprehensively explore the parameter space.

Table 6 outlines the parameters chosen for the sensitivity analysis, detailing their types of change (percentage, relative, and replace), the applied ranges (minimum and maximum), and the default values. These parameters were chosen based on their frequent use in streamflow calibration studies and their relevance within the SWAT+ framework. The sensitivity analysis aimed to identify the most influential parameters that improve model performance relative to observed data (Nair et al., 2025), thereby demonstrating the SWAT+ Toolbox's capacity to modify a range of SWAT+ parameter types.

Table 6 - List of SWAT+ sensitive parameters

Name	Description	Change Type	Min	Max
revap_co	Groundwater coefficient	Relative	0.02	0.2
revap_min	Threshold depth of water in the shallow aquifer	Replace	0	50
flo_min	Minimum aquifer storage	Relative	0	50
surlag	Surface runoff lag coefficient	Replace	0.05	24
cn2	Curve number	Percent	-20	40
canmx	Maximum canopy storage	Replace	1	10
slope	Average slope steepness in HRU	Relative	0.0001	0.9
alpha	Baseflow factor	Relative	0	1
esco	Evaporation soil compensation factor	Replace	0	1
ovn	Overland manning's roughness	Percent	-20	20
cn3_swf	Pothole evaporation coefficient	Percent	-30	30
epco	Plant uptake compensation factor	Replace	0	1
awc	Available water capacity of the soil layer	Relative	-0.5	0.5
latq_co	Lateral flow contribution to streamflow	Percent	0	0.05
k	Saturated hydraulic conductivity	Percent	-100	250

3.7.1.3 Performance Matrices

SWAT+ performance in streamflow simulation was assessed using the aforementioned objective functions. These functions evaluated the goodness-of-fit between simulated and observed discharge. The principal metrics comprised NSE, PBIAS, RMSE, MSE, and KGE. These metrics were selected to provide comprehensive quantitative indicators of model accuracy and reliability in representing streamflow dynamics.

SWAT+ was employed to understand historical processes and streamflow naturalisation, providing a process-driven representation of the catchment's hydrology. The model's performance during calibration and validation periods was assessed using established accuracy thresholds to evaluate its suitability for projecting future climate change impacts, particularly hydrological extremes. Based on this evaluation, SWAT+ outputs were used for historical performance assessment, sensitivity analysis, and improving understanding of catchment processes. However, the model was not utilised for simulating future streamflow changes under climate scenarios.

3.7.2 Rationale for the Dual-Model Approach

While SWAT+ is instrumental in establishing the physical water balance (**Equation 6**), defining the watershed response, and executing streamflow naturalisation, a preliminary evaluation confirmed the model's inherent challenges in the South Phuthiatsana catchment. Specifically, the model demonstrated difficulty capturing the highly variable daily flow dynamics and accurately reproducing the magnitude of hydrological extremes (high and low flows), a limitation often found in physically-based models in data-scarce regions.

To achieve a robust and predictively accurate assessment of future climate change impacts on extremes, a complementary approach was required. The XGBoost machine learning model was therefore strategically adopted to specifically address the predictive uncertainty of extremes and non-linear relationships. The SWAT+ model serves its essential purpose (physical process understanding and naturalisation), while XGBoost is employed as the main tool for simulating and predicting future streamflow and hydrological extremes under the SSP scenarios.

3.7.3 Extreme Gradient Boosting (XGBoost) Model Setup and Application

The (Extreme Gradient Boosting) model is an ensemble machine learning technique that utilises boosted decision trees, known for its superior performance and speed in capturing complex, non-linear relationships in hydrological time series. The model setup involves:

a) Feature selection: The same historical climate variables used to drive SWAT+ (daily precipitation, temperature, solar radiation, relative humidity, and wind speed) were used as input features for XGBoost.
b) Training and Testing: The observed historical streamflow timeseries (1984-2014) is split into a training period (01/01/1984 to 31/12/2006) and a testing period (01/01/2007 to 31/12/2014), mirroring the SWAT+ setup to ensure an objective and statistically comparable evaluation.
c) Hyperparameter Tuning: Optimal model configuration was achieved through cross-validation and tuning key hyperparameters (maximum depth, learning rate) to maximise predictive accuracy during the testing phase.

The validated XGBoost model is then used to predict streamflow under the downscaled SSP2-4.5 and SSP5-8.5 scenarios.

3.7.3.1 Model Description

A data-driven machine learning model was developed utilising the XGBoost technique to enhance the physically based SWAT+ model. XGBoost is a gradient boosting method employed in ensemble learning. The Extreme Gradient Boosting model employed in this study is a decision-tree-based ensemble learning technique crafted to effectively capture non-linear correlations in structured data. In contrast to artificial neural networks (ANNs), which are composed of interconnected layers of nodes (neurons) trained by back-propagation, XGBoost develops an additive ensemble of regression trees in a sequential manner. Every tree in the ensemble rectifies the residuals of its predecessors by minimising a regularised objective function through gradient descent.

While ANNs learn distributed representations through layered abstractions in deep architectures that are multilayer nonlinear transformations of input to progressively extract higher-level features, XGBoost partitions the feature space using decision rules at each node, resulting in a piecewise approximation of the target function. Additionally, this tree-based structure improves interpretability using measures such as feature significance, which are particularly useful in hydrological modeling. XGBoost is also computationally effective and resistant to overfitting, which makes it appropriate for streamflow forecasting, where it is crucial to capture temporal dependencies and variable interactions. The model's structure is governed by hyperparameters such as the maximum depth of trees (*max_depth*), learning rate (*eta*), and number of boosting iterations (*nrounds*), which jointly control its complexity and generalisation.

3.7.3.2 Data Preparation and Feature Engineering for XGBoost

The machine learning model XGBoost was trained using historical data on streamflow and key climate variables, namely precipitation and temperature. The data from the Masianokeng gauging station, which covered the years 1984–2014, matched the input parameters of the SWAT+ simulations, guaranteeing model consistency.

The XGBoost model was developed using historical streamflow records alongside key meteorological inputs such as precipitation and minimum and maximum temperature. These daily hydrometeorological datasets (1984–2014), including precipitation, temperature, and streamflow observed at the Masianokeng gauging station, were consistent with those employed in the SWAT+ model and served as the foundation for training the machine learning model.

This data was chronologically ordered, and feature engineering was performed to create lagged variables for both streamflow and precipitation, capturing essential temporal dependencies. Specific features included:

a) Current and lagged daily precipitation
b) Current and lagged daily maximum and minimum temperatures

c) Seasonality indicators
d) Lagged streamflow

The original chronological sequence was preserved when the data were divided into a training (70%) and a testing (30%) dataset. Before training, feature scaling, such as normalisation, was applied to the input variables to enhance model performance when relevant. Significantly, extreme hydrological values were preserved in the dataset, as they represent the central emphasis of the study's examination of hydrological extremes.

3.7.3.3 Model Training and Hyperparameter Tuning

Model training and tuning were implemented using the *xgboost* R package, ensuring reproducibility by setting a random seed. Hyperparameter tuning was conducted using grid search, with cross-validation applied to prevent overfitting. This process aimed to identify the optimal set of parameters that maximise predictive performance on unseen data. **Table 7** illustrates the optimal hyperparameters obtained for the XGBoost algorithm.

Table 7 - Hyperparameters for XGBoost model

Parameter	**Range**	**Optimal Model Values (Fitted Value)**	**Description**
'nrounds	100, 200, 300	100	Number of boosting iterations (trees)
max_depth	3, 5, 7	3	Maximum depth of a tree
eta	0.01, 0.1, 0.2	0.1	Learning rate (shrinkage)
gamma	0, 0.1	0.1	Minimum loss reduction required to make a further partition
colsample_bytree	0.7, 1.0	1	Subsample ratio of columns when constructing each tree
min_child_weight	1, 3	1	Minimum sum of instance weight (hessian) needed in a child
subsample	0.7, 1.0	0.7	Subsample ratio of the training instance'

3.7.3.4 Future Streamflow Prediction

After successful training and tuning, the XGBoost model was subjected to the bias corrected downscaled climate projections under SSP2-4.5 and SSP5-8.5 scenarios for future streamflow simulation. Recursive prediction was performed for future periods. This involved computing lagged precipitation features directly from the scenario data, while lagged streamflow features were dynamically updated using previous model predictions, ensuring temporal dependencies are maintained throughout the simulation process.

3.7.3.5 Model Validation and Performance Evaluation

The evaluation of the trained XGBoost model was conducted utilising metrics that are standard in hydrological modeling. These metrics include NSE, PBIAS, KGE, and RMSE.

3.8 Evaluation of Future Climate Effects on Streamflow Dynamics and Extreme Hydrological Events

The calibrated XGBoost model was used to predict streamflow based on two selected SSPs mentioned above in order to evaluate the effects of future climate conditions on streamflow and hydrological extremes. Different emission trajectories are represented by these pathways. While SSP5-8.5 predicts a high-emissions future driven by extensive fossil fuel usage and modest mitigation efforts, SSP2-4.5 represents a balanced development scenario with moderate climate policy concerns. By employing these contrasting scenarios, the analysis aimed to capture a range of potential hydrological outcomes under differing global development directions.

A methodology based on the selection and analysis of high and low flow events from daily simulated streamflow data covering the period 1984–2014 (baseline) and 2041–2080 (future period) was used in this study to assess the possible effects of climate change on the extreme flow trends within the South Phuthiatsana catchment, as it was used in (Chakilu et al., 2023). Changes in extreme flow regimes across time were characterised by analysing daily streamflow data generated by the XGBoost model, forced with climate projections under SSP2-4.5 and SSP5-8.5 scenarios.

Flow frequency analysis and flow duration curves were applied to assess extreme streamflow events (floods and droughts) under historical and projected climates (SSP2-4.5 and SSP5-8.5). The process included the extraction of extreme flow series, the fitting of suitable statistical distributions, and the calculation of return periods through the use of frequency curves. An analysis of flow quantiles was conducted to characterise the overall hydrologic flow regimes. Daily streamflow data for the historical period from 1984 to 2014, as well as projections for future scenarios SSP2-4.5 and SSP5-8.5 covering the period from 2041 to 2080, were utilised to conduct all associated analyses.

3.8.1 Quantification of Hydrological Extremes

The primary objective of assessing climate change impacts on streamflow extremes requires precise and standardised metrics. The assessment is therefore based on predefined streamflow quantiles derived from the daily simulated streamflow time series for both the historical baseline (1984–2014) and the future SSP periods (2041–2080).

a) High Flow Extremes (Q_{10}): High flow conditions, often indicative of flood risk, are defined as the flow rate exceeded only 10% of the time. This quantile is widely utilised for its relevance to peak flow and flood management assessments.
b) Low Flow Extremes (Q_{90}): Low flow conditions, critical for water resource management, environmental flows, and drought analysis, are defined as the flow rate exceeded 90% of the time.

The proportional changes in the magnitude of these quantiles between the historical and future periods, as predicted by the XGBoost model, will serve as the primary metric for quantifying the impact of the SSP2-4.5 and SSP5-8.5 scenarios.

3.8.2 Low Flow Selection and Analysis

Analysis of low flow frequency was done to determine the lengths and magnitudes of droughts. There were two main methods used: fitting a Log-Pearson Type III distribution and fitting a Weibull distribution to annual minimum 7-day average flows. 7-Day Annual Minima (7DAM) was

extracted for every particular dataset. The daily streamflow was calculated as a 7-day rolling average (moving average). Each year's minimum 7-day average flow was then determined to create the yearly minimum series. L-moments for each scenario were computed based on the 7DAM series. L-moments can be used to parameterise distributions in hydrological frequency analysis since they are reliable substitutes for conventional moments and are less susceptible to outliers. These moments were then fitted to the Weibull distribution (using type *wei* in *lmomco*) (Asquith, 2024). The return period for low flows indicates the average flow size that should be equal to or less than once every given return period such as 5, 10, 25, 50, 100, and 200 years. The inverse of the non-exceedance probabilities was used to obtain low flow return levels from the fitted Weibull distribution using **Equation 7** below:

The percentile of non-exceedance for each value was calculated using the Weibull formula:

$$P = \frac{1}{T} \qquad \textit{Equation 7}$$

where T is the return period.

Given the limitations of the Weibull distribution in handling near-zero flow values, the Log-Pearson Type III method was additionally utilised to assess low flow conditions, as it's a widely accepted approach for streamflow evaluation. A log transformation (base 10) was performed on the 7DAM series for every scenario. All flow values before transformation were subjected to a modest constant in order to handle possible zero or near-zero flow values that are challenging for logarithmic transformation. The inverse of non-exceedance probability and the estimated Pearson Type III distribution were used to compute low-flow return periods in the log-transformed space. After applying 10x and deducting the previously added constant, these log-transformed estimations were subsequently back-transformed to the original flow units. Estimates of any consequent negative streamflow were set to zero.

3.8.3 High Flow Selection and Analysis

High flow frequency analysis is centred on estimating flood magnitudes for different return periods. The Annual Maximum Series (AMS) was extracted from each dataset, including historical

data, SSP2-4.5, and SSP5-8.5. This procedure entails the identification of the maximum daily flow value for each year. The AMS for each scenario was fitted to a Generalised Extreme Value (GEV) distribution utilising the maximum likelihood estimation method, as executed in the *extRemes* R package. Following the fitting of the GEV distribution, return levels were computed for designated return periods of 5, 10, 25, 50, 100, and 200 years. Return levels indicate the flow magnitude anticipated to be matched or surpassed on average once within a designated number of years. Confidence intervals at a 95% level were estimated to assess the uncertainty associated with the predictions.

3.8.4 Flow Quantile Analysis

The daily streamflow data for each scenario were subjected to a quantile analysis to provide a comprehensive understanding of hydrologic flow regimes. Specific flow quantiles Q5, Q10, Q25, Q50, Q75, Q90, and Q95 were computed, representing the flow values below which a given percentage of observations fall. According to standard Flow Duration Curve categorisation, Q5 and Q10 represent high flows typically associated with flood conditions, Q50 represents median flow, and Q75 to Q99 represent low flows indicative of drought or baseflow conditions. In this study, the 5th percentile (Q5) of the historical daily streamflow data was identified as the flood threshold and graphically represented on the quantile plot. This analysis enhances understanding of how the distribution of flows may shift under different climate scenarios, including changes in extreme high and low flow conditions.

3.9 Trend Detection and Statistical Analysis

Climate change impacts studies frequently employ the Sen's slope estimator and the Mann-Kendall test (Han & Bocchiola, 2025; Aziz et al., 2024; Haghighi et al., 2019). Mann-Kendall is a non-parametric trend analysis technique mainly used for trend identification in hydro-climatological data series (Aziz et al., 2024). Moreover, Sen’s Slope Estimator was applied alongside Mann-Kendall test for a more complete analysis. Sen’s slope provides a quantitative estimate of trend magnitude.

Statistical analyses were conducted on the hydrological indices obtained from historical (baseline) and future periods, with separate evaluations for SSP2-4.5 and SSP5-8.5 scenarios. All statistical tests were performed at a 5% significance level. Analyses were carried out using Microsoft Excel and the R programming environment, implemented via RStudio (version 2024.12.1+563).

4 Results

4.1 Introduction

This chapter presents the assessment results of climate change impacts on streamflow in the South Phuthiatsana catchment, based on simulations from the MPI-ESM1-2-LR climate model. Due to suboptimal performance with the SWAT+ model, the study utilised XGBoost as the primary tool for predicting future streamflow under anticipated climatic changes. The following sections present the detailed results from these analyses.

4.2 Characterisation of Historical Climate Patterns

4.2.1 Historical Patterns of Precipitation

Precipitation within the catchment demonstrates notable inter-annual variability, characterised by significant fluctuations in total annual rainfall across the observed period (1984 to 2014). The annual precipitation totals range broadly, from approximately 600 mm to over 1100 mm, indicating a dynamic hydrological regime. Visually, the plot (**Figure 10**) highlights years of exceptionally high precipitation, such as around 1988-1989, and periods of notably lower rainfall, as seen around 1992.

A marginal decline in annual precipitation is noted over the long run. The non-parametric Mann-Kendall trend test was employed to properly evaluate this pattern in the annual rainfall totals. The analysis revealed a slight negative trend, with Sen's slope demonstrating an average decline of 4.53 mm annually. **Figure 10** clearly depicts a decreasing trend in precipitation. Nonetheless, this identified trend was not statistically significant (Mann-Kendall p-value = 0.292), indicating that

the observed decrease may reasonably be attributed to natural climatic fluctuation rather than a conclusive systematic or directional alteration within the examined timeframe.

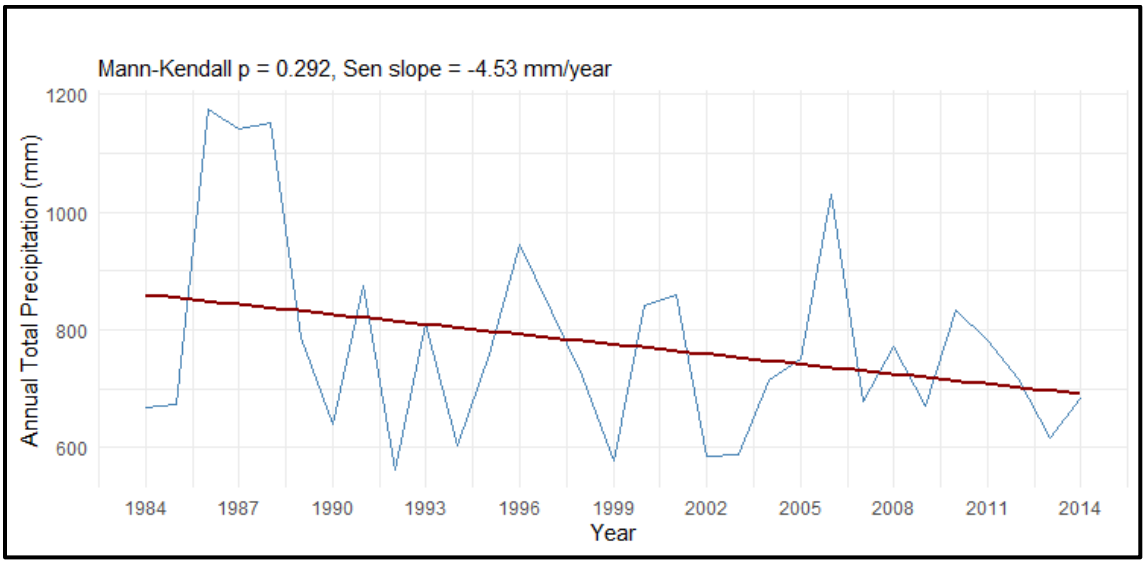

Figure 10 - Trend of annual historical precipitation from 1984 to 2014

The long-term monthly average precipitation for individual stations within the catchment, spanning the period 1984–2014, is presented in **Figure 29**. This figure comprises a series of bar plots, each illustrating the average monthly precipitation distribution for a specific rainfall station in the catchment.

Due to the observed low heterogeneity in the monthly precipitation differences among these individual stations, the interpretation primarily focuses on the general patterns that are consistent across most stations. While each station's plot provides granular detail, the overarching trends in seasonality are broadly similar, allowing for a consolidated discussion.

A distinct unimodal seasonal pattern of precipitation is observable throughout the basin. The wet season generally begins in October, with average monthly precipitation steadily rising through November and December. Precipitation often reaches its maximum in the summer months of January and February, with majority of stations recording their highest average monthly totals,

frequently exceeding 100 mm. Stations such as Khoshane, Masianokeng, and Matela frequently exhibit average monthly precipitation over 100 mm throughout these peak months.

4.2.2 Historical Patterns of Temperature

The annual maximum temperature (Tmax) in the South Phuthiatsana catchment demonstrates an upward trend during the examined historical period. **Figure 11 (a)** distinctly illustrates the underlying pattern, exhibiting a continuous increase from the beginning to the end of the data set. This ascending trend signifies a predominant warming pattern. The non-parametric Mann-Kendall trend test was employed to quantify the observed pattern in yearly maximum temperature. The analysis demonstrated a positive trend, with Sen's slope exhibiting an average annual increase of 0.035 °C. Yearly maximum temperature is estimated to have climbed by 0.035 degrees Celsius every year from 1984 to 2014. Moreover, the observed trend was confirmed to be statistically significant (Mann-Kendall p-value = 0.0381). The p-value, being below the conventional significance threshold of 0.05, suggests that the observed increase in annual maximum temperature cannot be assumed to be a purely random event and shows a significant systematic alteration throughout the historical period.

Similarly, the annual minimum temperature (Tmin) also demonstrates an increasing trend across the historical period. As illustrated in **Figure 11 (b),** the dashed green line representing the trend shows a consistent upward slope. The ‘Mann-Kendall’ statistical test for annual minimum temperature revealed a positive trend, with ‘Sen's slope’ indicating an average increase of 0.019 °C annually. This implies that the annual minimum temperature has, on average, risen by approximately 0.019 degrees Celsius each year from 1984 to 2014. This trend was also found to be statistically significant (Mann-Kendall p-value = 0.0249), being less than the 0.05 significance level. This statistical significance suggests that the observed increase in annual minimum temperature is unlikely due to chance and indicates a systematic change within the historical timeframe.

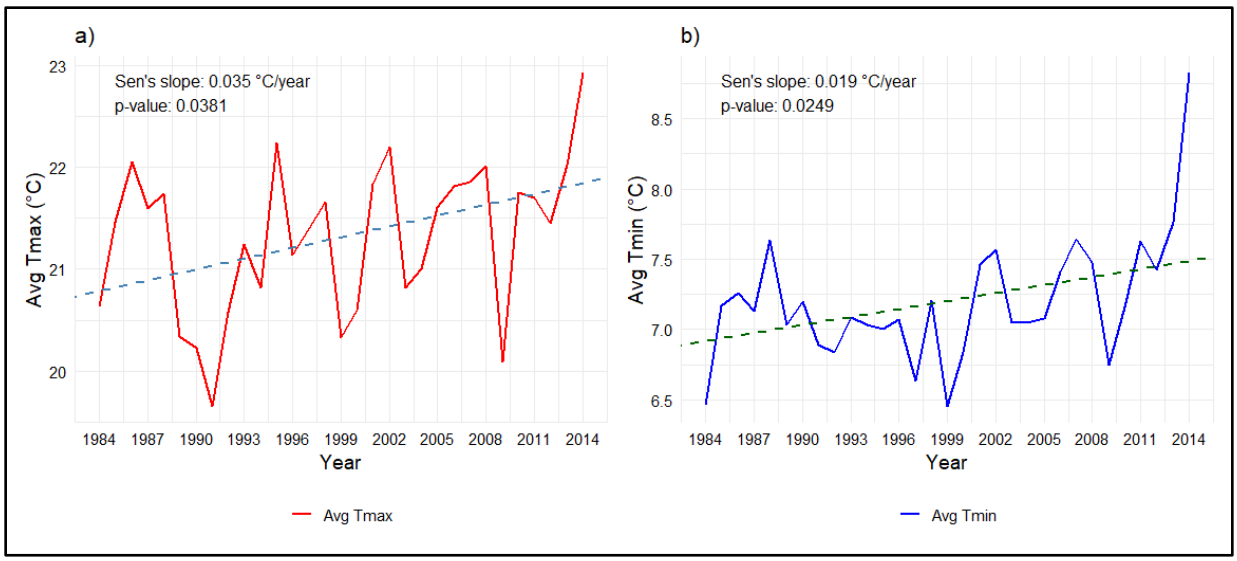

Figure 11 – (a) Annual Tmax and (b) Annual Tmin trend from 1984-2014, showing Sen's slope and Mann-Kendall p-value

4.3 Climate Projections: Changes in Precipitation and Temperature

4.3.1 Bias Correction

The MPI-ESM1-2-LR model demonstrated a varied performance in forecasting precipitation and temperature. Linear scaling effectively reduced precipitation biases, while quantile mapping efficiently corrected minimum and maximum temperatures, as illustrated in **Figure 12**.

Specifically, the raw model underestimated minimum temperatures during the winter months (May to August) and overestimated them for the rest of the year. Similarly, maximum temperatures were underestimated by the raw model throughout the entire period. The precision of the quantile mapping bias correction for minimum (Tmin) and maximum (Tmax) temperatures varied seasonally. Tmin correction showed larger errors, with notable underestimations during the winter months of May and July and a significant overestimation in the winter month of June, while exhibiting better performance in the spring and summer months. In contrast, Tmax correction had more pronounced underestimations during the late summer months to early autumn months (January to March) and overestimations during the late winter and early spring (June, August, and

September), with relatively moderate errors in the autumn (April) and late spring. Overall, the higher percentage errors observed for Tmin, particularly the substantial overestimation in June.

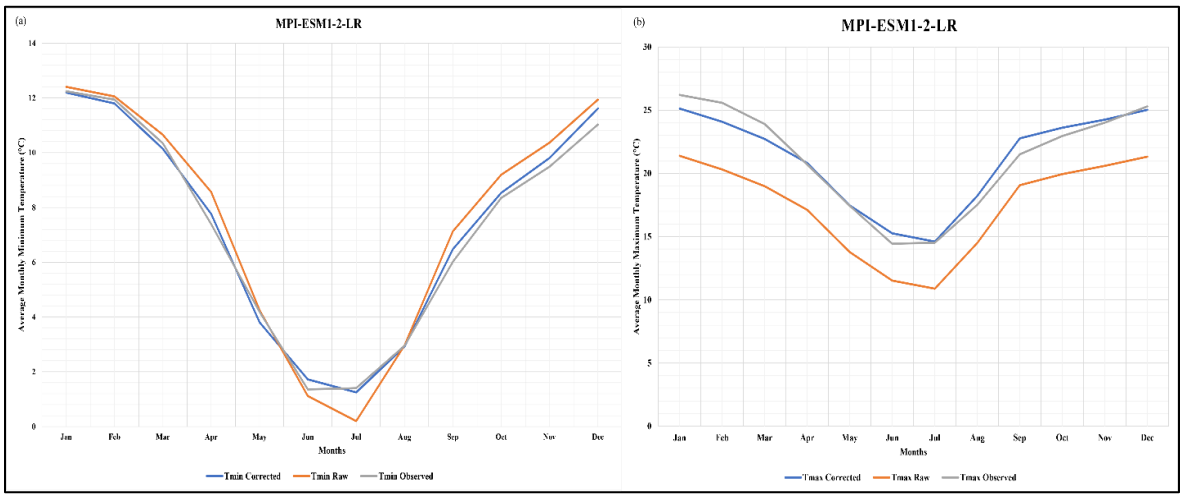

Figure 12 - Comparison of observed station data, raw and bias corrected MPI-ESM1-2-LR GCM in the South Phuthiatsana catchment for the baseline period (1984 - 2014); (a) Average monthly minimum and (b) Average monthly maximum temperatures

4.3.2 Projected Changes in Precipitation

As illustrated in **Figure 13**, projected monthly rainfall variations are anticipated to follow distinct seasonal trends based on the two analysed climate projections for the near term (2041–2060) and the middle of the century (2061–2080). The most significant rises in the near future take place in May under SSP5-8.5 (+60.78%) and July under SSP2-4.5 (+46.32%). In August, precipitation is predicted to decrease significantly under both scenarios, by −43.94% under SSP5-8.5 and −56.69% under SSP2-4.5. June also sees dryness under both pathways, while there are very minor changes in the following months.

Seasonal variations become increasingly noticeable in the mid-term. While SSP5-8.5 reveals a moderate increase (+36.74%), SSP2-4.5 reveals an alarming increase of +89.85% in July precipitation. Particularly under SSP5-8.5 (-55.13%) and, to a lesser extent, under SSP2-4.5 (-29.42%), August continues to decline. Significant drying is also observed in June for both scenarios (−46.21% for SSP2-4.5 and −44.10% for SSP5-8.5). Additionally, under SSP5-8.5, May precipitation rises by +34.95%, signalling a potential change in rainfall patterns in South Phuthiatsana catchment.

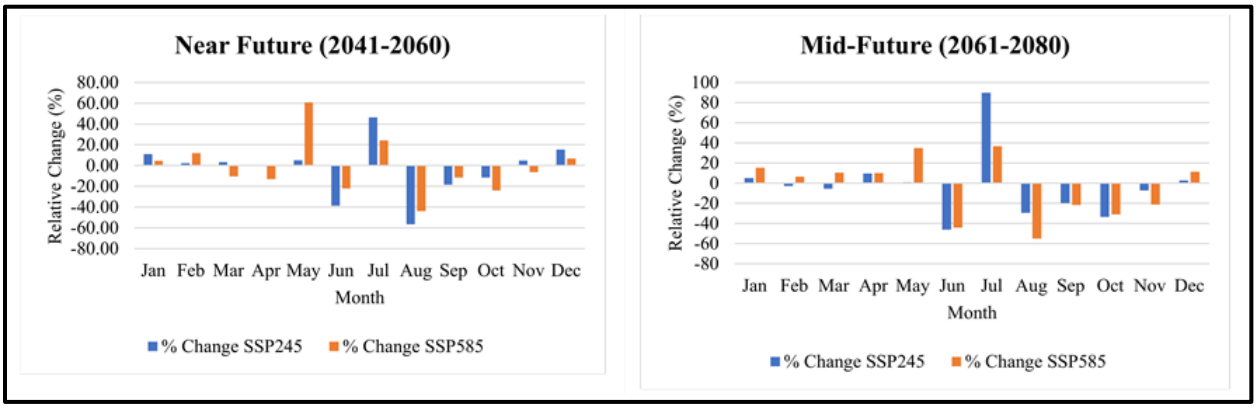

Figure 13 - Change in mean precipitation for near and mid-future under SSP2-4.5 and SSP5-8.5 relative to historical period

SSP2-4.5 and SSP5-8.5 project significant and distinct seasonal shifts in monthly precipitation for the South Phuthiatsana catchment. In the near-future (2041–2060), substantial increases in monthly mean precipitation are projected for July under SSP2-4.5 and May under SSP5-8.5. Conversely, significant drying, which result in drastically reduced monthly mean precipitation, is expected in August and June under both scenarios as illustrated in **Figure 14**. These patterns intensify in the mid-future (2061–2080), with an alarming increase in July precipitation under SSP2-4.5, while August and June continue to experience severe drying, particularly under SSP5-8.5. May precipitation also shows a notable rise under SSP5-8.5 in the mid-future, indicating a potential broader shift in seasonal rainfall distribution

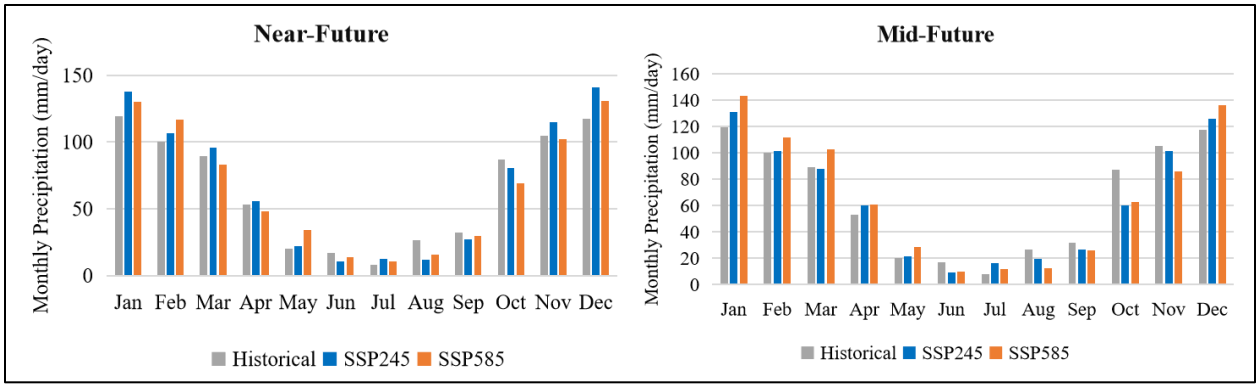

Figure 14 – Historical (1984-2014) and future (2041-2080) monthly and seasonal precipitation for SSP2-4.5 and SSP5-8.5

4.3.3 Projected Changes in Temperature

The projected changes in mean monthly temperatures show a steady warming trend under the SSP2-4.5 and SSP5-8.5 scenarios for both near and mid-future periods. SSP2-4.5 predicts below historical mean monthly temperatures for the entire period, whereas SSP5-8.5 projects higher mean monthly temperatures. While the seasonal temperature cycle is maintained, the magnitude of warming is generally consistent throughout the year, indicating a broad-scale increase in temperatures across all seasons. This is illustrated in **Figure 15** below.

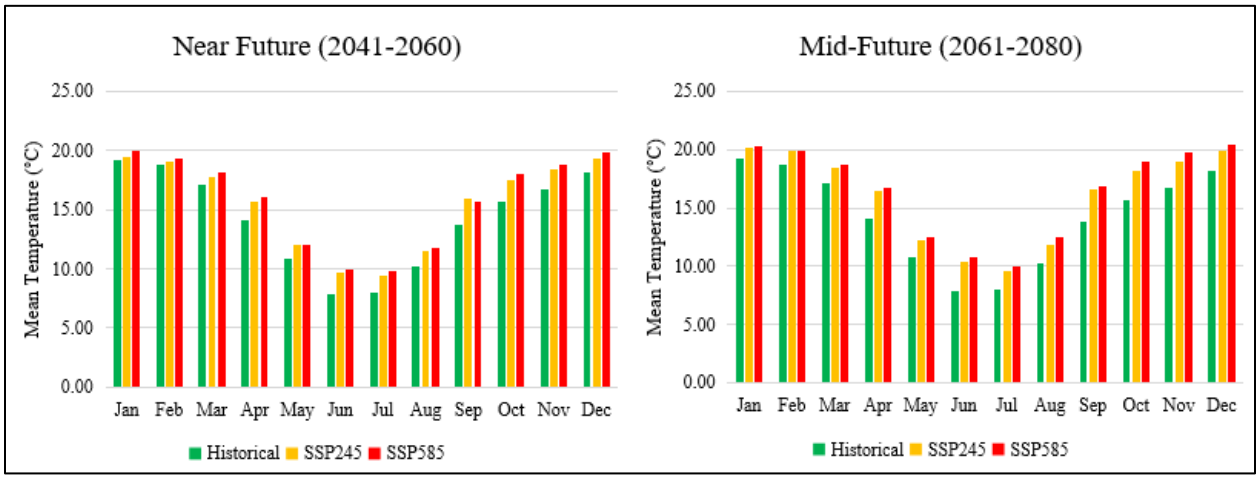

Figure 15 - Average monthly temperature for the near and mid-future periods in comparison to the historical period

In the mid-future, there is a noticeable rising trend in the mean temperature increases predicted under the SSP2-4.5 and SSP5-8.5 scenarios. **Figure 16** illustrates the overall projected change in temperatures and two future periods (2041 – 2060 and 2061 - 2080) with a rise by roughly 1.28°C under SSP2-4.5 and 1.57°C in SSP5-8.5 between 2041 and 2060 (near future). Moreover, mean temperature is also expected to increase by 1.84°C in SSP2-4.5 and by 2.26°C in SSP5-8.5 between 2061-2080 (mid-future). Interestingly, for both future periods under consideration, temperature rises are consistently higher under SSP5-8.5 than under SSP2-4.5. Generally, future temperature is projected to increase by 1.56°C and 1.91°C for SSP2-4.5 and SSP5-8.5, respectively. These projections, relative to the 1984–2014 historical, illustrate how different socio-economic and emission pathways could influence regional warming in the South Phuthiatsana catchment. Additionally, **Table 8** shows mean temperature changes under the above-mentioned scenarios. Under SSP5-8.5 mean temperature is expected to rise by 0.69°C as opposed to an increase of 0.56°C under SSP2-4.5°C from the from the near future to the mid-future. Nonetheless, these results demonstrate an obvious rise in the average temperature in both cases.

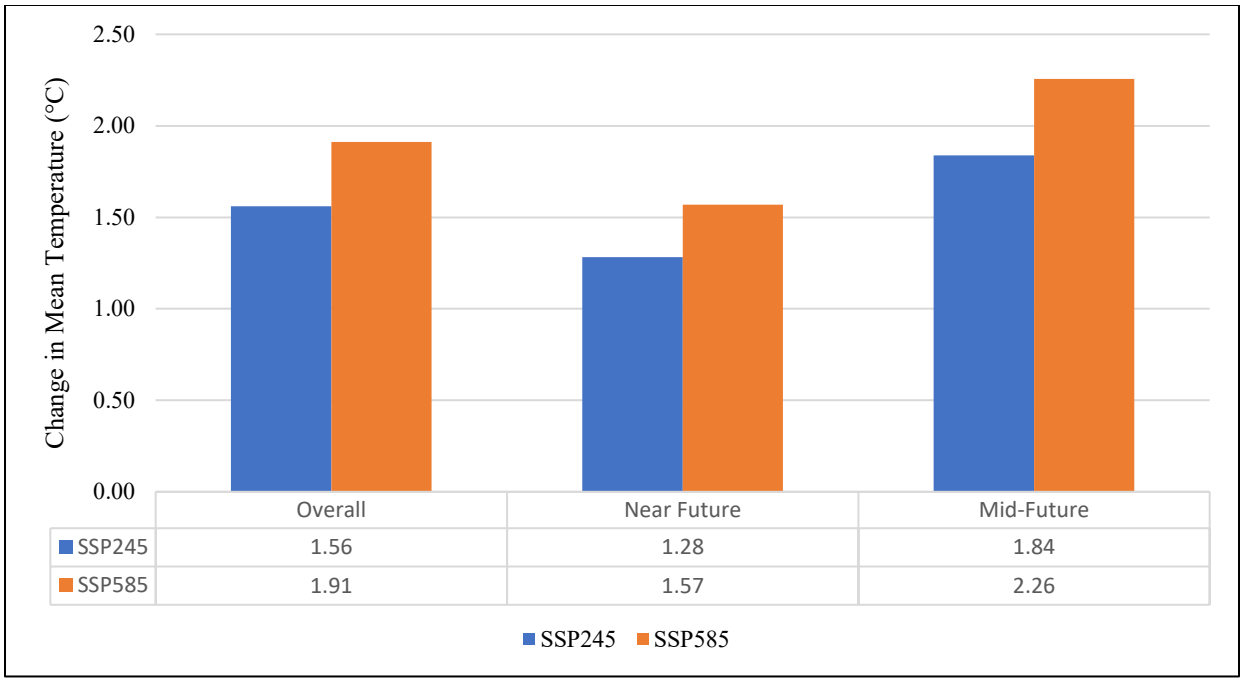

Figure 16 - Anticipated shifts in average temperature during the near- and mid-term periods under SSP2-4.5 and SSP5-8.5 pathways, illustrating a steady upward trend compared to the historical reference period

Table 8 - Mean temperature changes under SSP2-4.5 and SSP5-8.5 scenarios

Temperature °C					
Scenario	**Baseline**	**2041-2060 Average**	**2041-2060**	**2061-2080 Average**	**2061-2080**
SSP2-4.5	14.20	15.48	1.28	16.04	1.84
SSP5-8.5		15.77	1.57	16.46	2.26

4.4 Historical Streamflow Characteristics

Rainfall and baseflow from groundwater in the South Phuthiatsana catchment play a crucial role in maintaining flow of South Phuthiatsana river. This catchment is in the lowlands, therefore there is little to no contribution from snow as the country rarely experiences snowfall in the lowlands.

The Mann-Kendall test was used to determine whether a statistically significant monotonic trend was present in the mean annul streamflow data. The findings showed a negative Kendall's tau (-0.111) and a negative Sen's slope (-0.278 m3/s yearly), suggesting a downward trend in mean annual streamflow throughout the 1973–2014 baseline period. The test's p-value (0.651) exceeded the 0.05 threshold for significance. A linear regression analysis, shown in **Figure 17**, provides additional evidence for the existence of a slight declining trend (slope = -0.0393 m3/s annually). Only a little portion of the variability in the mean annual streamflow data can be explained by the linear model, according to the incredibly low coefficient of determination (R2 = 0.0262).

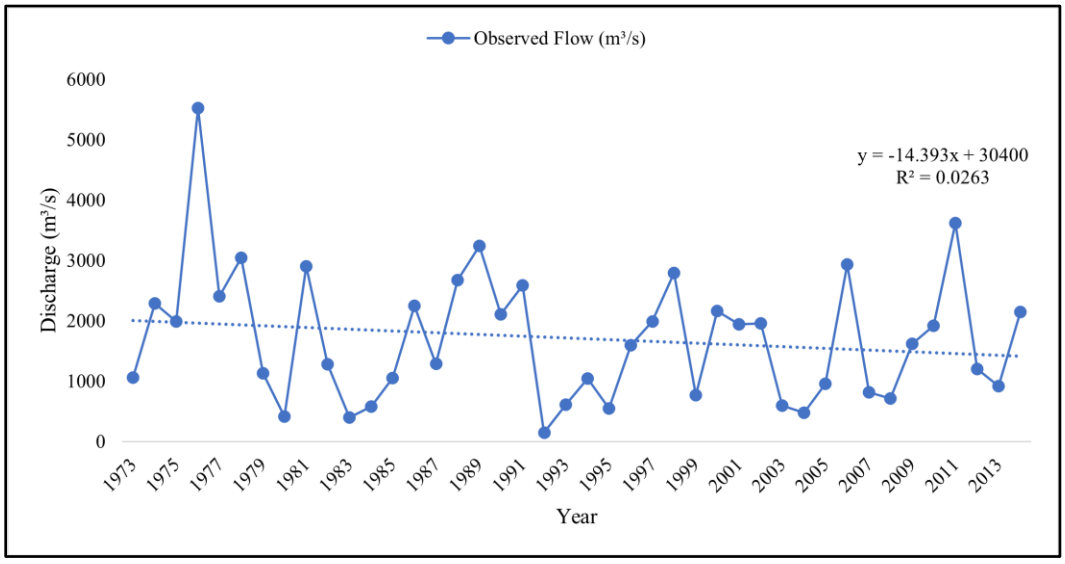

Figure 17 - Mean annual historical streamflow from 1973 to 2014 in Masianokeng gauging station

4.4.1 Seasonal Trends in Streamflow

Additionally, the monthly average streamflow data for all 42 years were subjected to Sen's slope estimators and the Mann-Kendall trend test in order to evaluate any potential changes in the

seasonal distribution of streamflow. **Table 9** summarises the results of this analysis for each month per year. Although the non-significant trends' directions changed throughout the year, with six months (January, February, March, August, September, October, and November) exhibiting a tendency toward decreasing streamflow and six months (April, May, June, July, and December) exhibiting a tendency toward increasing streamflow, none of these directional changes were statistically significant enough to be separated from natural variability. February and November had the largest magnitude of non-significant downward trend as indicated by the Sen's slope of -0.318 and -0.053 m^3/s per year, while May and June had the largest non-significant upward trend indicated by 0.022 m^3/s per year and 0.024 m^3/s per year.

Table 9 - Summary of monthly monotonic trend detection and rate-of-change estimates for average yearly streamflow

Month	Kendall's tau	p-value	Sen's Slope (m^3/s)/year	Tends Direction (Significance at α = 0.05)
January	-0.036	0.745	-0.023	Non-significant; downward
February	-0.152	0.159	-0.138	Non-significant; downward
March	-0.048	0.665	-0.022	Non-significant; downward
April	0.024	0.828	0.011	Non-significant; upward
May	0.101	0.351	0.022	Non-significant; upward
June	0.168	0.119	0.024	Non-significant; upward
July	0.094	0.386	0.009	Non-significant; upward
August	-0.066	0.544	-0.004	Non-significant; downward
September	-0.157	0.146	-0.013	Non-significant; downward
October	-0.073	0.502	-0.011	Non-significant; downward
November	-0.134	0.217	-0.053	Non-significant; downward
December	0.013	0.914	0.009	Non-significant; upward

4.5 Streamflow Model Development and Historical Simulation

4.5.1 Identification of Key Parameters and Model Performance Assessment

Sensitivity analysis was carried out using the SWAT+ toolbox to identify the parameters that most significantly influenced streamflow. **Table 10** displays the results, which showed that seven parameters were the most sensitive.

Table 10 - Key parameters influencing model behaviour during calibration and testing phases

Parameter Name	Description	Minimum	Maximum	Fitted Value
Revap_co	Groundwater coefficient	0.02	0.2	0.168
Revap_min	Threshold depth of water in the shallow aquifer	0	50	41.802
Flo_min	Minimum aquifer storage	0	50	25.201
Surlag	Surface runoff lag coefficient	0.05	24	1.158
Cn2	Curve number	-20	40	13.242
Canmax	Maximum canopy storage	1.0	50	1.041
Slope	Average slope steepness in HRU	0	0.9	0.866
Alpha	Baseflow factor	0	1.0	0.124
Esco	Evaporation soil compensation factor	0	1.0	0.000
Cn3_swf	Pothole evaporation coefficient	-30	30	-30.000
Latq_co	Lateral flow contribution to streamflow	0	0.05	0.050
k	Saturated hydraulic conductivity	-100	250	250

4.5.2 Performance of SWAT+ and XGBoost in Simulating Historical Streamflow

The Masianokeng gauging station's observed streamflow was used to calibrate and validate SWAT+. The NSE, KGE, Pbias, RMSE, and MSE are five commonly used statistical metrics that were used to evaluate the model's performance and are listed in **Table 11**. Although the model captured general flow patterns, NSE and KGE values for both calibration (0.17 and0.14) and

validation (0.20 and 0.35) revealed poor performance overall, indicating a limited ability to simulate daily streamflow variability as they are very low compared to the acceptable thresholds. Pbias showed mixed performance tendencies of the model to simulate observed streamflow, with positive Pbias (17.56%) during calibration, revealing that the model overestimates streamflow and also the negative Pbias during validation (-10.91%) indicating underestimation of streamflow. Generally, the Pbias values are within the acceptable range of percentage bias of ±25%. Both the RMSE and MSE are lower during the validation period (6.50 and 42.27, respectively) than during the calibration period (9.33 and 87.01), indicating a minor improvement in model performance during validation.

As illustrated in **Figure 18** below, the SWAT+ model typically underestimates peak flows over the full timeseries for both the calibration and validation timeframes. The timing of flow events is captured reasonably well, even though the model was poor in simulating the peak flows compared to low flows. The underrepresentation of peak flows aligns with the low NSE and KGE values.

Additionally, the SWAT+ simulation produced internal warnings that highlighted hydrological imbalances, including surface runoff in forested and wetland HRUs surpassing 50% of precipitation and unreasonably high biomass and evapotranspiration values. These challenges may be the result of miscalibrated land use parameters, constraints in the model framework, or inadequate depictions of important processes like evapotranspiration and infiltration in particular land covers.

Table 11 – SWAT+ performance metrics for calibration and validation at Masianokeng gauging station

Model	NSE	KGE	PBIAS (%)	RMSE	MSE
Calibration	0.17	0.14	17.56	9.33	87.01
Validation	0.20	0.35	-10.91	6.50	42.27

Similar outcomes have been observed in previous research conducted with the SWAT+ model. For example, Mogebisa (2021), observed similarly low NSE values (~ -0.08) in the Incomati River Basin, which were attributed to regional heterogeneity, biased climate input data, and missing observations. Abbaspour et al. (2015) also reported low NSE values ranging from 0.03 to 0.26 in a continental-scale hydrological study. In contrast, Emiru et al. (2021) achieved acceptable NSE values (between 0.40 and 0.49) during calibration and validation at selected stations, highlighting that model performance is often site-specific.

In the South Phuthiatsana catchment, Masianokeng gauging station is located downstream of the Metolong dam. As noted by Abbaspour et al. (2015), dam or reservoir operations can significantly influence streamflow dynamics in ways that are not well represented in SWAT+, potentially contributing to simulation errors. Generally, the following sources contribute to model uncertainty:

a) Conceptual simulations such as the SCS curve number method for flow partitioning
b) Watershed processes that are not mentioned in the program such as wind erosion and wetland processes
c) Program-included processes in the catchment such as data limitations (i.e., as water transfers), and
d) Poor input data quality

The model proved inadequate for accurate future streamflow prediction due to its poor performance, especially when NSE values dropped below generally recognised thresholds. Scenario analysis based on a model that performs poorly runs the risk of producing inaccurate or unusable conclusions. This is consistent with recent research findings that highlight the need to avoid using physically-based models such as SWAT for future impact assessments when they perform poorly in calibration and validation (NSE < 0.5), particularly in areas with limited data or hydrological complexity (Schutte et al., 2024; Sun et al., 2017; Moriasi et al., 2007).

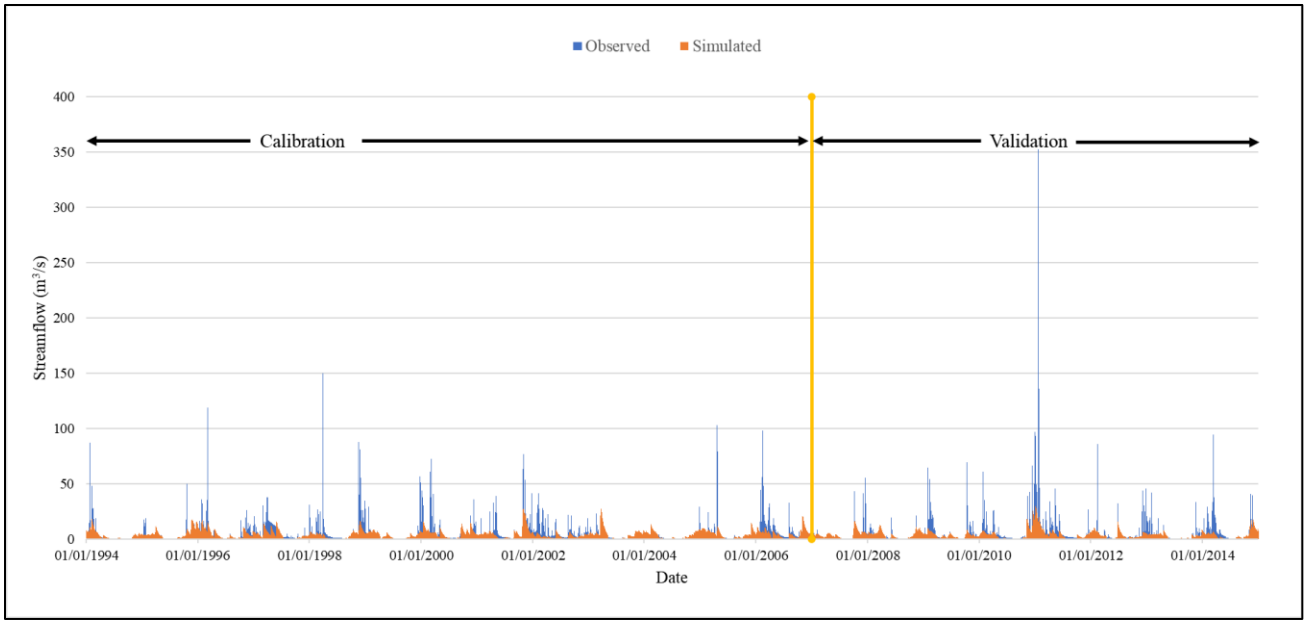

Figure 18 – SWAT+ model performance results showing time series alignment between observed and modeled streamflow at the Masianokeng gauging station, highlighting the model's limited ability to capture peak flows accurately.

The SWAT+ model output was also used to further assess model performance using water balance (WB) equation. **Table 12** and **Table 13** presents the aggregated annual average hydrological water balance components and key hydrological ratios for the simulated period (1984-2014). The inputs are listed under gains, while outputs are categorised as losses. The computed water balance (WB) error is -7.267 mm, indicating that total simulated losses exceeded inputs. While this discrepancy is relatively small in magnitude (about 1% of total precipitation), it nonetheless highlights a lack of mass conversation in the model outputs, which points to parameters representation or parameterisation (calibration). Furthermore, water balance ratios were also obtained from SWAT+ Editor, after running the model. SWAT+ Editor has a SWAT+ Check option which is the program for checking whether the results are within typical ranges (Arnold et al., 2012). It also helps in identifying typical parameter ranges.

Table 12 - Water balance components (mm) and annual water balance ratios from SWAT+ model simulation

Component	Gains	Losses
Precipitation (Pr)	726.796	
Evapotranspiration (ET)		483.307
Percolation (Perc)		249.967
Surface Runoff (SURQ)		0.075
Lateral Flow (LATQ)		0.714
Total	**726.796**	**734.063**
Water Balance (Gains – Losses)	-7.267	

Table 13 - Annual water balance ratios

Water Balance Ratios	Ratio values
Streamflow/Precipitation	0.29
Baseflow/Total Flow	1
Surface Runoff/Total Flow	0
Percolation/Precipitation	0.34
Deep Recharge/Precipitation	0.02
ET/Precipitation	0.66

On the other hand, the streamflow in South Phuthiatsana was successfully simulated by the extreme gradient boosting model as illustrated in **Figure 19**. The comparison of the simulated and actual streamflow demonstrates that, with the exception of extremely high flows, XGBoost was

fairly accurate in capturing the observed streamflow patterns. While the model learns patterns from the data, the training time has a significant effect on the XGBoost ability to make predictions. Throughout validation, the model is continuously observed to evaluate its capacity for generalisation and applicability. Observed daily streamflow data for South Phuthiatsana catchment obtained from Masianokeng gauging station (outlet), spanning from 1984 to 2014 was used for streamflow simulation at the catchment outlet. This data was split into training data (1984 to 2005) and validation data (2006 to 2014). Model performance metrics such as NSE, KGE, PBIAS, and RMSE were used to assess the model as shown in **Table 14**.

Table 14 – XGBoost performance metrics for training and validation at Masianokeng gauging station

Model	**NSE**	**PBIAS (%)**	**KGE**	**RMSE**
Training	0.89	0.00	0.89	3.23
Validation	0.62	-0.70	0.71	6.97

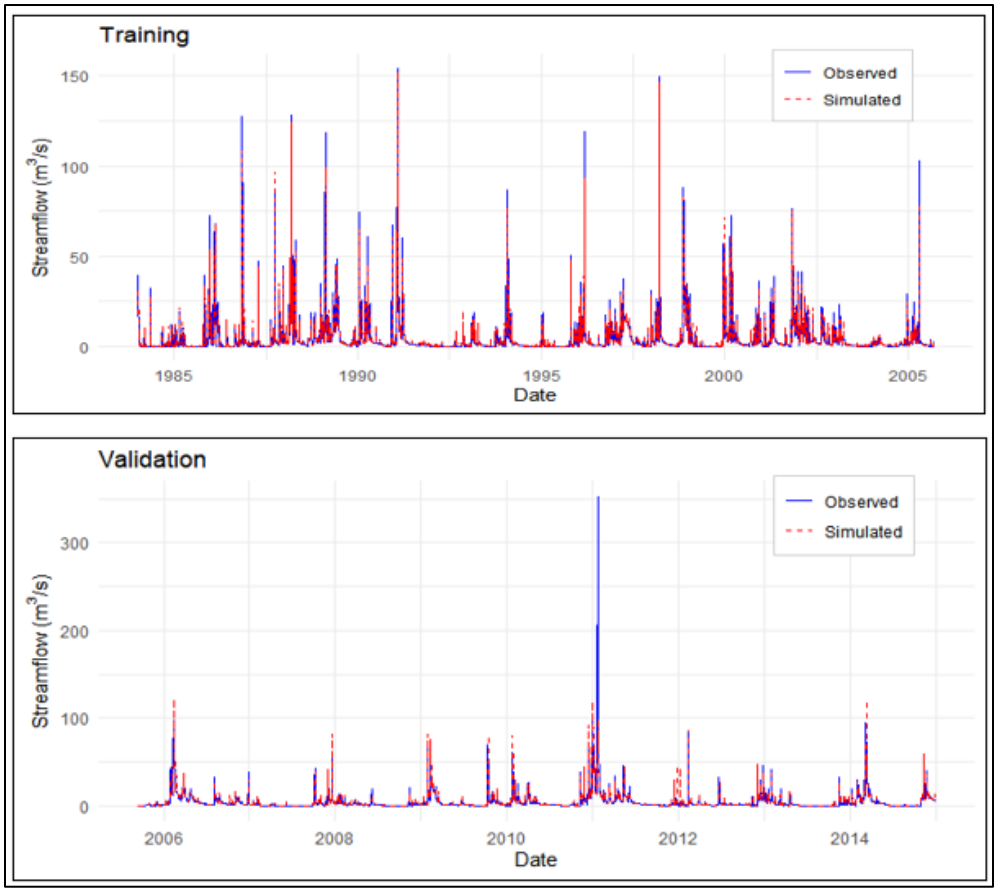

Figure 19 - Training (a) and validation (b) XGBoost results of timeseries comparison between observed streamflow and simulated streamflow

In general, ***Figure 19*** illustrates how well the XGBoost model can accurately represent the daily streamflow in the Masianokeng gauging station's South Phuthiatsana watershed. As demonstrated by acceptable goodness-of-fit measures utilised in hydrological research, the simulated streamflow values correspond to the observed streamflow. NSE was the primary metric used to assess the XGBoost performance; during calibration and validation, it was 0.89 and 0.62, respectively. For calibration and validation, the model's percentage bias was 0.00 and -0.70, which falls within an acceptable range of ±25. **Table 14** shows general performance of the model using different metrics. Generally, this indicates the applicability of XGBoost model for different scenarios including future scenarios in climate change studies. Hence, this model was used to predict future streamflow

at daily timestep and further, hydrological extremes were analysed under different climate scenarios.

4.6 Projected Impacts of Climate Change on Streamflow

Monthly streamflow projections for 2041–2080 for SSP2-4.5 and SSP5-8.5 are displayed in relation to the historical, spanning from 1984–2014. **Figure 20** below presents a comparison of long-term monthly mean streamflow. Under historical conditions, streamflow exhibits a relatively low and stable seasonal pattern, with small peaks from January to April (wet season) and low flows from June to October (dry season). In contrast, both future scenarios indicate significant changes in streamflow magnitude and timing.

Projected streamflow under SSP2-4.5 rises significantly from December to May, which is normally the wet season, with February and March expected to experience the highest peak flows. Dry season flows (June–October), although still lower, remain higher compared to historical levels, suggesting a possible extension of the high-flow period. The catchment's rainy season, which begins in November and ends in early April, probably has an impact on the uptrend in streamflow during the same period.

The SSP5-8.5 scenario shows a similar but more pronounced trend, with markedly higher streamflow during the summer, particularly from December to April. Furthermore, streamflow during the dry season (June–October) is also expected to be higher than historical levels, indicating a general increase in runoff or baseflow throughout the year. This however, shows a more consistent dry season flows with historical flow than the SSP2-4.5, hinting to variability in climate impacts or a non-linear hydrological response to warming. Overall, the projected changes in streamflow suggest that climate change may not only increase streamflow but also alters the seasonality of flow.

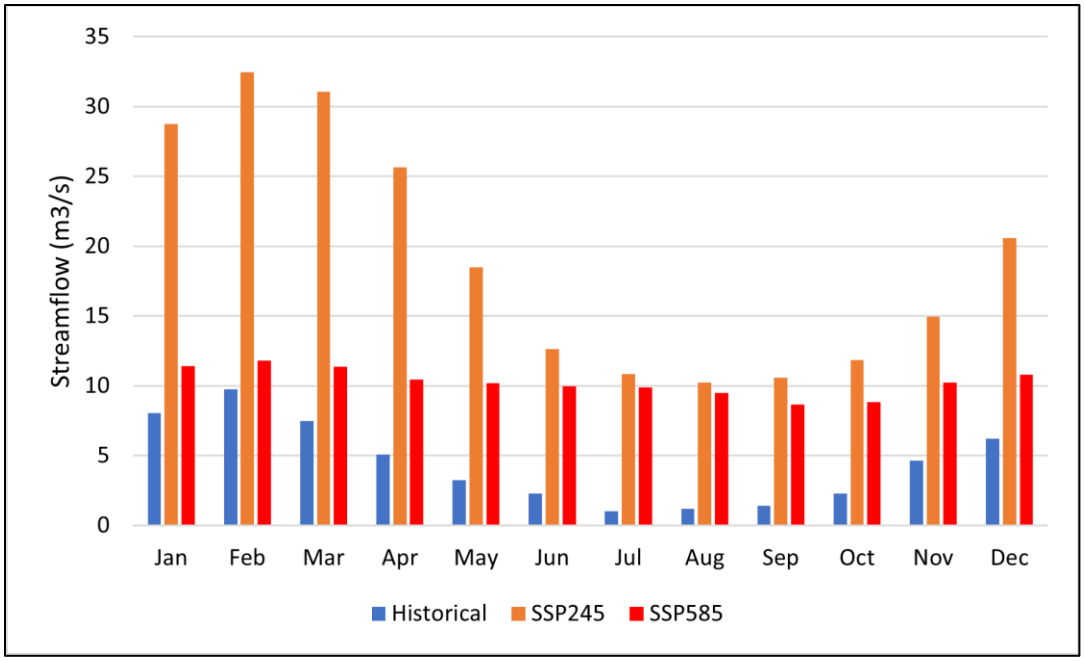

Figure 20 – Long-term average monthly streamflow, presenting historical observations and projected changes under SSP2-4.5 and SSP5-8.5, based on MPI-ESM1-2-LR model simulations

The mean streamflow for the dry and wet seasons is compared in **Figure 21** between historical conditions and future scenarios (SSP2-4.5 and SSP5-8.5). Historically, the rainy season has seen substantially higher streamflow than the dry season. Both seasons display an increase in streamflow under SSP2-4.5, with the rainy season exhibiting the greatest total values. While rainy season flow is lower than in SSP2-4.5 but still greater than historical levels, dry season flow in SSP5-8.5 is comparable to SSP2-4.5 and significantly higher than historical levels. As a result, SSP5-8.5 reduces the seasonal contrast in streamflow, suggesting a less pronounced difference between wet and dry periods.

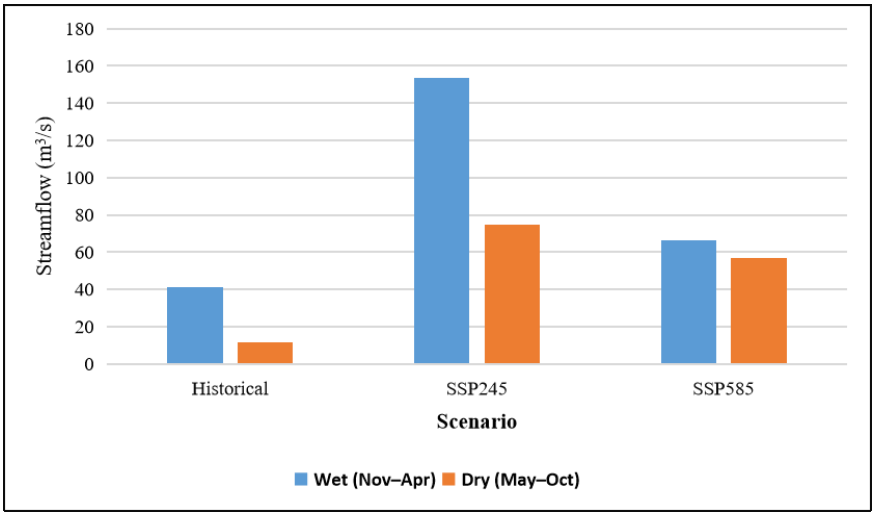

Figure 21 – Mean streamflow during wet and dry seasons across the historical period and projected climate pathways (SSP2-4.5 and SSP5-8.5)

Additionally, as shown in **Table 15**, the Mann-Kendall trend test and Sen's slope were used to try to further analyse the effects of climate change on streamflow. With a very low Kendall's tau (0.0151) and a small Sen's slope of 0.0126 m3/s annually, the baseline scenario showed no discernible trend ($p = 0.919$) and a slight positive direction. Under SSP2-4.5, there is a rather high increasing trend (Kendall's tau = 0.187) with an annual rise of 0.0760 m3/s. A signal of change may be emerging under this moderate emissions scenario, even if the trend is near the threshold and not statistically significant at the 5% level ($p = 0.0911$). SSP5-8.5 scenario shows no statistically significant trend ($p = 0.600$). Negative tau (-0.0590) and weak Sen's slope (-0.00541) indicate a weak and insignificant downward trend over time.

Comparatively, only SSP2-4.5 scenario reveals a moderate increasing trend when comparing the three scenarios, which indicate sensitivity to mid-range emission paths. While SSP5-8.5 shows a slight decline, both the baseline and SSP5-8.5 scenarios reveal little to no observable trends. The monthly Mann-Kendall trend test remains more or less the same for all the scenarios.

Table 15 – Summary of annual monotonic trend analysis and rate-of-change estimates for the baseline period and projected climate conditions in the South Phuthiatsana catchment

	Annual			Monthly		
Scenario	**MK_p**	**MK_tau**	**Sen's_slope**	**MK_p**	**MK_tau**	**Sen's_slope**
Baseline	0.919	0.0151	0.0126	0.118	0.0543	0.00134
SSP2-4.5	0.0911	0.187	0.0760	0.593	0.0163	0.000304
SSP5-8.5	0.600	-0.0590	-0.00541	0.426	-0.0243	-0.000319

4.7 Impacts of Climate Change on Extreme Hydrological Events

4.7.1 Impacts of Climate Change on High Flows

The high flow duration curve (HFDC), based on annual maximum daily streamflows, indicates a steady decline in high flow magnitudes under both future climate scenarios (SSP2-4.5 and SSP5-8.5) relative to the historical baseline (1984–2014). **Figure 22** highlights changes in high flow regimes across scenarios, with SSP5-8.5 showing the most pronounced reduction in high flow events throughout the projected period.

Three exceedance probability thresholds (0.1, 0.5, and 0.9) are used to quantify the changes; these values correspond to extreme, moderate, and more common high flow episodes, respectively. At the 10% exceedance probability (extreme high flows), flow magnitudes decrease by 12.5% under SSP2-4.5 and by 54.8% under SSP5-8.5. At the median exceedance level (50%), the reductions become more pronounced, reaching 67.4% under SSP2-4.5 and 66.6% under SSP5-8.5. SSP2-4.5 reduces flows by 54.8%, whereas SSP5-8.5 reduces flows by 60.1% for frequent high flows (90% exceedance). **Table 16** shows the percentage changes across the two climate scenarios relative to the baseline.

Generally, both future scenarios project substantial decline in high flow magnitudes across all exceedance probabilities, with SSP5-8.5 generally exhibiting more pronounced changes at the extreme end (10% or 0.10). SSP5-8.5 generally lies below the baseline and the SSP2-4.5, indicating larger reductions in high flow extremes. Nevertheless, SSP2-4.5 briefly drops below SSP5-8.5 at around 0.3 exceedance probability and quickly returns above it after mid exceedance probability (0.5), and settles between the baseline and SSP5-8.5 scenario as the probability increases. This indicates how the reduction of moderate and frequent high flow magnitudes will vary depending on future climatic scenarios.

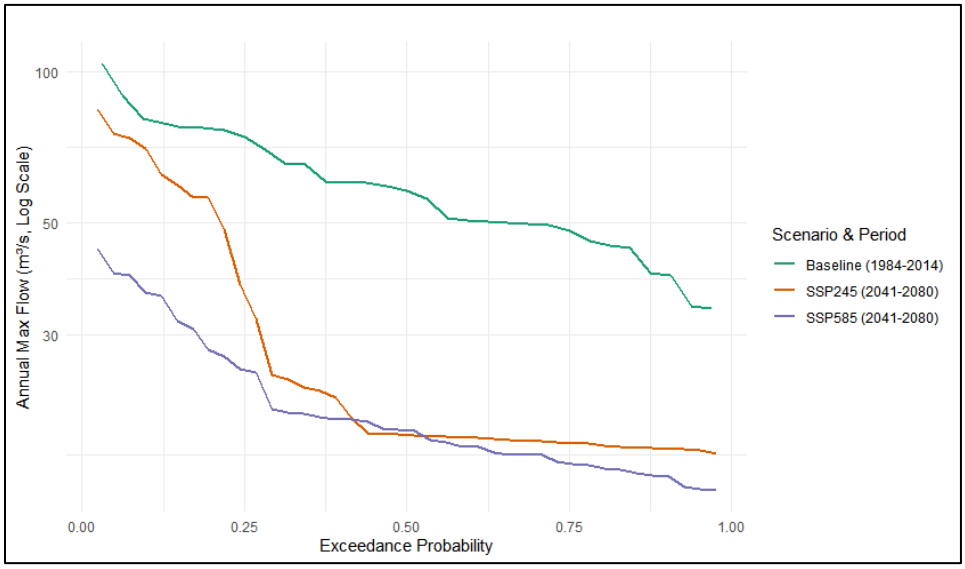

Figure 22 – High flow duration curve historical and future climate scenarios and their periods

Table 16 – Percentage change in high flows under both climate scenarios relative to baseline

Probability	**SSP2-4.5 (%)**	**SSP5-8.5**
0.1	-12.5	-54.8
0.5	-67.4	-66.6
0.9	-54.8	-60.1

The average monthly number of days throughout the 1984–2014 baseline period and future scenarios (2041-2080) when streamflow exceeds 90th percentile (Q10) threshold is shown in **Figure 23**. High-flow circumstances are represented by the Q10 threshold, and days above this threshold are regarded as hydrologically exceptional events on the high-flow end. A higher frequency of these events has been recorded in Q1, particularly throughout the months of January to March. This was probably caused by summer runoff and early autumn precipitation. February was the month with the highest frequency of streamflow extremes, with an average of over 12 days with high flow. In contrast, winter and spring months (June to October) experiences no high flow days across all the scenarios.

Predictions for 2041-2080 under SSP2-4.5 and SSP5-8.5 emissions scenarios show significant drop in high flows frequency in almost every month. While high events do happen in the SSP2-4.5 scenario, they are much less often than in the baseline. There are only one to three high-flow days each month from January to April, which is a significant decrease from the summer maxima of the baseline. There is a more significant change in the high emissions scenario. Decline of seasonal high flow extremes is essentially indicated by the average high flow days for almost every month approaching zero. SSP5-8.5 shows a constant low number of high flow days on average, potentially signalling further investigation.

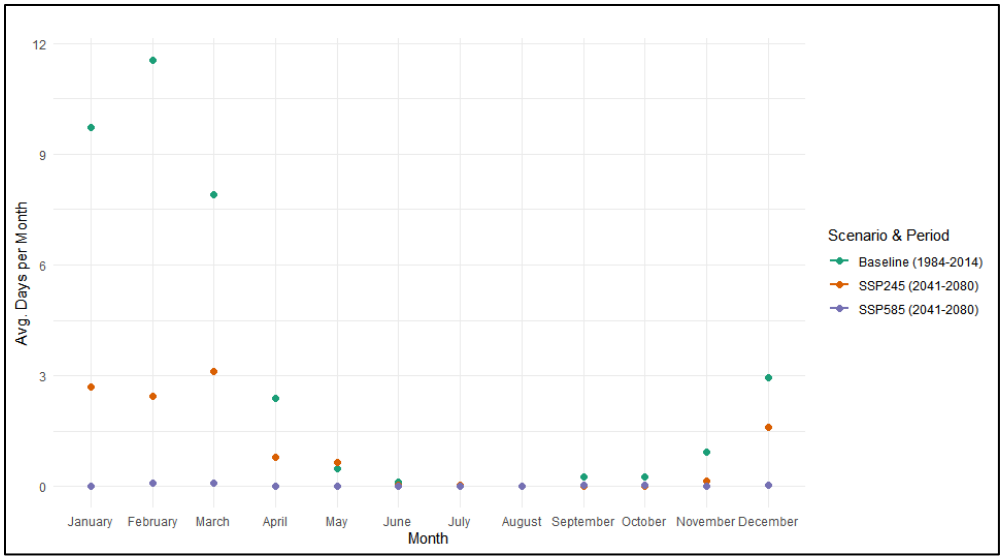

Figure 23 – Average number of days per month that flow condition exceeds high flow threshold (Q10)

4.7.2 Impacts of Climate Change on Low Flows

The low flow duration curve (LFDC) was constructed for the historical period (1984-2014) and future climate scenarios (SSP2-4.5 and SSP5-8.5) indicating notable changes in the 7-day minimum flow regime as illustrated in **Figure 24** below. The LFDC shows the relationship between flow magnitude and non-exceedance probability, with values plotted on a logarithmic scale to highlight differences in low flow behaviour.

Both future scenarios exhibit a consistent decrease in low flow magnitudes compared to the baseline across the majority of the probability range. Under anticipated climate change, this downward shift suggests a general worsening of low flow conditions. However, each scenario has a different pattern and degree of change. Quantitively, under SSSP5-8.5, the median 7-day minimum flow at probability 0.5, decreases by approximately -28.2% analysed in relation to the historical. While in SSP2-4.5, the reduction is approximately -23.5% at the same probability level. At higher probabilities (P = 0.9), representing more frequently occurring low flows, SSP5-8.5 shows lower flows than SSP2-4.5, indicating a more persistent reduction in water availability

under the emission scenario, with -25.7% for SSP5-8.5 and -0.9 for SSP2-4.5 as indicated in **Table 17**.

The crossover between the SSP2-4.5 and SSP5-8.5 curves at approximately P = 0.4–0.5 is an intriguing aspect of the LFDCs. SSP2-4.5 shows the lowest flows at low non-exceedance probabilities (rare events at P < 0.4), indicating that extreme low flow episodes in this scenario are more severe. SSP5-8.5, on the other hand, shows lower flows at greater probabilities, suggesting that moderate low flow conditions are more common and last longer in this situation. While SSP245 may be linked to sharper, more intense low flow extremes, SSP585 suggests a more prolonged decrease in low flows, which is consistent with broader hydrological drying. This pattern suggests that the nature of low flow risks varies among emission paths.

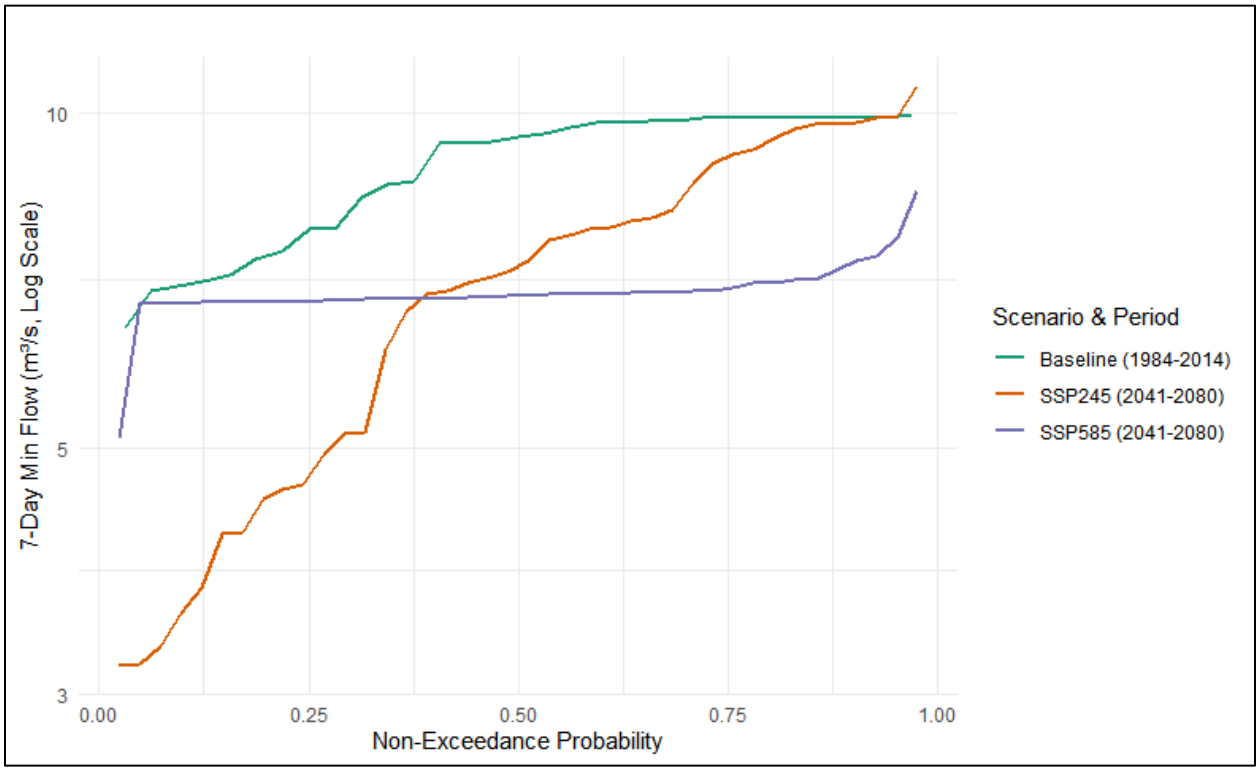

Figure 24 – Low flow duration for baseline (1984-2014), and future climate scenarios (2041-2080)

Table 17 – Percentage change in low flow under both climate scenarios relative to baseline

Probability	SSP2-4.5 (%)	SSP5-8.5
0.1	-49.3	-3.5
0.5	-23.5	-28.2
0.9	-0.9	-25.7

Figure 25 presents average monthly number of days where streamflow falls below its historical 90th percentile (Q90) threshold, derived from the 1984-2014 baseline period. The Q90 threshold defines a low streamflow condition, and days below the Q90 are considered low flow days. Historically, low flow days were more prevalent in spring and early summer (August to December), reaching a peak in October of approximately 7 days. the period spanning January through July generally saw a lower number of low flow days.

Future projections for 2041–2080 reveal substantial differences between the two emissions scenarios. When compared to the baseline, the average monthly number of low streamflow days in the SSP2-4.5 scenario reveals a mixed trend. The highest increases are projected in September, followed by October and November, with more than 12 low-flow days in those months. Notably, April also shows a marked rise in low-flow frequency, indicating reduced streamflow soon after the rainy season. Overall, these results suggest that low streamflow events are likely to become more frequent throughout the year, exceeding historical norms, even under a moderate emissions scenario.

Additionally, in comparison to the baseline and the SSP2-4.5 scenario, the fossil-fuelled scenario consistently predicts a significantly higher average monthly number of low streamflow days. The SSP5-8.5 estimates show a much higher number of days with low flows for almost every month. This increase is particularly noticeable in the second half of the year, with months like September and October exhibiting predicted averages of about 20 and 24 days, respectively. This suggests that low streamflow episodes are likely to grow increasingly frequent throughout the year. Under a high emissions future, these values show a sharp rise in the frequency of streamflow dry

conditions, as they are significantly greater than both the historical baseline and the SSP2-4.5 estimates.

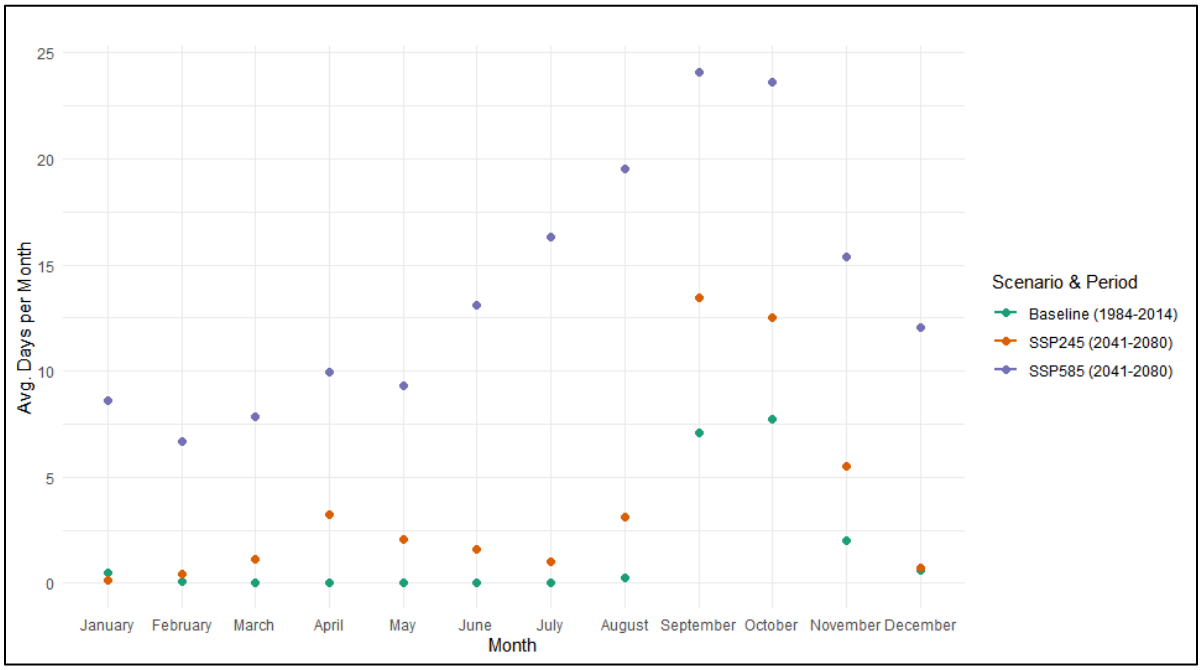

Figure 25 – Average number of days per month that flow conditions fall below a specific low-flow threshold (Q90)

4.8 Flow Frequency Analysis

Flow frequency analysis is a widely used technique in hydrology to assess the probability of occurrence of extreme flow events, such as floods. In this study, annual maximum and minimum streamflow data from the South Phuthiatsana catchment were analysed to estimate the frequency and magnitude of high-flow and low flow events.

4.8.1 High Flow Analysis (Flood Frequency)

A significant anticipated change in the extent of extreme flood events across the various climatic scenarios is depicted by the high flow frequency curves as illustrated in **Figure 26** below. One significant finding is that, for any given return period, the expected peak flows for both projected climatic scenarios (SSP2-4.5 and SSP5-8.5 spanning 2041-2080) are significantly lower than those

observed during the historical baseline era (1984-2014). For example, a flood event that was previously thought to have a 100-year return time and reach about 300 m^3/s is predicted to occur in both future scenarios at a significantly lower amplitude of about 30–40 m^3/s. This significant drop in peak flows raises the possibility that future flood occurrences in the South Phuthiatsana catchment will be less intense. Furthermore, the projected high flow magnitudes for SP2-4.5 and SSP5-8.5 seem to be very similar, with the majority of their respective confidence ranges overlapping. It also indicates that for high flow occurrences, the estimated flood magnitudes in the South Phuthiatsana catchment could not be significantly different depending on the future emissions pathway selected. This however points back to the use of single GCM model as opposed to an ensemble mean for several GCMs.

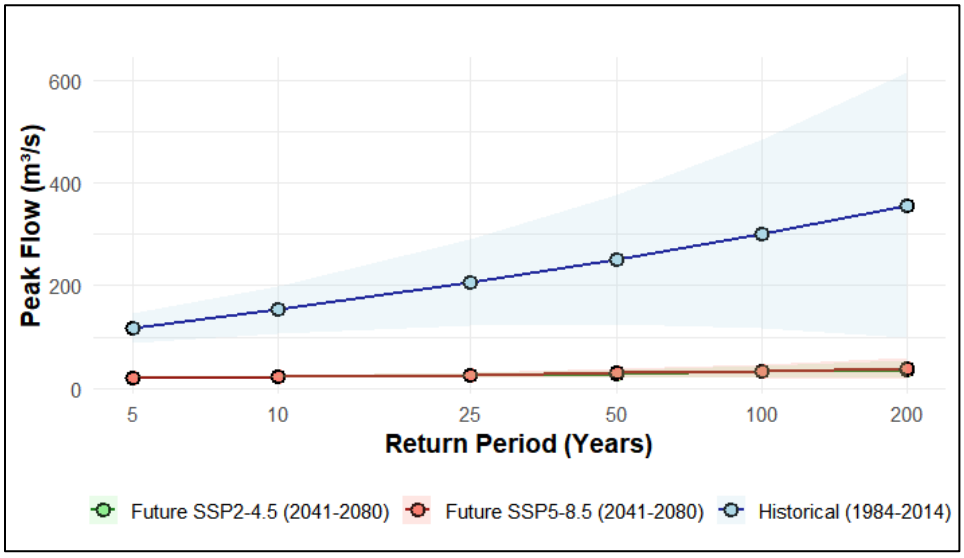

Figure 26 – High flow frequency curve for historical and two future climate scenarios (SSP2-4.5 and SSP5-8.5)

4.8.2 Low Flow Analysis

Using the 7-day minimum flow values recorded annually and analysed with the Log-Pearson Type III method, the resulting flow-duration curves illustrate a marked contrast between observed historical conditions and projected low streamflow scenarios, as depicted **Figure 27** below. Throughout all return periods, from 5-year to 200-year occurrences, the historical baseline (1984-

2014) constantly shows a 7-day annual minimum flow of effectively 0 m 3 /s. This suggests that in the past, regardless of the intensity of the drought episode, the river often had periods of total drying or maintained zero flow for at least seven days in a row annually. However, both projected climate pathways for the 2041–2080 timeframe (corresponding to SSP2-4.5 and SSP5-8.5) reveal a significant change from past conditions, showing positive values for 7-day annual minimum flows even during rare (200-year) low-flow events. This implies a significant reduction in the future severity of drought, which could lead to the river becoming more perennial or experiencing shorter times of no flow. Across all return periods, a consistent pattern is also observed, with the higher emissions scenario; SSP5-8.5 projecting slightly higher minimum flows than SSP2-4.5. Generally, analysis of hydrological extremes in the South Phuthiatsana catchment indicates a need for further investigation into the complex hydro-climatic processes governing streamflow in the catchment.

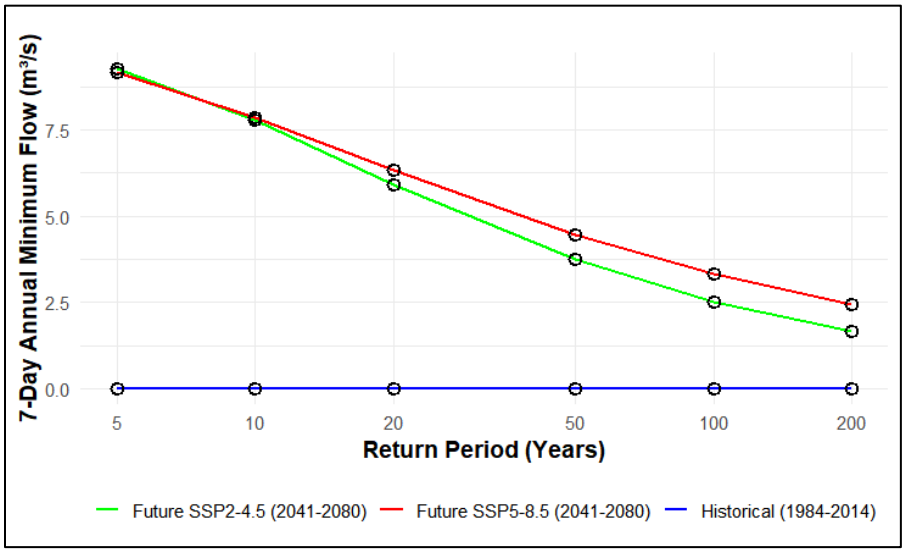

Figure 27 – Low flow frequency curves for the historical period and future climate projections (SSP2-4.5 and SSP5-8.5)

4.8.3 Hydrologic Regimes Analysis

The analysis of hydrologic flow regimes, represented by various flow quantiles in **Figure 28**, provides a thorough overview of the expected changes to the entire range of daily streamflow. The

streamflow regime analysis illustrates shifts across the whole range of flow conditions, from extremely low (Q1) to very high (Q98) flows. The historical flood threshold of 17.52 m^3/s is highlighted in **Figure 28** corresponding to the 95th percentile of historical flows.

The projected magnitudes of Q1, Q5, and Q10 are consistently higher in future scenarios compared to historical near-zero values, suggesting a shift towards less severe absolute minimum flow magnitudes and a decreased frequency of periods with extremely low or no flow. However, in the 1st and 5th percentiles, future projected streamflow indicates positive flow magnitudes, suggesting a decreased frequency of days with extremely low or now flow. Both future scenarios predict streamflow values that are much higher than those of the historical period as they go towards the mid-range flow quantiles (Q25, Q50, and Q75). The predicted median flows for SSP2-4.5 and SSP5-8.5 are significantly greater than the historical median flow (Q50) indicating a generally changed seasonal flow patterns that contribute to increased baseflows, implying an overall increase in normal or average daily flow conditions in the future.

On the other hand, a clear decline in magnitude is anticipated for both future climatic scenarios in comparison to historical conditions for the high flow quantiles (Q90, Q95, and Q98). The historical 98th percentile flow (Q98) is significantly higher than the SSP2-4.5 and SSP5-8.5 scenarios. This is in agreement with the high flow frequency analysis regarding the reduced flood magnitude.

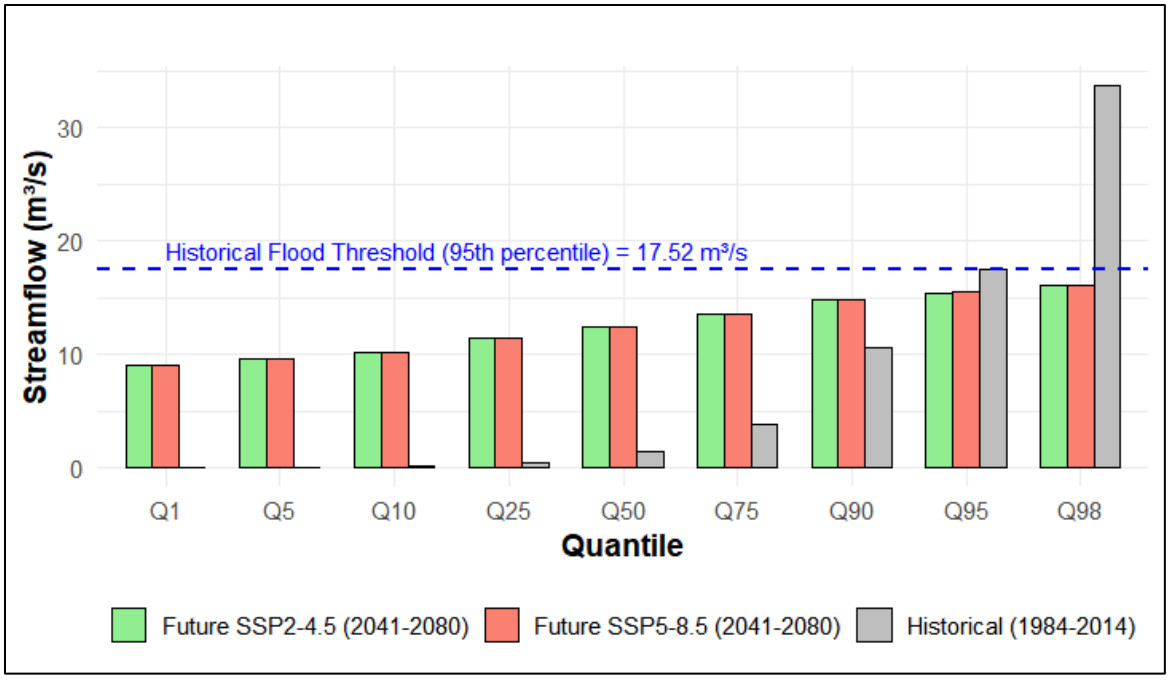

Figure 28 – Projected alterations in hydrologic flow patterns illustrated through streamflow quantiles (m^3/s), contrasting historical data (1984–2014) with anticipated conditions for 2041–2080 under two climate projection pathways.

4.9 Summary

This subsection presents a structured summary of the analytical results in relation to the study's specific objectives. **Table *18*** links each objective to its corresponding key findings and supporting visual references, thereby enhancing clarity, traceability, and coherence within the results chapter.

Table 18 - Summary of research objectives, corresponding key results, and supporting visual references.

Objective	Key Output/Results	Reference (Figure/Table)
1. Assess historical trends and variability in key climate variables	Identified warming trends and seasonal shifts in precipitation from 1984-2014	**Figure 10**, **Figure 11**, **Figure 14**, and **Table 8**
2. Evaluate projected changes in precipitation and temperature under SSP2-4.5 and SSP5-8.5	Projected increase in temperature and variable precipitation patterns for 2041–2080	**Figure 13**, **Figure 15**, and **Figure 16**
3. Simulate future streamflow patterns using hydrological modeling	SWAT+ showed poor performance in capturing peaks; XGBoost provided improved simulation of future streamflow	**Figure 18**, **Figure 19**, **Table *11***, and **Table 14**
4. Analyse effects of projected climate change on hydrological extremes	Decline in high flows (Q98) and increase in low flows (Q1); altered flow regime	**Figure *22*** - **Figure 23Figure 28**, and **Table *17***

5 Discussion

5.1 Introduction

This chapter discusses the key findings of the study, which aimed to assess the impacts of climate change on streamflow in the South Phuthiatsana catchment using bias-corrected outputs from the MPI-ESM1-2-LR global climate model. Initially, the physically-based SWAT+ hydrological model was applied for historical simulation and process understanding. However, due to its limitations in accurately capturing observed streamflow dynamics especially for future projections the XGBoost machine learning algorithm was adopted as the primary tool for predicting future streamflow and assessing hydrological impacts.

The discussion integrates insights from model performance evaluations, climate projections, and hydrological impact analyses. Drawing on advancements from the Coupled Model Intercomparison Project Phase 6 (CMIP6) and the growing success of data-driven approaches in hydrological forecasting, this study demonstrates the value of machine learning in simulating streamflow regimes and hydrological extremes under changing climate conditions. The findings offer new perspectives on the use of advanced modeling techniques for climate impact assessment and carry important implications for water resource management in the South Phuthiatsana catchment.

5.2 Climate Change Projections and Historical Context

5.2.1 Historical Precipitation Patterns and Observed Trends

Precipitation in the catchment varies significantly from year to year over the 1984-2014 period, with annual amounts fluctuating between roughly 600 mm and more than 1100 mm. These shifts are influenced by large-scale climate systems like the El Niño–Southern Oscillation (ENSO) and the Indian Ocean Dipole (IOD), which shape regional moisture patterns and atmospheric dynamics across Southern Africa (Roffe et al., 2024; Dieppois et al., 2016). **Figure 10** captures these variations, including wetter conditions around 1988-1989 and a pronounced dry spell in 1992.

Such fluctuations create ongoing challenges for managing water supplies and planning agricultural activities, often triggering cycles of drought and flooding (Lesotho's Climate Action, 2025).

A gradual reduction in total annual precipitation over the study period was identified through Mann-Kendall's rank-based trend assessment, with Sen's estimator indicating an average yearly decline of approximately 4.53 mm. While **Figure 10** visually reflects this downward movement, the associated p-value of 0.292 indicates that the trend lacks statistical strength, pointing instead to natural variability rather than a definitive long-term change. This finding aligns with assessments across the wider Orange-Senqu River Basin, where studies often find that the high inter-annual variability driven by phenomena like ENSO and IOD (Roffe et al., 2024) overrides clear long-term trends in mean annual rainfall, especially in the Lesotho Highlands where orographic effects are complex (Mpheshea et al., 2025). While some climate models project future precipitation declines for Southern Africa (Engelbrecht et al., 2024), the current observed record in the South Phuthiatsana catchment remains within the bounds of this high natural variability.

Long-term monthly precipitation data also reveal a consistent unimodal seasonal cycle (**Figure 29**). Given the low spatial variability across monitoring stations, a catchment-wide interpretation is appropriate. The wet season typically begins in October, peaks in January-February, and is driven by the seasonal migration of the Intertropical Convergence Zone (ITCZ) and subtropical high-pressure systems (Engelbrecht et al., 2024; Zhuang et al., 2020). Monthly totals during peak months often exceed 100 mm, particularly at stations like Khoshane, Masianokeng, and Matela. A pronounced dry season occurs from May to August. This distinct seasonality, wet summers and dry winters is characteristic of the Southern African Summer Rainfall Zone (SRZ) and carries important implications for agriculture, water supply, and hydrological extremes.

5.2.2 Historical Temperature Patterns and Observed Trends

The South Phuthiatsana catchment's annual maximum and minimum temperature increase from 1984 to 2014 are consistent with larger regional and continental climatic trends. These findings indicate a statistically significant warming, with Tmax increasing by an average of 0.035 °C annually (Mann-Kendall p-value = 0.0381) and Tmin increasing by 0.019 °C annually (Mann-

Kendall p-value = 0.0249). These results underscore a noticeable systematic alteration in the thermal regime of the catchment, which is unlikely to be attributed to natural variability alone.

Importantly, the observed warming in the South Phuthiatsana catchment reflects broader climatic trends documented across Africa and globally. The Intergovernmental Panel on Climate Change (IPCC) Sixth Assessment Report (AR6), specifically Chapter 9 on Africa, confirms that increasing mean and extreme temperature trends are prevalent across the continent and are largely attributable to human-caused climate change (Trisos et al., 2022). While the IPCC report provides a continental overview, broader regional studies further corroborate these patterns. For instance, research across Southern Africa has consistently documented observed increases in both mean and extreme temperatures over similar historical periods, often linking these changes to large-scale atmospheric circulation patterns, oceanic phenomena, and anthropogenic forcing (Engelbrecht et al., 2024). Studies focusing on specific sub-regions within Southern Africa, even if not directly on Lesotho, provide valuable contextual support, showing similar warming trajectories in neighbouring areas or regions with analogous climatic characteristics (Ngwenya & Mukwada, 2024).

The observed differential warming rates between Tmax and Tmin, with Tmax showing a slightly higher rate of increase, is an important aspect of the observed warming. While some regions exhibit a narrowing of the diurnal temperature range (DTR) due to faster Tmin warming, the observed pattern in South Phuthiatsana catchment suggests that the increases in daytime maximums are a prominent feature of the warming. In Lesotho, particularly in high-altitude (eastern) stations such as Mokhotlong, Oxbow, and Qachasnek, both Tmax and Tmin have increased significantly over the past 70 to 80 years, and in those high-altitude areas the Tmax trend is strong. Conversely, in lowland and foothill stations on the western side, significant warming has been more consistent for Tmin than for Tmax (Nhalpo, 2017).

The asymmetry with maximum temperature increasing more sharply than minimum temperature aligns with broader trends observed in the Maloti-Drakensberg region over the period 1960-2016. Effects such as reduced cloud cover during daytime, changes in atmospheric circulation that allow more solar heating, and possibly reductions in moisture/evaporation may be contributing to stronger daytime warming (Mohamed and Mukwada, 2019).

Crucially, higher maximum temperatures directly enhance potential evapotranspiration (PET) rates, leading to increased atmospheric water demand. This heightened evaporative demand, in turn, can contribute to reduced soil moisture availability, decreased runoff generation, and consequently, diminished streamflow, especially during dry periods or extended droughts (Onyutha et al., 2024; Scheff & Frierson, 2014). Equally, although Tmin warming is less pronounced, its increase contributes to an overall warmer environment, further supporting higher PET and potentially reducing the duration or intensity of cold-season processes that could contribute to streamflow. To properly evaluate their combined impact on the water balance and hydrological extremes of the catchment, it is essential to comprehend the complex nature of these different warming patterns.

The statistical significance of the identified temperature trends highlights that the observed warming in the South Phuthiatsana catchment indicates a systematic climatic change rather than just natural inter-annual variability. This carries significant consequences for upcoming climate projections and, importantly, for the lasting sustainability and fluctuations of water resources and hydrological extremes in the catchment area. The data indicates a persistent warming trend, highlighting a greater susceptibility to climate-related hydrological risks. Higher temperatures can specifically intensify the hydrological cycle; on one hand, they drive more severe and prolonged droughts through enhanced evaporation, which reduces baseflow and increases the likelihood of low flow extremes (Ellenburg et al., 2018). On the other hand, a warmer atmosphere holds more moisture, potentially leading to more intense precipitation events when they do occur, thereby increasing the risk of flash floods and high flow extremes (Prein et al., 2016). These findings provide a robust foundation for developing informed climate change adaptation and mitigation plans that specifically target the impacts on streamflow regimes and the management of hydrological extremes within the South Phuthiatsana catchment.

5.2.3 Effectiveness of Bias Correction and Implications for Projections

Temperature and precipitation data accuracy was successfully increased using bias correction. The majority of biases in the raw GCM output were eliminated through linear scaling and quantile mapping, especially the seasonal underestimating of minimum and maximum temperatures. Bias

corrected precipitation and temperature are critical for reliable hydrological modeling, as temperature and precipitation drive evapotranspiration, and runoff processes.

The observed weak downward trend in precipitation and streamflow during the historical baseline period supports the initial hypothesis of a drying tendency in the catchment, although these trends were not statistically significant. Projected climate data under both SSP2-4.5 and SSP5-8.5 scenarios indicate consistent increases in temperature by 1.56°C and 1.91°C, respectively; along with highly variable seasonal changes in precipitation. July and May may experience significant increases, consistent with global and regional patterns of amplified warming under high emissions pathways (IPCC, 2021; O'Neill et al., 2017), while June and August show substantial drying under both scenarios. These projections suggest a potential shift in rainfall seasonality, which may alter peak runoff timing and hydrological stress periods.

5.2.4 Projected Climate Changes (Precipitation and Temperature)

Projected climatic pathways represented by SSP2-4.5 and SSP5-8.5 indicate significant changes in rainfall and temperature patterns within the South Phuthiatsana catchment, extending the observed warming trajectory into the periods 2041-2060 and 2061-2080.

The projections indicate distinct seasonal variations in precipitation, with significant drying projected for August and June under both scenarios, particularly distinct in August (-56.69% in near-future SSP2-4.5) and June (-46.21% in mid-future SSP2-4.5). On the other hand, substantial increases are projected for July (up to +89.85% in mid-future SSP2-4.5) and May (+60.78% in near-future SSP5-8.5) (**Figure 13** and **Figure 16**). This projected intensification of seasonal variability, with concurrent periods of increased and decreased rainfall, is a common feature of future climate projections for semi-arid and subtropical regions. While there is often higher uncertainty in precipitation projections compared to temperature, particularly at regional scales, many climate models for Southern Africa suggest an increase in rainfall intensity alongside changes in seasonal distribution and more frequent dry spells (Trisos et al., 2022). The specific magnitudes and timing of these shifts in the South Phuthiatsana catchment warrant critical

comparison with other downscaled climate projections for the Maloti-Drakensberg region, where a complex topography can lead to localised variations in rainfall responses.

Consistent with the historical observations, future projections indicate a robust and pervasive warming trend across all seasons and future periods. Projections indicate a marked upward trend in mean monthly temperatures, with estimated increases of approximately 1.84°C for SSP2-4.5 and 2.26°C for SSP5-8.5 by the mid-century period (2061-2080) in comparison to baseline conditions (**Figure 14**, **Figure 15** and **Table 8**). The sustained nature of this warming, with the higher emission scenario (SSP5-8.5) consistently showing greater increases, aligns strongly with global and regional climate model outputs. The IPCC AR6 further emphasises that temperatures across Africa are projected to rise significantly throughout the 21st century, with warming rates generally exceeding the global mean (Trisos et al., 2022). Regional climate modeling efforts for Southern Africa consistently project significant temperature increases across all seasons, regardless of the emission pathway, although the magnitude of warming is directly tied to the emissions scenario (Engelbrecht et al., 2024). The maintenance of the seasonal temperature cycle, alongside an increase in the absolute magnitude of warming, is also a common feature of climate model projections for the region. These projections for the South Phuthiatsana catchment thus represent a robust signal of future warming.

5.3 Historical Streamflow Characteristics and Model Performance

Analysis of mean annual streamflow data for the South Phuthiatsana River (1973-2014) reveals a weak, non-significant declining trend, with Sen's slope at -0.278 m^3/s/year and Kendall's tau at -0.111. Linear regression corroborates this slight decline (slope = -0.0393 m^3/s/year), but the result lacks statistical significance ($p = 0.651$) and explanatory power ($R^2 = 0.0262$). This suggests that the variability in streamflow is largely governed by factors beyond a simple temporal trend; likely the interplay of climatic and catchment-specific dynamics. A similar non-significant decline was observed in annual precipitation (Mann-Kendall $p = 0.292$), reinforcing the intuitive hydrological link between rainfall inputs and streamflow outputs, as supported by regional studies in Southern Africa (Hadebe & Dube, 2023).

Interestingly, this streamflow tendency contrasts with statistically significant warming trends in both Tmax and Tmin over the 1984-2014 period, increasing at 0.035 °C and 0.019 °C per year respectively. Elevated temperatures are known to enhance evaporative demand, reducing effective precipitation and increasing moisture stress, even if rainfall remains constant or declines only marginally (Yahaya et al., 2024). This aligns with broader findings that suggest warming alone can exacerbate water scarcity by intensifying evapotranspiration losses (IPCC, 2021). Therefore, the weak decline in streamflow may be a function of both marginal precipitations decrease and increasing atmospheric water demand, supporting a hydrologically plausible, if statistically inconclusive, trend toward reduced runoff in the catchment.

5.3.1 Streamflow Model Performance, Sensitivity, and Uncertainty

The initial hydrological modeling efforts utilised the physically-based SWAT+ model for historical streamflow simulation and process understanding in the South Phuthiatsana catchment. Sobol sensitivity analysis revealed that the minimum threshold flow rate (flo_min), which dictates the shallow aquifer's contribution to baseflow, was the most sensitive parameter influencing simulated streamflow. This highlighted the model's heavy reliance on sub-surface flow mechanisms, a finding consistent with other studies in groundwater-influenced catchments (Gasirabo et al., 2023). Other sensitive parameters included cn2 (SCS runoff curve number) and canmax (maximum canopy storage), emphasising the importance of surface runoff and interception. Conversely, esco (soil evaporation compensation factor) showed the highest negative sensitivity, indicating that increased soil evaporation negatively impacted streamflow accuracy, which aligns with research on the critical role of evapotranspiration (Kumar & Mishra, 2025).

The SWAT+ model showed considerable difficulties in accurately replicating observed streamflow dynamics, even after extensive parameter sensitivity analysis and many calibration efforts. Initial model runs highlighted a persistent hydrology warning indicating excessive water yield, low surface runoff, and a high groundwater ratio. This aligns with the sensitivity analysis results, strongly suggesting the model disproportionately routed water through subsurface pathways while underrepresenting overland flow contributions which discovered as the common challenge in SWAT models (Gasirabo et al., 2023). Land use summary evaluations further supported this

imbalance, identifying extreme evapotranspiration values and excessive surface runoff in certain land uses, alongside unusually high biomass yields, implying misrepresentation of water balance components and overestimated plant productivity (Arnold et al., 2012).

These observations are quantitatively supported by the water balance and partitioning ratios. The streamflow-to-precipitation ratio of 0.29 indicates that only 29% of total precipitation exits the catchment as streamflow, within acceptable limits for temperate, semi-humid environments such as Lesotho and the broader Orange River Basin (Mahasa et al., 2023). However, this streamflow is entirely composed of baseflow (100%), with no surface runoff contribution (0.00), reinforcing earlier warnings and suggesting the model failure to simulate quick-flow responses typically associated with storm events and overland flow.

Furthermore, 66% of precipitation is lost through evapotranspiration, a value that falls within global and regional normal but warrants caution due to its spatial concentration and potential link to parameter overestimation. The percolation-to-precipitation ratio (0.34) and deep recharge (0.02) also point to excessive vertical movement of water through the soil profile, contributing to sustained but unrealistic baseflow dominance. Generally, these findings suggest that while overall water budget closure is numerically acceptable (-7.27 mm imbalance), the internal flow partitioning is physically inconsistent with expected hydrological behaviour in South Phuthiatsana catchment terrain and climate. As such, these results highlight the need for better representation of surface runoff processes, more localised calibration of ET and plant growth parameters, and possibly improved resolution soil and land use datasets.

With NSE values of 0.17 and 0.20 and KGE of 0.14 and 0.35 for the calibration and validation periods, respectively, the SWAT+ model performed poorly in simulating historical streamflow for the South Phuthiatsana catchment despite a thorough parameter sensitivity analysis and numerous calibration attempts. These numbers demonstrate the model's inadequate capacity to replicate known hydrological processes and are below the widely accepted threshold of 0.50 for adequate daily streamflow simulations (Abbaspour et al., 2015; Moriasi et al., 2007). Given these major performance limitations, direct prediction of future streamflow using the physically-based SWAT+ model under climatic conditions was deemed unreliable. In accordance with recommendations that

underperforming models should not be used for scenario analysis (Krysanova et al., 2018), an alternative approach was necessary.

Consequently, XGBoost machine learning algorithm was adopted. The XGBoost algorithm, trained using bias-adjusted climate inputs and historically recorded streamflow, was subsequently applied to estimate future discharge conditions aligned with SSP2-4.5 and SSP5-8.5 trajectories. The resulting simulations form the basis for investigating how projected climatic changes may influence streamflow extremes and broader watershed dynamics. The transition to a data-driven modeling approach, such as XGBoost, reflects a growing trend in hydrological research, particularly in cases where physically based models face limitations due to catchment complexity or data scarcity, as machine learning techniques are well-suited to capturing intricate, non-linear patterns (Vogeti et al., 2022).

5.4 Projected Hydrological Impacts of Climate Change on Streamflow

A detailed examination of streamflow behaviour encompassing flow patterns, monthly discharge trends, and the frequency of extreme events using the XGBoost model reveals notable and multifaceted changes in the hydrological system projected for 2041–2080. These findings highlight the pressing importance of implementing flexible and resilient water governance approaches within the South Phuthiatsana catchment.

5.4.1 Shifts in Extreme High Flows (Floods)

The findings from the XGBoost model consistently show that the frequency and size of high-flow occurrences are expected to significantly decline. This is evidenced by the high-flow frequency curve (**Figure 26**), where projected peak flows for both SSP2-4.5 and SSP5-8.5 scenarios are significantly smaller than historical values for any given return period. For instance, the Q98 flow (exceeded only 2% of the time, representing very high flood events) is projected to decrease by over 52% under both scenarios (from approximately 33.7 m^3/s historically to around 16.1 m^3/s). This substantial decrease is further supported by quantile analysis (**Figure 28**), where the highest flow percentiles (Q90, Q95, and Q98) from XGBoost simulations show a marked decrease in magnitude compared to historical flows, consistently falling below the historical flood threshold.

The monthly high-flow day analysis further reinforces this trend, showing projected decreases in the number of days exceeding the historical Q10 threshold across almost all months. This is consistent with broader trends indicating a reduction in monthly exceedance days due to climate change, altering flood seasonality and duration (Thompson et al., 2021). Collectively, these outcomes indicate a reduction in flood risk regarding peak magnitude and event frequency, potentially relieving stress on infrastructure and property from flood damages. This decrease is directly linked to the projected changes in seasonal rainfall patterns and an increase in evapotranspiration due to rising air temperatures, both of which reduce the water available for rapid runoff generation and negatively affect streamflow. Similar hydrological modeling studies have also documented reductions in high-flow quantiles under future scenarios (Sapač et al., 2019). For example, in water-stressed, semi-arid catchments within the Western Cape or the Limpopo River Basin, hydrological projections also show a decline in extreme high flow events (Botai et al., 2021). This counter-intuitive trend is attributed to the combined effect of increased PET losses and longer dry spells that prevent the soil from reaching the saturation levels required to generate large-scale storm runoff (Benti et al., 2025, Mokua et al., 2024). This shift toward fewer extreme high flows could be a consequence of increased evaporative demand and potentially more dispersed rainfall events, preventing the buildup of conditions for large flood peaks.

5.4.2 Low Flow Dynamics and Drought Implications

Conversely, the low-flow frequency curves (**Figure 27**) indicate a significant relief of extreme drought conditions with a decreased chance of total drying. A dramatic shift is observed from a historical period with near-zero 7-day annual minimum flows to future scenarios with positive flow magnitudes. For example, the Q1 flow (exceeded 99% of the time) increases from a historical near-zero (0.0006 m^3/s) to approximately 9.0 m^3/s under both SSPs, signifying a major change from what was possibly an intermittent or sometimes dry river to one with constant, substantial baseflow. The Q5 and Q10 flows are also expected to rise significantly. These findings align with research using XGBoost for low-flow forecasting, which has shown its efficacy in capturing extremes (Laimighofer et al., 2022).

The frequency of low-flow days, however, presents a more complex picture. The elevated emissions pathway, represented by SSP5-8.5, exhibits a higher frequency of days when flow goes below the historical Q90 level in a number of months, particularly in late spring and early summer (**Figure 25**). This implies that the South Phuthiatsana catchment is anticipated to have more frequent low flows (i.e., longer length of moderate dry periods) than it has historically, even though absolute minimum flows are predicted to increase. Other CMIP6-based hydrological evaluations have documented this twofold reaction, which consists of more frequent sub-threshold situations and greater absolute minima (Hasan et al., 2023). Potential drivers include heightened evaporative demand from increased air temperatures, changes in precipitation regimes leading to longer dry spells, and diminished groundwater contributions. The slightly larger 7-day minima projected by SSP5-8.5 compared to SSP2-4.5 might reflect how the XGBoost model reacts to warmer and more evaporative conditions, potentially leading to larger absolute low flows under the warmest pathway even as baseline flows overall decrease (Mutlu et al., 2025). The persistence of moderate dry spells despite higher absolute minima points to a complex interplay of factors, where increased temperatures drive evaporative losses, even if overall water availability remains higher due to changes in rainfall distribution (Yılmaz & Tosunoğlu, 2024). This apparent paradox where severe low-flow conditions (Q_5) appear less frequent or intense, while moderate low-flow events (Q_{90} exceedances) increase is increasingly plausible under projected climate conditions across semi-arid Southern Africa. For example, recent studies show divergent trends in low-flow quantiles, with some catchments experiencing decreases in extreme low flows but increases in moderate drought frequency. Similarly, streamflow-based drought assessments across the Cape Provinces highlight a rise in hydrological drought frequency despite mixed severity patterns (Botai et al., 2024). These findings align with a growing recognition of baseflow-dominated regimes, where extended dry intervals produce frequent moderate droughts despite less pronounced extremes (Mokua et al., 2024).

5.4.3 Overall Hydrologic Regime Shifts

Based on XGBoost-projected streamflow, the comprehensive quantile analysis (***Figure 28***) shows a distinct reshaping of the entire flow distribution. High percentiles (Q90–Q98) contract, indicating fewer extreme highs, while low to mid-range percentiles (Q1–Q75) significantly increase,

indicating a generally wetter daily flow regime. For example, the Q25 flow is projected to increase from 0.41 m^3/s to 11.3 m^3/s (a 2600% increase), while the median flow (Q50) increases from 1.4 m^3/s to 12.4 m^3/s (770%), and the Q75 flow increases from 3.77 m^3/s to 13.5 m^3/s (260%). Similar trends have been observed in hydrological experiments using boosting algorithms, with XGBoost accurately simulating both low and median streamflow under shifting climate forcings (Mishra et al., 2024).

These dynamics suggest that the river may become more stable with higher baseline flows and fewer extremes, indicating changed hydrological behaviour. Climate-driven changes in precipitation intensity, evapotranspiration, and seasonality have been associated with similar shifts in streamflow distributions worldwide, moving from more variable regimes to more stable ones (Estrada et al., 2024). While the decrease in high flow extremes means less frequent significant flood-based recharge events, the overall trend towards generally higher mid-range flows translates to more water being available for a larger percentage of the year. This increased stability, while generally beneficial, might alter ecological dynamics that depend on natural flow variability.

5.5 Implications for Water Resources Management

The anticipated climatic changes, marked by increased temperatures and altered precipitation patterns, along with specific changes in streamflow extremes and regimes projected by XGBoost mode, will significantly impact water resources management in the South Phuthiatsana catchment.

The projected decrease in flood frequency and severity in the South Phuthiatsana catchment suggests reduced risks to human safety and agricultural productivity. However, this reduction may also disrupt natural flood pulses, which play a vital role in sediment transport, groundwater recharge, and the ecological integrity of riparian zones. These findings align with broader concerns in semi-arid regions, where diminished flood activity can compromise key ecohydrological functions (Calderwood et al., 2024). Such trade-offs highlight the need for integrated water resource planning that balances flood risk reduction with ecosystem sustainability.

The complex shifts in low flows present both opportunities and challenges. While the potential reduction in the most severe dry-outs (avoiding zero-flow times) is beneficial for aquatic life and

ensuring a constant water supply, the projected increase in the number of historically low-flow days in some months, for example, September and October, suggests continued or even increased water stress during these periods. This could strain current water allocation systems and intensify competition for scarce resources across domestic, agricultural (where increased low flows could benefit irrigation downstream), and industrial sectors, mostly in the prolonged dry season (May-September). Proactive strategies, such as improved water conservation measures, efficient irrigation techniques, and the development of alternative water sources, will be critical (Döll et al., 2016).

Furthermore, the overall trend toward generally higher mid-range flows implies more water availability for a large percentage of the year. This offers opportunities for improved water collection and storage, particularly when combined with anticipated seasonal increases in winter precipitation. However, the reduction in high-flow extremes might mean less frequent major flood-based recharge events. The observed shifts in climate and hydrological responses, as indicated by model results, underscore the need for robust early warning systems addressing both water scarcity and localised flash flood risks. Adaptive water management strategies should be responsive to changes in rainfall timing and magnitude, while existing water harvesting systems may require redesign or enhancement to accommodate more frequent or intense rainfall events (Gabriela & Vladimir, 2022). Most importantly, these changes will have a significant influence on the livelihoods of communities dependent on the South Phuthiatsana river, as well as on Maseru and neighbouring towns that rely on the catchment for water. The changes will also significantly impact aquatic biodiversity and ecosystem health.

Despite the modeling constraints, the knowledge gained from this study about these particular shifts in flow extremes and regime is crucial for creating proactive and adaptive water management plans in the South Phuthiatsana catchment, ensuring long-term water security in the face of climate change.

5.6 Uncertainty, Limitations, and Future Research Directions

The results and projected impacts must be interpreted within the context of the acknowledged limitations and the inherent uncertainties of the climate impact modeling chain. This section

explicitly discusses the trade-offs made and the sources of uncertainty across the modeling framework.

5.6.1 Hydrological Model Limitations and Methodological Trade-offs

This study's primary limitation stems from the poor performance of the physically-based SWAT+ model in simulating historical streamflow for the South Phuthiatsana catchment. Despite extensive calibration efforts and sensitivity analysis, the model consistently misrepresented hydrological processes, most notably by disproportionately routing flow through subsurface pathways and producing negligible surface runoff. This compromised the credibility of its process-based outputs and raised concerns about its applicability in this particular hydrological and climatic context.

As a result, the study employed the XGBoost machine learning model as an alternative, prioritising empirical performance over process representation. This shift, while improving predictive accuracy, is a methodological trade-off that limited the ability to interpret projections in terms of catchment-scale physical processes (changes in groundwater contribution or ET partitioning), highlighting a fundamental limitation in the explanatory power of the final impact results. Moreover, the climate and streamflow data quality available for model training also restricted the satisfactory performance of the models.

5.6.2 Sources of Climate and Scenario Uncertainty

The projections are subject to uncertainties originating from various stages of the climate modeling process:

a) GCM Model Uncertainty: This study specifically utilised results from one GCM, MPI-ESM1-2-LR. While this model was selected based on its ability to simulate past climate, dependence on a single model inevitably introduces GCM uncertainty, as different GCMs may forecast different climate futures due to variations in their underlying physical processes and parameterisations.
b) Scenario Uncertainty: Although two future emissions scenarios (SSP2-4.5 and SSP5-8.5) were examined, they depict only a limited range of potential climate trajectories based on human socioeconomic choices (IPCC, 2021).

c) Bias Correction Uncertainty: Despite the application of bias correction techniques (multiplicative quantile mapping and linear scaling) to lessen systematic biases in raw GCM outputs, some uncertainties remain, especially those pertaining to GCM structural faults or their capacity to accurately depict extreme occurrences at finer scales. The statistical downscaling process itself relies on assumptions, such as the stationarity of historical relationships, which may not hold perfectly under a changing climate, potentially introducing additional uncertainties into the projected climate inputs (Tootoonchi et al., 2023).

5.6.3 Critical Limitations of the XGBoost Algorithm

A key limitation of the XGBoost algorithm is its limited sensitivity to the different future climatic forcings. Despite differing emission scenarios between SSP2-4.5 and SSP5-8.5, the model produced similar streamflow outputs under both scenarios. This suggests that the model may not adequately capture non-linear hydrological responses to more extreme climate conditions, potentially due to the nature of the input features or the training data range (Mulu et al., 2025). This sensitivity often arises from statistical models being trained on historical data that may not fully encompass the range of future climatic conditions, forcing the model to extrapolate rather than simulate physical processes (Martel et al., 2024).

5.6.4 Recommendations for Future Research

To yield more comprehensive findings about the future of South Phuthiatsana catchment's water resources, future research should focus on:

a) Multi-Model Ensemble: Utilising a multi-model ensemble mean of GCMs to better characterise the range of plausible future climate conditions and significantly reduce model-specific uncertainties (IPCC, 2021).
b) Integrating Anthropogenic Factors: While the current study focused on climate-driven variables, future research should explicitly account for local-scale human interventions such as land use changes, water demand management, dam operations, urbanisation, or water transfers (Hoang et al., 2016; Chawanda et al., 2023). Integrating these anthropogenic factors

is crucial for a holistic understanding of water availability and demand in a changing environment, as these factors can significantly impact flow regimes.

6 Conclusion and Recommendations

6.1 Introduction

This chapter presents a summary of the major results and interpretations from the investigation into how climate change is expected to affect streamflow within the South Phuthiatsana catchment. It begins with a summary of the methodological framework, emphasising the challenges encountered with the SWAT+ model and the rationale for transitioning to the XGBoost model. The chapter then presents the core results related to future climate projections and their anticipated effects on streamflow dynamics, including analyses of extreme hydrological events and potential regime shifts. Finally, it provides recommendations for water resource management, aimed at supporting proactive and adaptive strategies to enhance water security under changing climatic conditions.

6.2 Conclusion

The South Phuthiatsana catchment, as a key hydrological system supporting municipal, industrial, and agricultural water demands in Maseru and surrounding areas, underscores the necessity of robust and accurate streamflow simulation to inform long-term water resource management under changing climatic conditions. This research focused on assessing the impacts of anticipated climatic changes on streamflow, utilising bias-corrected outputs from the MPI-ESM1-2-LR General Circulation Model (GCM).

While bias correction successfully enhanced the accuracy of temperature and precipitation projections, SWAT+ exhibited poor performance in simulating historical daily streamflow. This was evidenced by low NSE and KGE values, indicating its limited ability to capture the dynamic behaviour (timing and magnitude of peaks and troughs) of streamflow. Furthermore, the model showed significant hydrological imbalances and generally underestimated streamflow. These limitations, highlighted through a comprehensive sensitivity analysis, revealed the dominant role of subsurface flow mechanisms such as minimum threshold flow rate (flo_min) and the influence of surface runoff generation (cn2) and interception (canmax) in the catchment's hydrology. Due to these performance issues, direct streamflow projections under future climate scenarios were not

performed. Direct streamflow forecasts under future climate scenarios have been considered unreliable due to these basic performance problems with the SWAT+ in simulating historical streamflow conditions. As a result, a strong data-driven machine learning technique, the XGBoost model was used as a substitute to predict future streamflow, enabling a thorough examination of hydrological effects.

The examination of bias-corrected downscaled climate projections consistently showed a steady warming trend throughout all future periods and scenarios, with SSP5-8.5 predicting more severe temperature increases. Precipitation projections revealed large seasonal variations, with significant drying projected for June and August, alongside possible increases in July and May. These climate shifts align with the observed weak declining trend in historical mean annual streamflow and non-significant monthly decreases in critical periods (February and November), suggesting a potential for reduced water availability.

Additionally, the hydrology of the catchment underwent a complex but noticeable shift as a result of the XGBoost-based study of future streamflow extremes and regime shifts. The study predicts a considerable decline in the amplitude of extreme high flows (over 52% reduction for the Q98 flow), which suggests a possible relief of severe flood hazards, in contrast to a general increase in high-flow occurrences. A fundamental change from historically intermittent or near-dry conditions to a more perennial flow regime with significant baseflow is indicated by the analysis's simultaneous significant increase in low flows (Q1 flows rising from near-zero to around 9.0 m^3/s).

Generally, these results clearly point to a change in the South Phuthiatsana catchment toward more variable but simultaneously more stable (buffered) hydrological and climatic conditions. Although there were issues with the physical-based SWAT+ model's performance, the thorough hydrological extremes analysis using the XGBoost model and the strong insights obtained from the bias-corrected climate projections offer an essential quantitative basis for comprehending the likely effects of climate change. This knowledge is vital for creating proactive and adaptive water management plans in the South Phuthiatsana catchment, which will ultimately guarantee sustainable water security.

6.3 Recommendations

Drawing from the validated climate projections and the anticipated effects of shifting flow patterns within the South Phuthiatsana catchment, the following recommendations are framed as actionable mandates to enhance water resource management and policy coherence.

6.3.1 Recommendations for Water Resource Management

These recommendations directly address the projected shifts in hydrological extremes and the overall flow regime:

a) Prioritise Drought Frequency Resilience over Flood Defence: Given the significant projected decline in extreme high flows (Q_{98} reducing by over 52%), the strategic focus and allocation of infrastructure funding should shift away from large-scale flood control defence projects. Instead, water management policy should mandate the prioritisation of resilience measures to manage the anticipated increased frequency of moderate low-flow periods (Q_{90} exceedances).
b) Integrate Climate Metrics into Operational Planning: Water managers must formally integrate the XGBoost-derived flow quantiles (Q_5, Q_{10}, Q_{90}, Q_{50}) into the next revision cycle of the South Phuthiatsana Integrated Catchment Management Plan. This is vital to update operational flood thresholds and drought management triggers, ensuring that infrastructure is managed based on new climate realities rather than historical extremes.
c) Optimise Storage for Perennial Flow: The finding of a fundamental shift toward a more perennial flow regime (Q_1 increasing from near-zero to 9.0 m^3/s) presents an opportunity. Water storage infrastructure should be optimised to capture the now higher, more stable baseflow rather than relying solely on high-magnitude flood pulses for recharge. This includes scaling up and optimising rainwater harvesting and enhancing decentralised storage capacity to buffer the longer dry spells projected between rainfall events.

6.3.2 Recommendations for Modeling and Scientific Advancement

To address the methodological limitations identified in this study, particularly those related to uncertainty, several key actions are recommended. First, to mitigate the inherent uncertainty

associated with the reliance on a single global climate model (GCM) (MPI-ESM1-2-LR), and to address the observed insensitivity of the XGBoost model to variations across Shared Socioeconomic Pathways (SSPs), it is imperative that water authorities mandate the use of a multi-model ensemble. Specifically, future climate change impact assessments should incorporate at least five GCMs from the CMIP6 archive. This ensemble approach will yield a more comprehensive and reliable probability distribution of future outcomes, thereby improving the quality of information available to decision-makers.

Additionally, there is a strong need to develop and adopt an integrated hybrid modeling framework that combines the process-based realism of SWAT+ particularly valuable for interpreting water balance dynamics with the high predictive performance of XGBoost, especially in forecasting extreme events. This hybrid approach is crucial not only for improving forecasting accuracy across different scenarios but also for enhancing transparency and building trust among end-users and stakeholders.

References

Abbaspour, K.C., Rouholahnejad, E., Vaghefi, S., Srinivasan, R., Yang, H., Kløve, B., 2015. A continental-scale hydrology and water quality model for Europe: Calibration and uncertainty of a high-resolution large-scale SWAT model. Journal of Hydrology 524, 733–752. https://doi.org/10.1016/j.jhydrol.2015.03.027

Abdulahi, S.D., Abate, B., Harka, A.E., Husen, S.B., 2022. Response of climate change impact on streamflow: the case of the Upper Awash sub-basin, Ethiopia. Journal of Water and Climate Change 13, 607–628. https://doi.org/10.2166/wcc.2021.251

Abdule, A.M., Muluneh, A., Woldemichael, A., 2024. Modeling climate change projection and its impact on the streamflow in the Yadot watershed, Genale Dawa basin, Ethiopia. Journal of Water and Climate Change 15, 3487–3505. https://doi.org/10.2166/wcc.2024.404

Abeshu, G.W., Tian, F., Wild, T., Zhao, M., Turner, S., Chowdhury, A.F.M.K., Vernon, C.R., Hu, H., Zhuang, Y., Hejazi, M., Li, H.-Y., 2023. Enhancing the representation of water management in global hydrological models. Geosci. Model Dev. 16, 5449–5472. https://doi.org/10.5194/gmd-16-5449-2023

Adeniyi, M.O., 2016. The consequences of the IPCC AR5 RCPs 4.5 and 8.5 climate change scenarios on precipitation in West Africa. Climatic Change 139, 245–263. https://doi.org/10.1007/s10584-016-1774-2

Akoko, G., Le, T.H., Gomi, T., Kato, T., 2021. A Review of SWAT Model Application in Africa. Water 13, 1313. https://doi.org/10.3390/w13091313

Alexander, P., Henry, R., Rabin, S., Arneth, A., Rounsevell, M., 2023. Mapping the shared socio-economic pathways onto the Nature Futures Framework at the global scale. Sustain Sci. https://doi.org/10.1007/s11625-023-01415-z

Alfieri, L., Bisselink, B., Dottori, F., Naumann, G., De Roo, A., Salamon, P., Wyser, K., Feyen, L., 2017. Global projections of river flood risk in a warmer world. Earth's Future 5, 171–182. https://doi.org/10.1002/2016EF000485

Ali, M., Jamei, M., Prasad, R., Karbasi, M., Xiang, Y., Cai, B., Abdulla, S., Ahsan Farooque, A., Labban, A.H., 2023. New achievements on daily reference evapotranspiration forecasting: Potential assessment of multivariate signal decomposition schemes. Ecological Indicators 155, 111030. https://doi.org/10.1016/j.ecolind.2023.111030

Althoff, D., Rodrigues, L.N., 2021. Goodness-of-fit criteria for hydrological models: Model calibration and performance assessment. Journal of Hydrology 600, 126674. https://doi.org/10.1016/j.jhydrol.2021.126674

Arfasa, G.F., Owusu-Sekyere, E., Doke, D.A., 2024. Climate Change Projections and Impacts on Future Temperature, Precipitation, and Stream flow in the Vea Catchment, Ghana. Environmental Challenges 14, 100813. https://doi.org/10.1016/j.envc.2023.100813

Asquith, W., 2024. Cran R Project.

Assfaw, M.T., Neka, B.G., Ayele, E.G., 2023. Modeling the impact of climate change on streamflow responses in the Kessem watershed, Middle Awash sub-basin, Ethiopia. Journal of Water and Climate Change 14, 4837–4859. https://doi.org/10.2166/wcc.2023.541

Ayalew, D.W., Asefa, T., Moges, M.A., Leyew, S.M., 2022. Evaluating the potential impact of climate change on the hydrology of *Ribb* catchment, Lake Tana Basin, Ethiopia. Journal of Water and Climate Change 13, 190–205. https://doi.org/10.2166/wcc.2021.049

Bai, P., Liu, X., 2018. Evaluation of Five Satellite-Based Precipitation Products in Two Gauge-Scarce Basins on the Tibetan Plateau. Remote Sensing 10, 1316. https://doi.org/10.3390/rs10081316

Banda, V.D., Dzwairo, R.B., Singh, S.K., Kanyerere, T., 2024. Quantifying the influence of climate change on streamflow of Rietspruit sub-basin, South Africa. Journal of Water and Climate Change 15, 2282–2308. https://doi.org/10.2166/wcc.2024.690

Basheer, A.K., Lu, H., Omer, A., Ali, A.B., Abdelgader, A.M.S., 2016. Impacts of climate change under CMIP5 RCP scenarios on the streamflow in the Dinder River and ecosystem habitats in Dinder National Park, Sudan. Hydrol. Earth Syst. Sci. 20, 1331–1353. https://doi.org/10.5194/hess-20-1331-2016

Bekele, D., Alamirew, T., Kebede, A., Zeleke, G., M. Melesse, A., 2019. Modeling Climate Change Impact on the Hydrology of Keleta Watershed in the Awash River Basin, Ethiopia. Environ Model Assess 24, 95–107. https://doi.org/10.1007/s10666-018-9619-1

Benti, K.K., Dinka, M.O., Rwanga, S.S., Aredo, M.R., 2025. Assessing Streamflow Response to Climate Change Under Shared Socioeconomic Pathways (SSPs) in the Olifants River Basin, South Africa. Hydrology 12, 244. https://doi.org/10.3390/hydrology12090244

Bieger, K., Arnold, J.G., Rathjens, H., White, M.J., Bosch, D.D., Allen, P.M., Volk, M., Srinivasan, R., 2017. Introduction to SWAT +, A Completely Restructured Version of the Soil and Water Assessment Tool. J American Water Resour Assoc 53, 115–130. https://doi.org/10.1111/1752-1688.12482

Bienvenido-Huertas, D., Sánchez-García, D., Rubio-Bellido, C., 2022. Influence of the RCP scenarios on the effectiveness of adaptive strategies in buildings around the world. Building and Environment 208, 108631. https://doi.org/10.1016/j.buildenv.2021.108631

Botai, C.M., De Wit, J.P., Botai, J.O., 2024. Temporal Variability of Hydroclimatic Extremes: A Case Study of Vhembe, uMgungundlovu, and Lejweleputswa District Municipalities in South Africa. Water 16, 2924. https://doi.org/10.3390/w16202924

Brunner, M.I., Melsen, L.A., Newman, A.J., Wood, A.W., Clark, M.P., 2020. Future streamflow regime changes in the United States: assessment using functional classification. Hydrol. Earth Syst. Sci. 24, 3951–3966. https://doi.org/10.5194/hess-24-3951-2020

Byun, K., Sharma, A., Wang, J., Tank, J.L., Hamlet, A.F., 2022. Intercomparison of Dynamically and Statistically Downscaled Climate Change Projections over the Midwest and Great Lakes Region. Journal of Hydrometeorology 23, 659–679. https://doi.org/10.1175/JHM-D-20-0282.1

Calderwood, A.J., Rodriguez, A., Foglia, L., Dahlke, H.E., 2024. Evaluating levee setback distance for the co-benefits of groundwater recharge and riparian ecosystem function. Front. Environ. Sci. 12, 1421237. https://doi.org/10.3389/fenvs.2024.1421237

Chakilu, G.G., Sándor, S., Zoltán, T., 2023. The Dynamics of Hydrological Extremes under the Highest Emission Climate Change Scenario in the Headwater Catchments of the Upper Blue Nile Basin, Ethiopia. Water 15, 358. https://doi.org/10.3390/w15020358

Chawanda, C.J., George, C., Thiery, W., Griensven, A.V., Tech, J., Arnold, J., Srinivasan, R., 2020. User-friendly workflows for catchment modelling: Towards reproducible SWAT+ model studies. Environmental Modelling & Software 134, 104812. https://doi.org/10.1016/j.envsoft.2020.104812

Chawanda, C.J., Nkwasa, A., Thiery, W., Van Griensven, A., 2024. Combined impacts of climate and land-use change on future water resources in Africa. Hydrol. Earth Syst. Sci. 28, 117–138. https://doi.org/10.5194/hess-28-117-2024

Chen, T., Guestrin, C., 2016. XGBoost: A Scalable Tree Boosting System, in: Proceedings of the 22nd ACM SIGKDD International Conference on Knowledge Discovery and Data Mining. Presented at the KDD '16: The 22nd ACM SIGKDD International Conference on Knowledge Discovery and Data Mining, ACM, San Francisco California USA, pp. 785–794. https://doi.org/10.1145/2939672.2939785

Chen, W., Cui, H., Zheng, J., 2024. Prediction of Clausius–Clapeyron Scaling of Daily Precipitation Extremes over China. Journal of Climate 37, 165–177. https://doi.org/10.1175/JCLI-D-23-0030.1

Cheng, L., Von Schuckmann, K., Minière, A., Hakuba, M.Z., Purkey, S., Schmidt, G.A., Pan, Y., 2024. Ocean heat content in 2023. Nat Rev Earth Environ 5, 232–234. https://doi.org/10.1038/s43017-024-00539-9

Cohen, J., 2021. GISS and NCCS Contribute to CMIP6 International Climate Model Intercomparison Project.

Copernicus Climate Change Service, 2021. CMIP6 predictions underpinning the C3S decadal prediction prototypes. https://doi.org/10.24381/CDS.C82DEDDB

Cruz-Gaistardo, C.O., 2016. Report of the World Soil Classification Congress. South Africa, 2016. Presented at the International Soil Classification Congress 2016, Bloemfontein, South Africa.

D. N. Moriasi, J. G. Arnold, M. W. Van Liew, R. L. Bingner, R. D. Harmel, T. L. Veith, 2007. Model Evaluation Guidelines for Systematic Quantification of Accuracy in Watershed Simulations. Transactions of the ASABE 50, 885–900. https://doi.org/10.13031/2013.23153

Daniel, H., Abate, B., 2022. Effect of climate change on streamflow in the Gelana watershed, Rift valley basin, Ethiopia. Journal of Water and Climate Change 13, 2205–2232. https://doi.org/10.2166/wcc.2022.059

De Girolamo, A.M., Lo Porto, A., Pappagallo, G., Gallart, F., 2015. Assessing flow regime alterations in a temporary river – the River Celone case study. Journal of Hydrology and Hydromechanics 63, 263–272. https://doi.org/10.1515/johh-2015-0027

Dieppois, B., Pohl, B., Rouault, M., New, M., Lawler, D., Keenlyside, N., 2016. Interannual to interdecadal variability of winter and summer southern African rainfall, and their teleconnections. JGR Atmospheres 121, 6215–6239. https://doi.org/10.1002/2015JD024576

Dierauer, J.R., Allen, D.M., Whitfield, P.H., 2021. Climate change impacts on snow and streamflow drought regimes in four ecoregions of British Columbia. Canadian Water Resources Journal / Revue canadienne des ressources hydriques 46, 168–193. https://doi.org/10.1080/07011784.2021.1960894

Dobson, B., Liu, L., Mijic, A., 2024. Modelling water quantity and quality for integrated water cycle management with the Water Systems Integrated Modelling framework (WSIMOD) software. Geosci. Model Dev. 17, 4495–4513. https://doi.org/10.5194/gmd-17-4495-2024

Döll, P., Douville, H., Güntner, A., Müller Schmied, H., Wada, Y., 2016. Modelling Freshwater Resources at the Global Scale: Challenges and Prospects. Surv Geophys 37, 195–221. https://doi.org/10.1007/s10712-015-9343-1

Dondeyne, S., Vanierschot, L., Langohr, R., Ranst, E.V., Deckers, J., 2014. The soil map of the Flemish region converted to the 3rd edition of the World Reference Base for soil resources. https://doi.org/10.13140/2.1.4381.4089

Eccles, R., Zhang, H., Hamilton, D., 2019. A review of the effects of climate change on riverine flooding in subtropical and tropical regions. Journal of Water and Climate Change 10, 687–707. https://doi.org/10.2166/wcc.2019.175

Eckstein, D., Künzel, V., Schäfer, L., 2021. Global Climate Risk Index 2021: Who Suffers Most from Extreme Weather Events? (Indices). German Watch.

Ellenburg, W.L., Cruise, J.F., Singh, V.P., 2018. The role of evapotranspiration in streamflow modeling – An analysis using entropy. Journal of Hydrology 567, 290–304. https://doi.org/10.1016/j.jhydrol.2018.09.048

El-Samra, R., Haddad, A., Alameddine, I., Bou-Zeid, E., El-Fadel, M., 2024. Downscaling Climatic Variables at a River Basin Scale: Statistical Validation and Ensemble Projection under Climate Change Scenarios. Climate 12, 27. https://doi.org/10.3390/cli12020027

Enayati, M., Bozorg-Haddad, O., Bazrafshan, J., Hejabi, S., Chu, X., 2021. Bias correction capabilities of quantile mapping methods for rainfall and temperature variables. Journal of Water and Climate Change 12, 401–419. https://doi.org/10.2166/wcc.2020.261

Engelbrecht, F.A., Steinkopf, J., Padavatan, J., Midgley, G.F., 2024. Projections of Future Climate Change in Southern Africa and the Potential for Regional Tipping Points, in: Von Maltitz, G.P., Midgley, G.F., Veitch, J., Brümmer, C., Rötter, R.P., Viehberg, F.A., Veste, M. (Eds.), Sustainability of Southern African Ecosystems under Global Change, Ecological Studies. Springer International Publishing, Cham, pp. 169–190. https://doi.org/10.1007/978-3-031-10948-5_7

Estrada, L., Garcia, X., Saló-Grau, J., Marcé, R., Munné, A., Acuña, V., 2024. Spatio-temporal patterns and trends of streamflow in water-scarce Mediterranean basins. Hydrol. Earth Syst. Sci. 28, 5353–5373. https://doi.org/10.5194/hess-28-5353-2024

Fan, X., Duan, Q., Shen, C., Wu, Y., Xing, C., 2020. Global surface air temperatures in CMIP6: historical performance and future changes. Environ. Res. Lett. 15, 104056. https://doi.org/10.1088/1748-9326/abb051

FAO, 2023. Lesotho: Land Cover - Atlas 2017-2023 (No. 2665927). Maseru.

Fobo, L., 2021. Predicting hydrological droughts from a Standardized precipitation index (SPI) in South Phuthiatsana River basin, Lesotho. (Thesis).

Gasirabo, A., Xi, C., Kurban, A., Liu, T., Baligira, H.R., Umuhoza, J., Umugwaneza, A., Dufatanye Edovia, U., 2023. SWAT model calibration for hydrological modeling using concurrent methods, a case of the Nile Nyabarongo River basin in Rwanda. Front. Water 5, 1268593. https://doi.org/10.3389/frwa.2023.1268593

Gidden, M.J., Riahi, K., Smith, S.J., Fujimori, S., Luderer, G., Kriegler, E., Van Vuuren, D.P., Van Den Berg, M., Feng, L., Klein, D., Calvin, K., Doelman, J.C., Frank, S., Fricko, O., Harmsen, M., Hasegawa, T., Havlik, P., Hilaire, J., Hoesly, R., Horing, J., Popp, A., Stehfest, E., Takahashi, K., 2019. Global emissions pathways under different socioeconomic scenarios for use in CMIP6: a

dataset of harmonized emissions trajectories through the end of the century. Geosci. Model Dev. 12, 1443–1475. https://doi.org/10.5194/gmd-12-1443-2019

Gradiyanto, F., Parmantoro, P.N., Suharyanto, 2025. Impact of climate change on Kupang River flow and hydrological extremes in Greater Pekalongan, Indonesia. Water Science and Engineering 18, 69–77. https://doi.org/10.1016/j.wse.2024.03.005

Gutjahr, O., Putrasahan, D., Lohmann, K., Jungclaus, J.H., Von Storch, J.-S., Brüggemann, N., Haak, H., Stössel, A., 2019. Max Planck Institute Earth System Model (MPI-ESM1.2) for the High-Resolution Model Intercomparison Project (HighResMIP). Geosci. Model Dev. 12, 3241–3281. https://doi.org/10.5194/gmd-12-3241-2019

Han, X., Bocchiola, D., 2025. Analysis of future climate variability under CMIP6 scenarios based on a downscaling method considering wet days in the upper Yangtze River basin, China. Theor Appl Climatol 156, 101. https://doi.org/10.1007/s00704-024-05331-9

Hasan, M.M., Strong, C., Brooks, P.D., Burian, S.J., Barber, M.E., 2023. Quantifying climate change impacts on low flows of small high mountain watersheds: A nonstationary approach. Journal of Hydrology: Regional Studies 48, 101463. https://doi.org/10.1016/j.ejrh.2023.101463

Heidy Gabriela, R.M., Jose Vladimir, C.T., 2022. Rainwater harvesting system as a strategy for adaptation on climate change: A review. IOP Conf. Ser.: Earth Environ. Sci. 1121, 012007. https://doi.org/10.1088/1755-1315/1121/1/012007

Hlalele, B.M., 2020. Variability analysis of dry spells for improving agribusiness management in Lesotho. Jàmbá Journal of Disaster Risk Studies 12. https://doi.org/10.4102/jamba.v12i1.814

Hoang, L.P., Lauri, H., Kummu, M., Koponen, J., Van Vliet, M.T.H., Supit, I., Leemans, R., Kabat, P., Ludwig, F., 2016. Mekong River flow and hydrological extremes under climate change. Hydrol. Earth Syst. Sci. 20, 3027–3041. https://doi.org/10.5194/hess-20-3027-2016

Ibrahim, U.A., Dan'azumi, S., 2020. An overview of some hydrological models in water resourcesengineering systems. Faculty of Engineering, University of Maiduguri, Maiduguri, Nigeria 16, 285–292.

Intergovernmental Panel On Climate Change (Ipcc), 2023. Climate Change 2022 – Impacts, Adaptation and Vulnerability: Working Group II Contribution to the Sixth Assessment Report of the Intergovernmental Panel on Climate Change, 1st ed. Cambridge University Press. https://doi.org/10.1017/9781009325844

IPCC, 2021. Climate Change 2021: The Physical Science Basis. Contribution of Working Group I to the Sixth Assessment Report of the Intergovernmental Panel on Climate Change (In Press).

IPCC, Thorne, P.W., Trisos, C., Romero, J., Aldunce, P., Barrett, K., Blanco, G., Cheung, W.W.L., Connors, S., Denton, F., Diongue-Niang, A., Dodman, D., Garschagen, M., Geden, O., Hayward, B., Jones, C., Jotzo, F., Krug, T., Lasco, R., Lee, Y.-Y., Masson-Delmotte, V., Meinshausen, M., Mintenbeck, K., Mokssit, A., Otto, F.E.L., Pathak, M., Pirani, A., Poloczanska, E., Pörtner, H.-O., Revi, A., Roberts, D.C., Roy, J., Ruane, A.C., Skea, J., Shukla, P.R., Slade, R., Slangen, A., Sokona, Y., Sörensson, A.A., Tignor, M., Van Vuuren, D., Wei, Y.-M., Winkler, H., Zhai, P., Zommers, Z., Hourcade, J.-C., Johnson, F.X., Pachauri, S., Simpson, N.P., Singh, C., Thomas, A., Totin, E., Arias, P., Bustamante, M., Elgizouli, I., Flato, G., Howden, M., Méndez-Vallejo, C., Pereira, J.J., Pichs-Madruga, R., Rose, S.K., Saheb, Y., Sánchez Rodríguez, R., Ürge-Vorsatz, D., Xiao, C., Yassaa, N., Alegría, A., Armour, K., Bednar-Friedl, B., Blok, K., Cissé, G., Dentener, F., Eriksen, S., Fischer, E., Garner, G., Guivarch, C., Haasnoot, M., Hansen, G., Hauser, M., Hawkins, E., Hermans, T., Kopp, R., Leprince-Ringuet, N., Lewis, J., Ley, D., Ludden, C., Niamir, L., Nicholls, Z., Some, S., Szopa, S., Trewin, B., Van Der Wijst, K.-I., Winter, G., Witting, M., Birt, A., Ha, M., Romero, J., Kim, J., Haites, E.F., Jung, Y., Stavins, R., Birt, A., 2023. IPCC, 2023: Climate Change 2023: Synthesis Report. Contribution of Working Groups I, II and III to the Sixth Assessment Report of the Intergovernmental Panel on Climate Change [Core Writing Team, H. Lee and J. Romero (eds.)]. IPCC, Geneva, Switzerland. Intergovernmental Panel on Climate Change (IPCC). https://doi.org/10.59327/IPCC/AR6-9789291691647

Irish Aid, 2015. Lesotho Climate Action Report

Ishfaq, Zhang, F., Meraj, G., Farooq, M., Muslim, M., Arshad, A., 2022. Soil and Water Assessment Tool for Simulating the Sediment and Water Yield of Alpine Catchments, in: Geospatial Modeling for Environmental Management. CRC Press, Boca Raton, pp. 37–57. https://doi.org/10.1201/9781003147107-4

Islam, Md.N., van Amstel, A., 2021. India: Climate Change Impacts, Mitigation and Adaptation in Developing Countries.

Islam, Md.R., Aziz, Md.T., Imran, H.M., Haque, A., 2024. HEC-HMS-based future streamflow simulation in the Dhaka River Basin under CMIP6 climatologic projections. https://doi.org/10.21203/rs.3.rs-4519681/v1

J. G. Arnold, D. N. Moriasi, P. W. Gassman, K. C. Abbaspour, M. J. White, R. Srinivasan, C. Santhi, R. D. Harmel, A. Van Griensven, M. W. Van Liew, N. Kannan, M. K. Jha, 2012. SWAT: Model Use, Calibration, and Validation. Transactions of the ASABE 55, 1491–1508. https://doi.org/10.13031/2013.42256

Jain, S.K., Singh, V.P., 2017. Hydrological Cycles, Models and Applications to Forecasting, in: Duan, Q., Pappenberger, F., Thielen, J., Wood, A., Cloke, H.L., Schaake, J.C. (Eds.), Handbook of Hydrometeorological Ensemble Forecasting. Springer Berlin Heidelberg, Berlin, Heidelberg, pp. 1–28. https://doi.org/10.1007/978-3-642-40457-3_20-1

Kakarndee, I., Kositsakulchai, E., 2020. Comparison between SWAT and SWAT+ for simulating streamflow in a paddy-field-dominated basin, northeast Thailand. E3S Web Conf. 187, 06002. https://doi.org/10.1051/e3sconf/202018706002

Khan, M., Khan, A.U., Khan, S., Khan, F.A., 2023. Assessing the impacts of climate change on streamflow dynamics: A machine learning perspective. Water Science & Technology 88, 2309–2331. https://doi.org/10.2166/wst.2023.340

Kini, K.R., Harrou, F., Madakyaru, M., Sun, Y., 2024. Enhanced data-driven monitoring of wastewater treatment plants using the Kolmogorov–Smirnov test. Environ. Sci.: Water Res. Technol. 10, 1464–1480. https://doi.org/10.1039/D3EW00829K

Kreienkamp, F., Paxian, A., Früh, B., Lorenz, P., Matulla, C., 2019. Evaluation of the empirical–statistical downscaling method EPISODES. Clim Dyn 52, 991–1026. https://doi.org/10.1007/s00382-018-4276-2

Krysanova, V., Donnelly, C., Gelfan, A., Gerten, D., Arheimer, B., Hattermann, F., Kundzewicz, Z.W., 2018. How the performance of hydrological models relates to credibility of projections under climate change. Hydrological Sciences Journal 63, 696–720. https://doi.org/10.1080/02626667.2018.1446214

Kumar, S.B., Mishra, A., 2025. Enhancing the Stability of Hydrological Modelling through Multivariable Calibration Schemes Using the Satellite-Based Soil Moisture and Evapotranspiration. Water Resour Manage 39, 3213–3234. https://doi.org/10.1007/s11269-025-04104-x

Kumar, V., Kedam, N., Sharma, K.V., Mehta, D.J., Caloiero, T., 2023. Advanced Machine Learning Techniques to Improve Hydrological Prediction: A Comparative Analysis of Streamflow Prediction Models. Water 15, 2572. https://doi.org/10.3390/w15142572

Laimighofer, J., Melcher, M., Laaha, G., 2022. Low-flow estimation beyond the mean – expectile loss and extreme gradient boosting for spatiotemporal low-flow prediction in Austria. Hydrol. Earth Syst. Sci. 26, 4553–4574. https://doi.org/10.5194/hess-26-4553-2022

Lane, R.A., Kay, A.L., 2021. Climate Change Impact on the Magnitude and Timing of Hydrological Extremes Across Great Britain. Front. Water 3, 684982. https://doi.org/10.3389/frwa.2021.684982

Legrand, C., Hingray, B., Wilhelm, B., Ménégoz, M., 2024. Assessing downscaling methods to simulate hydrologically relevant weather scenarios from a global atmospheric reanalysis: case

study of the upper Rhône River (1902–2009). Hydrol. Earth Syst. Sci. 28, 2139–2166. https://doi.org/10.5194/hess-28-2139-2024

Lesotho's Climate Action, 2025. Lesotho Climate Change Portal. Vulnerability, Impacts and Adaptation. URL https://climatechangelesotho.gov.ls/index.php/vulnerability-impacts-adaptation/ (accessed 4.7.25).

Li, C., Fang, H., 2021. Assessment of climate change impacts on the streamflow for the Mun River in the Mekong Basin, Southeast Asia: Using SWAT model. CATENA 201, 105199. https://doi.org/10.1016/j.catena.2021.105199

Li, S., Chen, Y., Wei, W., Fang, G., Duan, W., 2024. The increase in extreme precipitation and its proportion over global land. Journal of Hydrology 628, 130456. https://doi.org/10.1016/j.jhydrol.2023.130456

LMS, 2021. The Kingdom of Lesotho's Third National Communication on Climate Change,. Lesotho Meteorological Services., Maseru.

LMS, 2017. Lesotho's Nationally Determined Contribution under the United Nations Framework Convention on Climate Change, Maseru, Lesotho. Ministry of Energy and Meteorology., Lesotho.

López-Ballesteros, A., Nielsen, A., Castellanos-Osorio, G., Trolle, D., Senent-Aparicio, J., 2023. DSOLMap, a novel high-resolution global digital soil property map for the SWAT + model: Development and hydrological evaluation. CATENA 231, 107339. https://doi.org/10.1016/j.catena.2023.107339

Lopez-Gomez, I., Wan, Z.Y., Zepeda-Núñez, L., Schneider, T., Anderson, J., Sha, F., 2025. Dynamical-generative downscaling of climate model ensembles. Proc. Natl. Acad. Sci. U.S.A. 122, e2420288122. https://doi.org/10.1073/pnas.2420288122

Ma, W., Zhang, Xiao, Shen, Y., Xie, J., Zuo, G., Zhang, Xu, Jin, T., 2024. Incorporating Recursive Feature Elimination and Decomposed Ensemble Modeling for Monthly Runoff Prediction. Water 16, 3102. https://doi.org/10.3390/w16213102

Mahasa, P.S., Xulu, S., Mbatha, N., 2023. Characterization of Evapotranspiration in the Orange River Basin of South Africa-Lesotho with Climate and MODIS Data. Water 15, 1501. https://doi.org/10.3390/w15081501

Maliehe, M., Mulungu, D.M.M., 2017. Assessment of water availability for competing uses using SWAT and WEAP in South Phuthiatsana catchment, Lesotho. Physics and Chemistry of the Earth, Parts A/B/C 100, 305–316. https://doi.org/10.1016/j.pce.2017.02.014

Maraun, D., 2016. Bias Correcting Climate Change Simulations - a Critical Review. Curr Clim Change Rep 2, 211–220. https://doi.org/10.1007/s40641-016-0050-x

Marin, M., Clinciu, I., Tudose, N.C., Ungurean, C., Adorjani, A., Mihalache, A.L., Davidescu, A.A., Davidescu, Șerban O., Dinca, L., Cacovean, H., 2020. Assessing the vulnerability of water resources in the context of climate changes in a small forested watershed using SWAT: A review. Environmental Research 184, 109330. https://doi.org/10.1016/j.envres.2020.109330

Markus, M., Cai, X., Sriver, R., 2019. Extreme Floods and Droughts under Future Climate Scenarios. Water 11, 1720. https://doi.org/10.3390/w11081720

Martel, J.-L., Brissette, F., Arsenault, R., Turcotte, R., Castañeda-Gonzalez, M., Armstrong, W., Mailhot, E., Pelletier-Dumont, J., Rondeau-Genesse, G., Caron, L.-P., 2024. Assessing the adequacy of traditional hydrological models for climate change impact studies: A case for long-short-term memory (LSTM) neural networks. https://doi.org/10.5194/egusphere-2024-2133

Martinho, A.D., Hippert, H.S., Goliatt, L., 2023. Short-term streamflow modeling using data-intelligence evolutionary machine learning models. Sci Rep 13, 13824. https://doi.org/10.1038/s41598-023-41113-5

Meinshausen, M., Nicholls, Z.R.J., Lewis, J., Gidden, M.J., Vogel, E., Freund, M., Beyerle, U., Gessner, C., Nauels, A., Bauer, N., Canadell, J.G., Daniel, J.S., John, A., Krummel, P.B., Luderer, G., Meinshausen, N., Montzka, S.A., Rayner, P.J., Reimann, S., Smith, S.J., Van Den Berg, M., Velders, G.J.M., Vollmer, M.K., Wang, R.H.J., 2020. The shared socio-economic pathway (SSP)

greenhouse gas concentrations and their extensions to 2500. Geosci. Model Dev. 13, 3571–3605. https://doi.org/10.5194/gmd-13-3571-2020

Mendlik, T., Gobiet, A., 2016. Selecting climate simulations for impact studies based on multivariate patterns of climate change. Climatic Change 135, 381–393. https://doi.org/10.1007/s10584-015-1582-0

Meresa, H., Tischbein, B., Mekonnen, T., 2022. Climate change impact on extreme precipitation and peak flood magnitude and frequency: observations from CMIP6 and hydrological models. Nat Hazards 111, 2649–2679. https://doi.org/10.1007/s11069-021-05152-3

Mishra, B.R., Vogeti, R.K., Jauhari, R., Raju, K.S., Kumar, D.N., 2024. Boosting algorithms for projecting streamflow in the Lower Godavari Basin for different climate change scenarios. Water Science & Technology 89, 613–634. https://doi.org/10.2166/wst.2024.011

Mogebisa, T., 2021. Potential impacts of climate change on hydrological extremes in the Incomati River Basin. Univerity of Cape Town, Cape Town.

Moges, D.M., Virro, H., Kmoch, A., Cibin, R., Rohith, R.A.N., Martínez-Salvador, A., Conesa-García, C., Uuemaa, E., 2024. Streamflow Prediction with Time-Lag-Informed Random Forest and Its Performance Compared to SWAT in Diverse Catchments. Water 16, 2805. https://doi.org/10.3390/w16192805

Mohamed, A.A., Mukwada, G., 2019. Temperature Changes in the Maloti-Drakensberg Region: An Analysis of Trends for the 1960–2016 Period. Atmosphere 10, 471. https://doi.org/10.3390/atmos10080471

Mokua, R.A., Glenday, J., Mazvimavi, D., 2024. Evaluating the spatial and temporal variation in baseflow across headwater streams in the Jonkershoek valley, South Africa. Proc. IAHS 385, 239–246. https://doi.org/10.5194/piahs-385-239-2024

Montanari, A., Young, G., Savenije, H.H.G., Hughes, D., Wagener, T., Ren, L.L., Koutsoyiannis, D., Cudennec, C., Toth, E., Grimaldi, S., Blöschl, G., Sivapalan, M., Beven, K., Gupta, H., Hipsey,

M., Schaefli, B., Arheimer, B., Boegh, E., Schymanski, S.J., Di Baldassarre, G., Yu, B., Hubert, P., Huang, Y., Schumann, A., Post, D.A., Srinivasan, V., Harman, C., Thompson, S., Rogger, M., Viglione, A., McMillan, H., Characklis, G., Pang, Z., Belyaev, V., 2013. "Panta Rhei—Everything Flows": Change in hydrology and society—The IAHS Scientific Decade 2013–2022. Hydrological Sciences Journal 58, 1256–1275. https://doi.org/10.1080/02626667.2013.809088

Mpheshea, L.E., Blamey, R.C., Reason, C.J.C., 2024. The influence of ENSO-type on rainfall characteristics over Southern Africa during the austral summer. https://doi.org/10.21203/rs.3.rs-4600172/v1

Muhammed, M.A., Hailu, B.T., Miehe, G., Wraase, L., Nauss, T., Zeuss, D., 2023. High-resolution digital elevation models and orthomosaics generated from historical aerial photographs (since the 1960s) of the Bale Mountains in Ethiopia. Earth Syst. Sci. Data 15, 5535–5552. https://doi.org/10.5194/essd-15-5535-2023

Mukheef, R.A.H., Hassan, W.H., Alquzweeni, S., 2024. Projections of temperature and precipitation trends using CMhyd under CMIP6 scenarios: A case study of Iraq's Middle and West. Atmospheric Research 306, 107470. https://doi.org/10.1016/j.atmosres.2024.107470

Mulu, A., Kassa, S.B., Wossene, M.L., Meshesha, T.M., Fenta, A.A., Hailu, Y.B., 2025. Runoff estimation using the SCS-CN method and GIS: a case study in the Wuseta watershed, upper blue Nile Basin, Ethiopia. Discov Water 5, 32. https://doi.org/10.1007/s43832-025-00216-y

Nair, G.S., Karunanidhi, D., Subramani, T., 2025. Hydrological modeling for the Bharathapuzha River basin of South India using SWAT model. Desalination and Water Treatment 321, 100975. https://doi.org/10.1016/j.dwt.2024.100975

Nath, N.K., Singh, P.K., Kothari, M., Bhakar, S.R., Yadav, K.K., Panwar, N.L., 2024. Advances in Hydrological Modelling: A Comprehensive Review of SWAT Applications and Developments. EEC 30, S1–S5. https://doi.org/10.53550/EEC.2024.v30i05s.001

Ngcamu, B.S., 2023. Climate change effects on vulnerable populations in the Global South: a systematic review. Nat Hazards 118, 977–991. https://doi.org/10.1007/s11069-023-06070-2

Ngwenya, S.J., Mukwada, G., 2024. Impacts of climate hazards on households along the Drakensberg Mountains in the Free State Province of South Africa. GeoJournal 89, 66. https://doi.org/10.1007/s10708-024-11061-2

Nhemachena, C., Nhamo, L., Matchaya, G., Nhemachena, C.R., Muchara, B., Karuaihe, S.T., Mpandeli, S., 2020. Climate Change Impacts on Water and Agriculture Sectors in Southern Africa: Threats and Opportunities for Sustainable Development. Water 12, 2673. https://doi.org/10.3390/w12102673

Nhlapo, L.A., 2017. Temperature variability and change at various altitudes across Lesotho and adjoining areas: implications for agriculture. University of the Witwatersrand, Johannesburg

Niazkar, M., Menapace, A., Brentan, B., Piraei, R., Jimenez, D., Dhawan, P., Righetti, M., 2024. Applications of XGBoost in water resources engineering: A systematic literature review (Dec 2018–May 2023). Environmental Modelling & Software 174, 105971. https://doi.org/10.1016/j.envsoft.2024.105971

Nicholson, S.E., Funk, C., Fink, A.H., 2018. Rainfall over the African continent from the 19th through the 21st century. Global and Planetary Change 165, 114–127. https://doi.org/10.1016/j.gloplacha.2017.12.014

Nyeko, M., 2015. Hydrologic Modelling of Data Scarce Basin with SWAT Model: Capabilities and Limitations. Water Resour Manage 29, 81–94. https://doi.org/10.1007/s11269-014-0828-3

O'Neill, B.C., Kriegler, E., Ebi, K.L., Kemp-Benedict, E., Riahi, K., Rothman, D.S., Van Ruijven, B.J., Van Vuuren, D.P., Birkmann, J., Kok, K., Levy, M., Solecki, W., 2017. The roads ahead: Narratives for shared socioeconomic pathways describing world futures in the 21st century. Global Environmental Change 42, 169–180. https://doi.org/10.1016/j.gloenvcha.2015.01.004

Onyutha, C., Ayugi, B.O., Lim Kam Sian, K.T.C., Babaousmail, H., Arineitwe, W., Akobo, J.T., Chelangat, C., Mubialiwo, A., 2024. Sensitivity of Streamflow to Changing Rainfall and Evapotranspiration in Catchments Across the Nile Basin. Atmosphere 15, 1415. https://doi.org/10.3390/atmos15121415

Oo, H.T., Zin, W.W., Thin Kyi, C.C., 2019. Assessment of Future Climate Change Projections Using Multiple Global Climate Models. Civ Eng J 5, 2152–2166. https://doi.org/10.28991/cej-2019-03091401

Pandey, A., Himanshu, S.K., Mishra, S.K., Singh, V.P., 2016. Physically based soil erosion and sediment yield models revisited. CATENA 147, 595–620. https://doi.org/10.1016/j.catena.2016.08.002

Pandi, D., Kothandaraman, S., Kuppusamy, M., 2023. Simulation of Water Balance Components Using SWAT Model at Sub Catchment Level. Sustainability 15, 1438. https://doi.org/10.3390/su15021438

Parajuli, P.B., Risal, A., 2021. Evaluation of Climate Change on Streamflow, Sediment, and Nutrient Load at Watershed Scale. Climate 9, 165. https://doi.org/10.3390/cli9110165

Parding, K.M., Dobler, A., McSweeney, C.F., Landgren, O.A., Benestad, R., Erlandsen, H.B., Mezghani, A., Gregow, H., Räty, O., Viktor, E., El Zohbi, J., Christensen, O.B., Loukos, H., 2020. GCMeval – An interactive tool for evaluation and selection of climate model ensembles. Climate Services 18, 100167. https://doi.org/10.1016/j.cliser.2020.100167

Pereira, L.S., 2017. Water, Agriculture and Food: Challenges and Issues. Water Resour Manage 31, 2985–2999. https://doi.org/10.1007/s11269-017-1664-z

Petja, B., Mpandeli, S., Nhamo, L., Zvimba, J., 2023. Climate change impacts on water resources-implications & practical responses in selected SA systems.

Phetanan, K., Hong, S.M., Yun, D., Lee, J., Chotpantarat, S., Jeong, H., Cho, K.H., 2024. Enhancing flow rate prediction of the Chao Phraya River Basin using SWAT–LSTM model

coupling. Journal of Hydrology: Regional Studies 53, 101820. https://doi.org/10.1016/j.ejrh.2024.101820

Pierre, C., Grippa, M., Mougin, E., Guichard, F., Kergoat, L., 2016. Changes in Sahelian annual vegetation growth and phenology since 1960: A modeling approach. Global and Planetary Change 143, 162–174. https://doi.org/10.1016/j.gloplacha.2016.06.009

Pratap, S., Markonis, Y., 2022. The response of the hydrological cycle to temperature changes in recent and distant climatic history. Prog Earth Planet Sci 9, 30. https://doi.org/10.1186/s40645-022-00489-0

Prein, A.F., Rasmussen, R.M., Ikeda, K., Liu, C., Clark, M.P., Holland, G.J., 2017. The future intensification of hourly precipitation extremes. Nature Clim Change 7, 48–52. https://doi.org/10.1038/nclimate3168

Pulighe, G., Lupia, F., Chen, H., Yin, H., 2021. Modeling Climate Change Impacts on Water Balance of a Mediterranean Watershed Using SWAT+. Hydrology 8, 157. https://doi.org/10.3390/hydrology8040157

Rahman, K.U., Pham, Q.B., Jadoon, K.Z., Shahid, M., Kushwaha, D.P., Duan, Z., Mohammadi, B., Khedher, K.M., Anh, D.T., 2022. Comparison of machine learning and process-based SWAT model in simulating streamflow in the Upper Indus Basin. Appl Water Sci 12, 178. https://doi.org/10.1007/s13201-022-01692-6

Rajib, A., Liu, Z., Merwade, V., Tavakoly, A.A., Follum, M.L., 2020. Towards a large-scale locally relevant flood inundation modeling framework using SWAT and LISFLOOD-FP. Journal of Hydrology 581, 124406. https://doi.org/10.1016/j.jhydrol.2019.124406

Rami, F., Thompson, L., Solis-Cortes, L., 2023. Healthcare Disparities: Vulnerable and Marginalized Populations, in: Searight, H.R. (Ed.), Covid-19: Health Disparities and Ethical Challenges Across the Globe. Springer International Publishing, Cham, pp. 111–145. https://doi.org/10.1007/978-3-031-26200-5_6

Riahi, K., Van Vuuren, D.P., Kriegler, E., Edmonds, J., O'Neill, B.C., Fujimori, S., Bauer, N., Calvin, K., Dellink, R., Fricko, O., Lutz, W., Popp, A., Cuaresma, J.C., Kc, S., Leimbach, M., Jiang, L., Kram, T., Rao, S., Emmerling, J., Ebi, K., Hasegawa, T., Havlik, P., Humpenöder, F., Da Silva, L.A., Smith, S., Stehfest, E., Bosetti, V., Eom, J., Gernaat, D., Masui, T., Rogelj, J., Strefler, J., Drouet, L., Krey, V., Luderer, G., Harmsen, M., Takahashi, K., Baumstark, L., Doelman, J.C., Kainuma, M., Klimont, Z., Marangoni, G., Lotze-Campen, H., Obersteiner, M., Tabeau, A., Tavoni, M., 2017. The Shared Socioeconomic Pathways and their energy, land use, and greenhouse gas emissions implications: An overview. Global Environmental Change 42, 153–168. https://doi.org/10.1016/j.gloenvcha.2016.05.009

Roffe, S.J., Engelbrecht, F.A., Bamford, M.K., 2024. Southern African precipitation changes in a warmer world: insights from the PlioMIP2 mid-Pliocene warm period (~3.3–3.0 Ma) ensemble. Transactions of the Royal Society of South Africa 79, 155–175. https://doi.org/10.1080/0035919X.2024.2410945

Rufino, P.R., Gücker, B., Faramarzi, M., Boëchat, I.G., Cardozo, F.D.S., Santos, P.R., Zanin, G.D., Mataveli, G., Pereira, G., 2022. Evaluation of the SWAT Model for the Simulation of Flow and Water Balance Based on Orbital Data in a Poorly Monitored Basin in the Brazilian Amazon. Geographies 3, 1–18. https://doi.org/10.3390/geographies3010001

Saade, J., Atieh, M., Ghanimeh, S., Golmohammadi, G., 2021. Modeling Impact of Climate Change on Surface Water Availability Using SWAT Model in a Semi-Arid Basin: Case of El Kalb River, Lebanon. Hydrology 8, 134. https://doi.org/10.3390/hydrology8030134

Saedi, J., Sharifi, M.R., Saremi, A., Babazadeh, H., 2022. Assessing the impact of climate change and human activity on streamflow in a semiarid basin using precipitation and baseflow analysis. Sci Rep 12, 9228. https://doi.org/10.1038/s41598-022-13143-y

Samimi, M., Mirchi, A., Moriasi, D., Ahn, S., Alian, S., Taghvaeian, S., Sheng, Z., 2020. Modeling arid/semi-arid irrigated agricultural watersheds with SWAT: Applications, challenges, and solution strategies. Journal of Hydrology 590, 125418. https://doi.org/10.1016/j.jhydrol.2020.125418

Sane, M.L., Sambou, S., Leye, I., Ndione, D.M., Diatta, S., Ndiaye, I., Badji, M.L., Kane, S., 2020. Calibration and Validation of the SWAT Model on the Watershed of Bafing River, Main Upstream Tributary of Senegal River: Checking for the Influence of the Period of Study. OJMH 10, 81–104. https://doi.org/10.4236/ojmh.2020.104006

Sapač, K., Medved, A., Rusjan, S., Bezak, N., 2019. Investigation of Low- and High-Flow Characteristics of Karst Catchments under Climate Change. Water 11, 925. https://doi.org/10.3390/w11050925

Sawant, P.N., 2021. Soil and Water Assessment Tool Application in Natural Resources Management: A Systematic Review. IJAEB 14. https://doi.org/10.30954/0974-1712.03.2021.11

Scheff, J., Frierson, D.M.W., 2014. Scaling Potential Evapotranspiration with Greenhouse Warming. Journal of Climate 27, 1539–1558. https://doi.org/10.1175/JCLI-D-13-00233.1

Schutte, C., Van Der Laan, M., Van Der Merwe, B., 2024. Leveraging historic streamflow and weather data with deep learning for enhanced streamflow predictions. Journal of Hydroinformatics 26, 835–852. https://doi.org/10.2166/hydro.2024.268

Şebcioğlu Mutlu, Ş., Pala, A., Guven, A., 2025. Comparing traditional hydrological forecasting models with CatBoost algorithm: insights from CMIP6 climate scenarios. Journal of Water and Climate Change 16, 1186–1208. https://doi.org/10.2166/wcc.2025.775

Serdeczny, O., Adams, S., Baarsch, F., Coumou, D., Robinson, A., Hare, W., Schaeffer, M., Perrette, M., Reinhardt, J., 2017. Climate change impacts in Sub-Saharan Africa: from physical changes to their social repercussions. Reg Environ Change 17, 1585–1600. https://doi.org/10.1007/s10113-015-0910-2

Sheng, S., Chen, Q., Li, J., Chen, H., 2023. The Improved Reservoir Module of SWAT Model with a Dispatch Function and Its Application on Assessing the Impact of Climate Change and Human Activities on Runoff Change. Water 15, 2620. https://doi.org/10.3390/w15142620

Shiferaw, H., Gebremedhin, A., Gebretsadkan, T., Zenebe, A., 2018. Modelling hydrological response under climate change scenarios using SWAT model: the case of Ilala watershed, Northern Ethiopia. Model. Earth Syst. Environ. 4, 437–449. https://doi.org/10.1007/s40808-018-0439-8

Siabi, E.K., Awafo, E.A., Kabo-bah, A.T., Derkyi, N.S.A., Akpoti, K., Mortey, E.M., Yazdanie, M., 2023. Assessment of Shared Socioeconomic Pathway (SSP) climate scenarios and its impacts on the Greater Accra region. Urban Climate 49, 101432. https://doi.org/10.1016/j.uclim.2023.101432

Sirisena, T.A.J.G., Maskey, S., Bamunawala, J., Ranasinghe, R., 2021. Climate Change and Reservoir Impacts on 21st-Century Streamflow and Fluvial Sediment Loads in the Irrawaddy River, Myanmar. Front. Earth Sci. 9, 644527. https://doi.org/10.3389/feart.2021.644527

Slater, L.J., Arnal, L., Boucher, M.-A., Chang, A.Y.-Y., Moulds, S., Murphy, C., Nearing, G., Shalev, G., Shen, C., Speight, L., Villarini, G., Wilby, R.L., Wood, A., Zappa, M., 2023. Hybrid forecasting: blending climate predictions with AI models. Hydrol. Earth Syst. Sci. 27, 1865–1889. https://doi.org/10.5194/hess-27-1865-2023

Solanki, H., Vegad, U., Kushwaha, A., Mishra, V., 2025. Improving Streamflow Prediction Using Multiple Hydrological Models and Machine Learning Methods. Water Resources Research 61, e2024WR038192. https://doi.org/10.1029/2024WR038192

Song, Y.H., Chung, E.-S., Sung, J.H., 2019. Selection framework of representative general circulation models using the selected best bias correction method. Journal of Korea Water Resources Association 52, 337–347. https://doi.org/10.3741/JKWRA.2019.52.5.337

Sun, J., Yan, H., Bao, Z., Wang, G., 2022. Investigating Impacts of Climate Change on Runoff from the Qinhuai River by Using the SWAT Model and CMIP6 Scenarios. Water 14, 1778. https://doi.org/10.3390/w14111778

Sun, W., Wang, Y., Wang, G., Cui, X., Yu, J., Zuo, D., Xu, Z., 2017. Physically based distributed hydrological model calibration based on a short period of streamflow data: case studies in four Chinese basins. Hydrol. Earth Syst. Sci. 21, 251–265. https://doi.org/10.5194/hess-21-251-2017

Szczepanek, R., 2022. Daily Streamflow Forecasting in Mountainous Catchment Using XGBoost, LightGBM and CatBoost. Hydrology 9, 226. https://doi.org/10.3390/hydrology9120226

T Dube, L., 2024. Climate Variability over Southern Africa and Implications for Water Resources: A Review. AHM 1. https://doi.org/10.33552/AHM.2024.01.000517

Tarekegn, N., Abate, B., Muluneh, A., Dile, Y., 2022. Modeling the impact of climate change on the hydrology of Andasa watershed. Model. Earth Syst. Environ. 8, 103–119. https://doi.org/10.1007/s40808-020-01063-7

Taye, M.T., Dyer, E., 2024. Hydrologic Extremes in a Changing Climate: a Review of Extremes in East Africa. Curr Clim Change Rep 10, 1–11. https://doi.org/10.1007/s40641-024-00193-9

Terrier, M., Perrin, C., De Lavenne, A., Andréassian, V., Lerat, J., Vaze, J., 2021. Streamflow naturalization methods: a review. Hydrological Sciences Journal 66, 12–36. https://doi.org/10.1080/02626667.2020.1839080

Tetra Tech Inc, 2015. Lake Champlain Basin SWAT Model Configuration, Calibration and Validation. U.S. EPA Region 1 - New England, Boston.

Teweldebrihan, M.D., Dinka, M.O., 2024. The impact of climate change on the development of water resources. Global J. Environ. Sci. Manage. 10. https://doi.org/10.22034/gjesm.2024.03.25

Thompson, J.R., Gosling, S.N., Zaherpour, J., Laizé, C.L.R., 2021. Increasing Risk of Ecological Change to Major Rivers of the World With Global Warming. Earth's Future 9, e2021EF002048. https://doi.org/10.1029/2021EF002048

Tokarska, K.B., Stolpe, M.B., Sippel, S., Fischer, E.M., Smith, C.J., Lehner, F., Knutti, R., 2020. Past warming trend constrains future warming in CMIP6 models. Sci. Adv. 6, eaaz9549. https://doi.org/10.1126/sciadv.aaz9549

Tootoonchi, F., Todorović, A., Grabs, T., Teutschbein, C., 2023. Uni- and multivariate bias adjustment of climate model simulations in Nordic catchments: Effects on hydrological signatures

relevant for water resources management in a changing climate. Journal of Hydrology 623, 129807. https://doi.org/10.1016/j.jhydrol.2023.129807

Torabi Haghighi, A., Darabi, H., Shahedi, K., Solaimani, K., Kløve, B., 2020. A Scenario-Based Approach for Assessing the Hydrological Impacts of Land Use and Climate Change in the Marboreh Watershed, Iran. Environ Model Assess 25, 41–57. https://doi.org/10.1007/s10666-019-09665-x

UNCCD, 2022. Southern Africa: Leveraging the land, water and energy nexus in SADC.

USGS, 2000. EarthData.

Uuemaa, E., Ahi, S., Montibeller, B., Muru, M., Kmoch, A., 2020. Vertical Accuracy of Freely Available Global Digital Elevation Models (ASTER, AW3D30, MERIT, TanDEM-X, SRTM, and NASADEM). Remote Sensing 12, 3482. https://doi.org/10.3390/rs12213482

Van Loon, A.F., Rangecroft, S., Coxon, G., Breña Naranjo, J.A., Van Ogtrop, F., Van Lanen, H.A.J., 2019. Using paired catchments to quantify the human influence on hydrological droughts. Hydrol. Earth Syst. Sci. 23, 1725–1739. https://doi.org/10.5194/hess-23-1725-2019

Van Vuuren, D.P., Edmonds, J., Kainuma, M., Riahi, K., Thomson, A., Hibbard, K., Hurtt, G.C., Kram, T., Krey, V., Lamarque, J.-F., Masui, T., Meinshausen, M., Nakicenovic, N., Smith, S.J., Rose, S.K., 2011. The representative concentration pathways: an overview. Climatic Change 109, 5–31. https://doi.org/10.1007/s10584-011-0148-z

Veldkamp, T.I.E., Zhao, F., Ward, P.J., De Moel, H., Aerts, J.C.J.H., Schmied, H.M., Portmann, F.T., Masaki, Y., Pokhrel, Y., Liu, X., Satoh, Y., Gerten, D., Gosling, S.N., Zaherpour, J., Wada, Y., 2018. Human impact parameterizations in global hydrological models improve estimates of monthly discharges and hydrological extremes: a multi-model validation study. Environ. Res. Lett. 13, 055008. https://doi.org/10.1088/1748-9326/aab96f

Vogeti, R.K., Mishra, B.R., Raju, K.S., 2022. Machine learning algorithms for streamflow forecasting of Lower Godavari Basin. H2Open Journal 5, 670–685. https://doi.org/10.2166/h2oj.2022.240

Wang, Q., Deng, H., Jian, J., 2023. Hydrological Processes under Climate Change and Human Activities: Status and Challenges. Water 15, 4164. https://doi.org/10.3390/w15234164

Wang, S., Peng, H., 2024. Multiple spatio-temporal scale runoff forecasting and driving mechanism exploration by K-means optimized XGBoost and SHAP. Journal of Hydrology 630, 130650. https://doi.org/10.1016/j.jhydrol.2024.130650

WateriTech, 2023. Data Resources.

World Health Organization (WHO), 2023. Climate change.

Yahaya, I., Li, Z., Zhou, J., Jiang, S., Su, B., Huang, J., Xu, R., Havea, P.H., Jiang, T., 2024. Estimations of potential evapotranspiration from CMIP6 multi-model ensemble over Africa. Atmospheric Research 300, 107255. https://doi.org/10.1016/j.atmosres.2024.107255

Yang, Y., Chui, T.F.M., 2021. Modeling and interpreting hydrological responses of sustainable urban drainage systems with explainable machine learning methods. Hydrol. Earth Syst. Sci. 25, 5839–5858. https://doi.org/10.5194/hess-25-5839-2021

Yin, J., He, F., Xiong, Y.J., Qiu, G.Y., 2017. Effects of land use/land cover and climate changes on surface runoff in a semi-humid and semi-arid transition zone in northwest China. Hydrol. Earth Syst. Sci. 21, 183–196. https://doi.org/10.5194/hess-21-183-2017

Yılmaz, M., Tosunoğlu, F., 2024. Non-stationary low flow frequency analysis under climate change. Theor Appl Climatol 155, 7479–7497. https://doi.org/10.1007/s00704-024-05081-8

Zhang, L., Nan, Z., Xu, Y., Li, S., 2016. Hydrological Impacts of Land Use Change and Climate Variability in the Headwater Region of the Heihe River Basin, Northwest China. PLoS ONE 11, e0158394. https://doi.org/10.1371/journal.pone.0158394

Zhang, Y., Wu, X., Wu, S., Dai, J., Yu, L., Xue, W., Wang, F., Gao, A., Xue, C., 2021. A Framework for Methodological Options to Assess Climatic and Anthropogenic Influences on Streamflow. Front. Environ. Sci. 9, 765227. https://doi.org/10.3389/fenvs.2021.765227

Zheng, L., Diamond, J.M., Denton, D.L., 2013. Evaluation of whole effluent toxicity data characteristics and use of Welch's *T* -test in the test of significant toxicity analysis. Environmental Toxicology and Chemistry 32, 468–474. https://doi.org/10.1002/etc.2075

Zhuang, Q., Liu, S., Zhou, Z., 2020. Spatial Heterogeneity Analysis of Short-Duration Extreme Rainfall Events in Megacities in China. Water 12, 3364. https://doi.org/10.3390/w12123364

Appendices

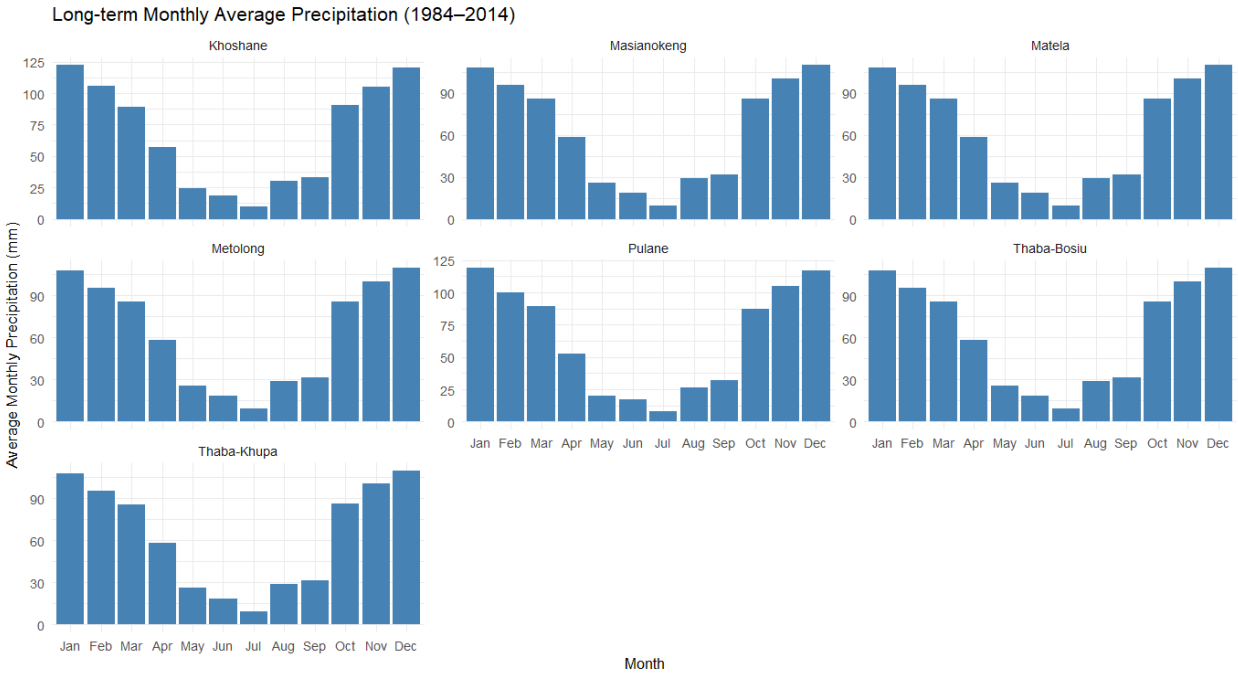

Figure 29 *- Long-term Monthly Average Precipitation (1984 - 2014)*